

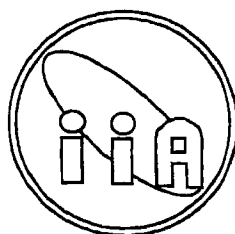
Star Formation: Circumstellar Environment around Young Stellar Objects

A thesis
submitted for the Degree of
Doctor of Philosophy

in
The Faculty of Science
Bangalore University

by

MANOJ PURAVANKARA



Indian Institute of Astrophysics

Bangalore 560 034, India

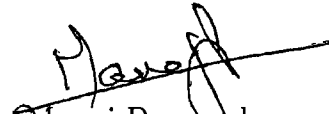
2004

Declaration

I hereby declare that the matter contained in this thesis is the result of the investigations carried out by me at the Indian Institute of Astrophysics, Bangalore, under the supervision of Dr. H. C. Bhatt. This work has not been submitted for the award of any degree, diploma, associateship, fellowship etc. of any university or institute.



Dr. H. C. Bhatt
(Thesis Supervisor)



Manoj Puravankara
(Ph.D. Candidate)

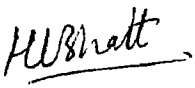
Indian Institute of Astrophysics
Bangalore 560 034, India

February, 2004

Certificate

This is to certify that the thesis entitled ' Star Formation: Circumstellar environment around young stellar objects' submitted to the Bangalore University by Mr. Manoj Puravankara for the award of the degree of Doctor of Philosophy in the faculty of Science, is based on the results of the investigations carried out by him under my supervision and guidance, at the Indian Institute of Astrophysics, Bangalore. This thesis has not been submitted for the award of any degree, diploma, associateship, fellowship etc. of any university or institute.

Indian Institute of Astrophysics,
Bangalore
February, 2004


Dr. H. C. Bhatt
(Thesis Supervisor)

Acknowledgements

I first of all wish to thank Harish Bhatt for his guidance and continuous support during the course of this work as my thesis advisor. It has been a pleasure and a great learning experience working with him.

I thank Dipankar Mallik, Chanda Jog and Mathew Mekkaden, who as the members of my doctoral committee, helped me in planning and refining this work. I have greatly benefitted from the discussions I have had with them.

I thank Jayant Murthy, Prajval Shastri, Sushma Mallik, G. C. Anupama, Ashok Pati, S. Chatterjee and Annapurni Subramaniam for interesting scientific discussions I have had with them.

I thank A. Vagiswari, Christina Birdie and all the other library staff for the excellent library facility offered at the Institute. I have benefitted a great deal from it. I also thank J. S. Nathan for all the help I have received from him as our system administrator.

I thank all the observing staff at the Vainu Bappu Observatory (VBO), Kavalur, for their efficient help during my observing runs. I also thank Muneer for helping me out in obtaining some of the spectra that have gone into this work. Thanks are due to P. S. Parihar and D. K. Sahu for all the assistance provided to me during my observations with HCT at CREST, Hosakote.

I am thankful and lucky to have had friends at IIA who made my Ph.D. years pleasant and memorable. I thank Arun, Dilip and Rajesh for those numerous discussions, both academic and on other issues, that I have had with them and for helping me start out in research in the early days. I thank Sivarani for being my IRAF 'Guru' and Shankar and Sridhar for initiating me to the wonderful world of IDL. Special thanks to Raji for proofreading the thesis and for her being an excellent friend throughout. I thank Maheswar for fruitful discussions and all those things that I have learned from him. Ravi has been a good friend and I thank him for those wonderful weekend 'sessions'. I also thank Srikanth, Rajguru, Pandey, Krishna, Swara, Bhargavi, Sanjoy, Pavan, Mangala, Jana, Geetha, Dharam, Suresh, Moja, Sudip, Geetanjali, Ambika, Shanmugham, Kathiravan, Shalima, Latha, Reji, Jayendra, Nagaraj,

Maiti and Vineet for making my stay at IIA light and enjoyable.

I wish to thank my friends Niruj, Rekesh, Amitesh and Dibyendu Nandy for the great times we have had together. Niruj, with his infectious enthusiasm for astronomy, has been kind of an ‘inspirational’ figure. He has indeed been a friend in need and has helped me through some rough patches.

I thank Prabha and Harish, Sharath and Prajval, Sushma and Dipankar and Raji and Raja for their cordial hospitality and those sumptuous dinners and wonderful evenings.

I am deeply indebted to Preeti for her constant encouragement and companionship.

Finally, I thank my parents without whose love, understanding and patient and enthusiastic support, it would not have been possible for me to achieve what I now have. I also thank my siblings Suraj and Sreeraj for their quiet and gentle encouragement and affection.

- *This research has made use of data products from the Two Micron All Sky Survey, which is a joint project of the University of Massachusetts and the Infrared Processing and Analysis Center/California Institute of Technology, funded by the National Aeronautics and Space Administration and the National Science Foundation.*
- *This research has made use of the SIMBAD database, operated at CDS, Strasbourg, France*
- *This research has made use of NASA’s Astrophysics Data System.*

List of Publications

Refereed Journals

1. POLARIZATION MEASUREMENTS OF VEGA-LIKE STARS
– Bhatt, H.C., **Manoj, P.**, *A&A*, **362**, 978 (2000)

2. KINEMATICS OF VEGA-LIKE STARS
–**Manoj, P.**, Bhatt, H.C., *Bull. Astron. Soc. India*, **29**, 313 (2001)

3. CIRCUMSTELLAR DISKS AROUND HERBIG AE/BE STARS: POLARIZATION, OUTFLOWS AND BINARY ORBITS
– Maheswar, G., **Manoj, P.**, Bhatt, H.C., *A&A* **387**, 1003 (2002)

4. NON-EMISSION-LINE YOUNG STARS OF INTERMEDIATE MASS
–**Manoj, P.**, Maheswar, G., Bhatt, H.C., *MNRAS*, **334**, 419 (2002)

5. CIRCUMSTELLAR ENVIRONMENT AROUND YOUNG STELLAR OBJECTS IN NEARBY OB ASSOCIATIONS
–**Manoj, P.**, Maheswar, G., Bhatt, H.C., *Bull. Astron. Soc. India*, **30**, 657 (2002)

6. INTERMEDIATE GALACTIC LATITUDE STARFORMING REGION - CG 12
– Maheswar, G., **Manoj, P.**, Bhatt, H.C., *Bull. Astron. Soc. India*, **30**, 651 (2002)

7. OPTICAL SPECTROSCOPIC AND 2MASS MEASUREMENTS OF STEPHENSON
 $H\alpha$ STARS

– Maheswar, G., **Manoj, P.**, Bhatt, H.C., *A&A*, **402**, 963, (2003)

8. MAGNETIC FIELDS IN COMETARY GLOBULES - III: CG 12

– Bhatt, H. C., Maheswar, G., **Manoj P.** - *MNRAS*, **348**, 83, (2004)

9. KINEMATICS OF VEGA-LIKE STARS AND TEMPORAL EVOLUTION OF THEIR
DUSTY DISKS

– **Manoj P.**, Maheswar, G., H. C. Bhatt - *in preperation*

Others

1. TEMPORAL EVOLUTION OF MAIN SEQUENCE DUST DISKS

– **Manoj, P.** & H. C. Bhatt in proceedings of the international Colloquium on “*Open Issues in Local Star Formation and ealy stellar Evolution*” held at Ouro Preto, Brazil during 5-10, April, 2003, *Astrophysics & Space Science Library*, Vol.299, p295, Kluwer Academic Publishers (2003)

2. AB AURIGAE

– Ashok, N. M., Chandrasekhar, T., Bhatt, H. C., **Manoj, P.**
IAU Circ., *7103*, 2, (1999)

3. ASTRONOMICAL SEEING AT MT. SARASWATI, HANLE

– **Manoj, P.**, Ravindra, B. & T. P. Prabhu
report of the project undertaken as part of graduate school
at Indian Institute of Astrophysics, (December 1998).

Contents

1	Introduction	1
1.1	An overview of star and planet formation	1
1.2	Circumstellar environment around young stars	4
1.3	Debris disks around main sequence stars	11
1.4	Evolution of circumstellar disks	12
1.5	Outline of the Thesis	15
2	Evolution of emission line activity in Herbig Ae/Be Stars	17
2.1	Introduction	17
2.2	The Sample	21
2.3	Observations and Analysis	26
2.4	Evolution of $H\alpha$ equivalent width with age	27
2.5	K-band excess and age	29
2.6	Discussion	34
2.7	Summary	37
3	Transition objects: Non-emission line young stars	39
3.1	Introduction	39
3.2	Non-emission line young stars of intermediate mass	41
3.2.1	Observations	41
3.2.2	Data compiled from literature	44

3.2.3	Stars in the Orion Nebula Cluster	49
3.2.4	HD 158352	53
3.2.5	HD 176386	54
3.3	Vega-like stars with high fractional dust luminosity	55
3.4	Discussion	61
3.5	Summary	62
4	Dust around main-sequence stars: Vega-like stars	64
4.1	Introduction	64
4.2	Polarization studies of Vega-like stars	65
4.3	Observations	66
4.4	Discussion	68
4.5	Conclusions	78
5	Kinematics of Vega-like stars and the temporal evolution of the dust disks	79
5.1	Introduction	79
5.2	Data	82
5.3	Analysis	82
5.3.1	Dustiness of Vega-like Stars	82
5.3.2	Kinematics - Transverse Velocities of Vega-like Stars	84
5.4	Results	84
5.5	Discussion	91
5.6	Conclusions	95
6	A disk census of nearby OB associations	97
6.1	Introduction	97
6.2	Data and analysis	100

6.3 Discussion	106
6.4 Summary and conclusions	109
7 Conclusions	111
A OPTICAL SPECTRA OF HERBIG Ae/Be STARS	116

Chapter 1

Introduction

1.1 An overview of star and planet formation

Formation of stars and planetary systems is one of the most fundamental problems in modern astrophysics. Until less than a decade ago, our solar system was the only planetary system that was known to us. In recent years the existence of planets around other sun-like stars has been established through a variety of ingenious observational techniques combined with the advances in the available facilities (Mayor & Queloz 1995; Marcy & Butler 1999; Marcy et al. 2000). More than a hundred extrasolar planetary systems have been identified so far. Now that the planetary systems are found to be quite common around stars, it is imperative that we compare and contrast the properties of planetary systems observed elsewhere with what is known about our own solar system and thereby gain insight into the processes which lead to the formation and control the evolution of planetary systems. Observational and theoretical studies of the last few decades have been able to establish that the formation of planetary system around a star is intimately connected to the star formation process itself and that the circumstellar disks found around most of the new born stars are analogous in their bulk properties to the protosolar nebula in which planets are thought to be formed (e.g., Beckwith 1999). The recognition of the fact that the collapse of magnetized, rotating molecular cloud cores, from which stars are

formed, naturally leads to the formation of protostellar disks has been one of the major triumphs of modern star formation theory (e.g, Shu et al. 1987). The study of star formation, therefore, is not only important in itself but also is essential to our understanding of the planet formation process and thereby of the origins of our solar system and that of our planet Earth.

Stars are believed to be formed in the dense and cold interiors of molecular clouds. In the current paradigm for star formation (e.g, Shu et al. 1987; Hartmann 1998), the process begins when a number of dense cores develop within a molecular cloud. For masses greater than Jeans mass given by,

$$M_J \sim 30M_\odot T^{3/2} n^{-1/2}$$

where M_\odot is the mass of the Sun, T is the temperature in K and n is the molecular hydrogen density in units of cm^{-3} , these dense cores will be unstable to gravitational collapse if thermal pressure is the principal force which counteracts gravity. Since dense cores of typical size ~ 0.1 pc must contract by a factor of 10^6 in linear dimensions to form a star, any small initial rotation of the star-forming cloud can be enormously magnified by conservation of angular momentum during rapid collapse. As a result, the nearly free-fall collapse of such a moderately rotating (angular velocity $\Omega < 10^{-13} s^{-1}$) core leads to the formation of a central protostar surrounded by a rapidly rotating nebular disk and remnant infalling envelope. The infalling envelope feeds the disk which in turn accretes matter on to the central protostar. In the early stages of the protostellar evolution the infall from the overlying envelope to the disk can be significantly high. This infall/accretion phase during which most of the stellar mass is acquired is heavily obscured with visual extinction as high as few hundreds of magnitudes. At some point during this phase a powerful stellar wind breaks out along the rotation/magnetic axis of the protostar/disk system which sweeps up the surrounding material and manifests itself observationally as bipolar outflows observed in the molecular lines, primarily in CO (e.g., Bachiller & Tafalla 1999). The main infall-outflow phase is thought to be as short as $< 10^5$ Myr. After the outflows have presumably cleared out the reservoir of mass from the protostellar envelope, the self-luminous central source surrounded by an accreting disk emerges from the natal

core and becomes visible at near-infrared and optical wavelengths as a young stellar object. In the Hertzsprung-Russell (HR) diagram it appears on the birthline and begins to contract quasi-statically along its evolutionary track towards the hydrogen-burning main sequence (Palla 1999). The star then is said to have entered its pre-main sequence phase. Pre-main sequence stars are associated with rich circumstellar environment. Circumstellar matter surrounding these young stars is distributed in a disk and probably also in an extended envelope of relatively low optical depth. A residual accretion at a low level ($\dot{M}_{acc} < 10^{-7} M_{\odot} \text{yr}^{-1}$) may be present during the pre-main sequence phase which can persist in some cases upto $\sim 10^7$ yr (Muzerolle et al. 2000). The disks dissipate on timescales of a few Myr on an average due to planet formation and other dispersal processes (Haisch et al. 2001; Hillenbrand 2002).

The low eccentricities and inclinations of the planets have long been used as evidence that the Solar system has formed from a flattened disk of gas and dust. In the standard model of planet formation (e.g., Lissauer 1993; Weidenschilling & Cuzzi 1993; Pollack et al. 1996; Ruden 1999) circumstellar disks surrounding young stars are considered to be the ‘birth place’ of planets. The process begins when the sub-micron sized dust grains, which are uniformly distributed and strongly coupled to the gas in the disk, grow through binary collisions. As they grow larger they settle gravitationally to the disk mid-plane forming a thin layer. In about 10^4 yr, particles can grow from micron size to meter size. Further growth in the mid-plane due to mutual collisions can cause the formation of roughly kilometer-sized bodies called planetesimals on timescales of a few thousand orbital periods. Planetesimals are massive enough to have largely decoupled from the gas and move on nearly circular, Keplerian orbits about the central star. Kilometer-sized planetesimals continue to further grow through pairwise inelastic collisions. This growth is aided by the increase in collision cross sections above the geometric value by the focussing nature of the gravitational interaction between colliding planetesimals. The increase in cross-section is greatest for the more massive planetesimals if the velocity dispersion among planetesimals remain sufficiently small. Thus the most massive planetesimals tend to gain mass more rapidly which causes its collision cross-section to increase even further. When the masses of these massive planetesimals grow beyond $100 M_{\oplus}$ (where M_{\oplus} is the mass

of the Earth) or so, they accrete gas from the disk to form giant gaseous planets. The smaller protoplanetary bodies left physically and dynamically isolated because of the runaway growth of the larger and massive planetesimals, can now grow collisionally only on much larger timescales ($\sim 10^8$ yr). The growth of terrestrial planets to their current masses continues long after the dispersal of the gas disk.

1.2 Circumstellar environment around young stars

As discussed in the previous Section, circumstellar disks are a necessary consequence of star formation process and stars are born with disks around them. Once the central star has emerged out of its parental cocoon, it becomes optically visible as a pre-main sequence star.

Pre-main sequence stars are young objects which have not started hydrogen burning at their center and which are quasi-statically contracting towards the main sequence in the HR diagram. The luminosity of these objects is primarily derived from the energy released from the gravitational contraction during the pre-main sequence evolution. Low mass pre-main sequence stars are called T Tauri stars and their intermediate mass counterparts are known as Herbig Ae/Be stars. These young stars were originally identified as stars with strong emission lines, especially in $H\alpha$, and irregular variations associated with dark or bright nebulosity. Pre-main sequence stars are invariably associated with rich and complex circumstellar environment and are very active. Observational signatures of the circumstellar environment of these stars include, emission lines in the spectra, strong variability, excess emission at infrared, sub-mm and mm wavelengths and intrinsic polarization of starlight.

The most important observational characteristic of pre-main sequence stars is the presence of a variety of emission lines in their spectra. To illustrate this, in Figure 1.1 we present the optical spectra of the prototype Herbig Ae star AB Aur in the blue and red region. Prominent emission lines seen are marked in the figure. Apart from the Balmer lines of hydrogen, the other lines like CaII, HeI, OI as well as many metallic lines are seen in emission in the spectra of pre-main sequence stars. Forbidden lines

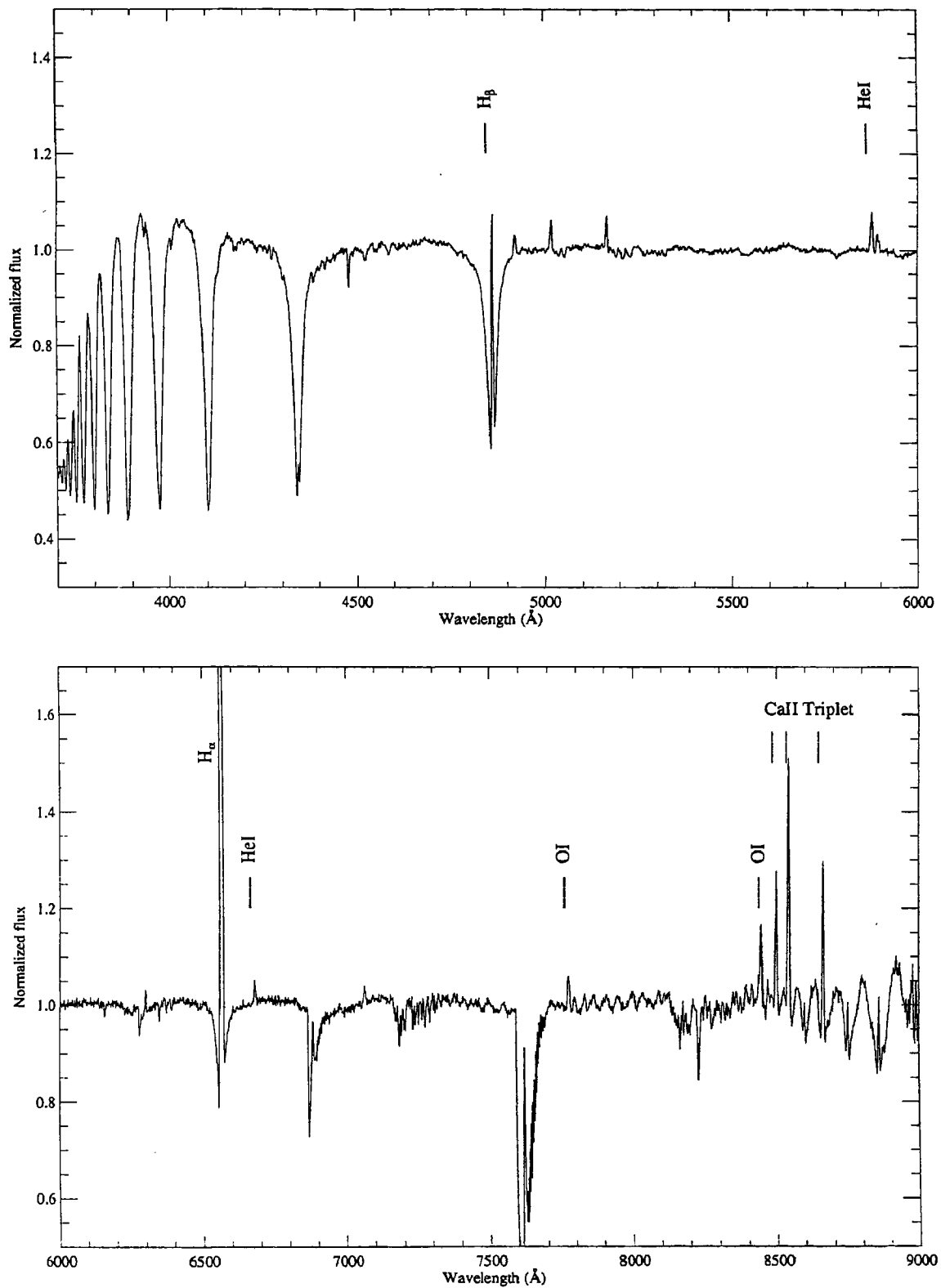


Figure 1.1: Optical spectra of Herbig Ae star AB Aur obtained with the Hanle Faint Object Spectrograph (HFOSC) on the 2 meter Himalayan Chandra Telescope at the Indian Astronomical Observatory, Hanle, India on 24th October 2003.

[OI] and [NII] are also found in the spectra of many of these young stars.

The origin of emission lines in T Tauri stars is currently understood in the framework of magnetospheric accretion model. In this model, the stellar magnetic field truncates the disk at some inner radius, and accretion continues onto the star by gas infall along magnetic field lines connecting the star to the disk near the truncation radius (Uchida & Shibata 1985; Koenigl 1991; Hartmann et al. 1994; Muzerolle et al. 1998). Observed characteristics of emission lines in T Tauri stars such as large line widths, blueward line asymmetries, and occasional inverse P Cygni profiles could be reproduced using magnetospheric accretion models where emission lines originate in the infall zone (Hartmann et al. 1994; Muzerolle et al. 1998, 2001). Such a model readily explains the optical and UV continuum excess emission and optical “veiling” seen in T Tauri stars as coming from the “accretion” shock formed when the infalling gas at free-fall velocities strikes the stellar photosphere (Bertout et al. 1988; Gullbring et al. 1998). The forbidden lines in T Tauri stars are found to be blue shifted with respect to the star in most cases. The widely accepted explanation is that an optically thick disk blocks the red shifted emission of the outflow close to the star. This has often been considered as an indirect evidence for the presence of optically thick disks around T Tauri stars, thereby supporting the contention that emission line activity in T Tauri stars is accretion driven.

However, in Herbig Ae/Be (HAeBe) stars the situation is less clear. Accretion disks as in the case of T Tauri stars has also been postulated for HAeBe stars (Lada & Adams 1992; Hillenbrand et al. 1992); but in the intermediate-mass young stars the UV/optical continuum excess and optical veiling which are used as the direct evidence for accretion is not observed unambiguously (Bohm & Catala 1993; Ghandour et al. 1994). Moreover, forbidden [OI] emission line profile is found to be more symmetric in HAeBe stars than in T Tauri stars, with strongly blue shifted profiles seen only in the most embedded objects (Böhm & Catala 1994; Corcoran & Ray 1997) suggesting the absence of optically thick obscuring disk. This has lead Böhm & Catala (1995) and Bouret & Catala (1998) to put forward the suggestion that the source of energy for the activity in HAeBe stars is linked to the star itself and that the emission line phenomenon could be explained as arising in a chromospheric wind, without

necessitating the presence of accretion disks. They have been able to reproduce the observed line profiles of $H\alpha$, MgII and CIV of HAeBe stars of P Cygni sub class based on their semi-empirical model of an expanding extended chromosphere, surrounded by a cool wind (Bouret & Catala 1998).

Nevertheless, accretion disks may still be present in HAeBe stars. The apparent absence of UV/optical continuum excess in HAeBe stars could be understood as a contrast effect because of the relatively high stellar luminosity of A and B type stars. Also, indications of far-UV excess in a number of HAeBe stars have been observed (e.g., Grady et al. 1993). From their study of the high resolution spectra of 30 HAeBe stars, Ghandour et al. (1994) have shown that while HAeBe stars show no evidence for excess optical continuum emission, they do show other spectroscopic signatures of disk accretion like inverse P Cygni profiles in $H\beta$ residual profiles and proportionality between forbidden line ([OI]) strengths and near-infrared excesses. Further, Corcoran & Ray (1998) have found that the line luminosities of forbidden [OI] and $H\alpha$ lines of HAeBe stars are correlated with the near-infrared excess in the same fashion as the T Tauri stars. All these evidence support the idea that HAeBe winds are accretion driven.

The prediction that the circumstellar disks are natural by products of star formation process has now been confirmed by a wealth of observational data, all of which provide compelling evidence for the presence of gas and dust disks around young stars (e.g., Beckwith & Sargent 1996; Mannings & Sargent 1997; Schneider et al. 1999; Millan-Gabet et al. 2001; Grady et al. 2001; Weinberger et al. 2002; Eisner et al. 2003). Direct images of disks surrounding young stars have provided information on the shape and structure of disks (e.g., McCaughrean & O'dell 1996). HST images of disk surface seen in scattered light show that the disks are "flared", i.e., the ratio H/R of scale height H of the disks over the distance R from the star is an increasing function of R . Flaring is expected for a gas-rich disk in hydrostatic equilibrium (Kenyon & Hartmann 1987). The flared shape seen in scattered light also indicates the presence of sub-micron sized grains which are well mixed with the gas at all vertical heights.

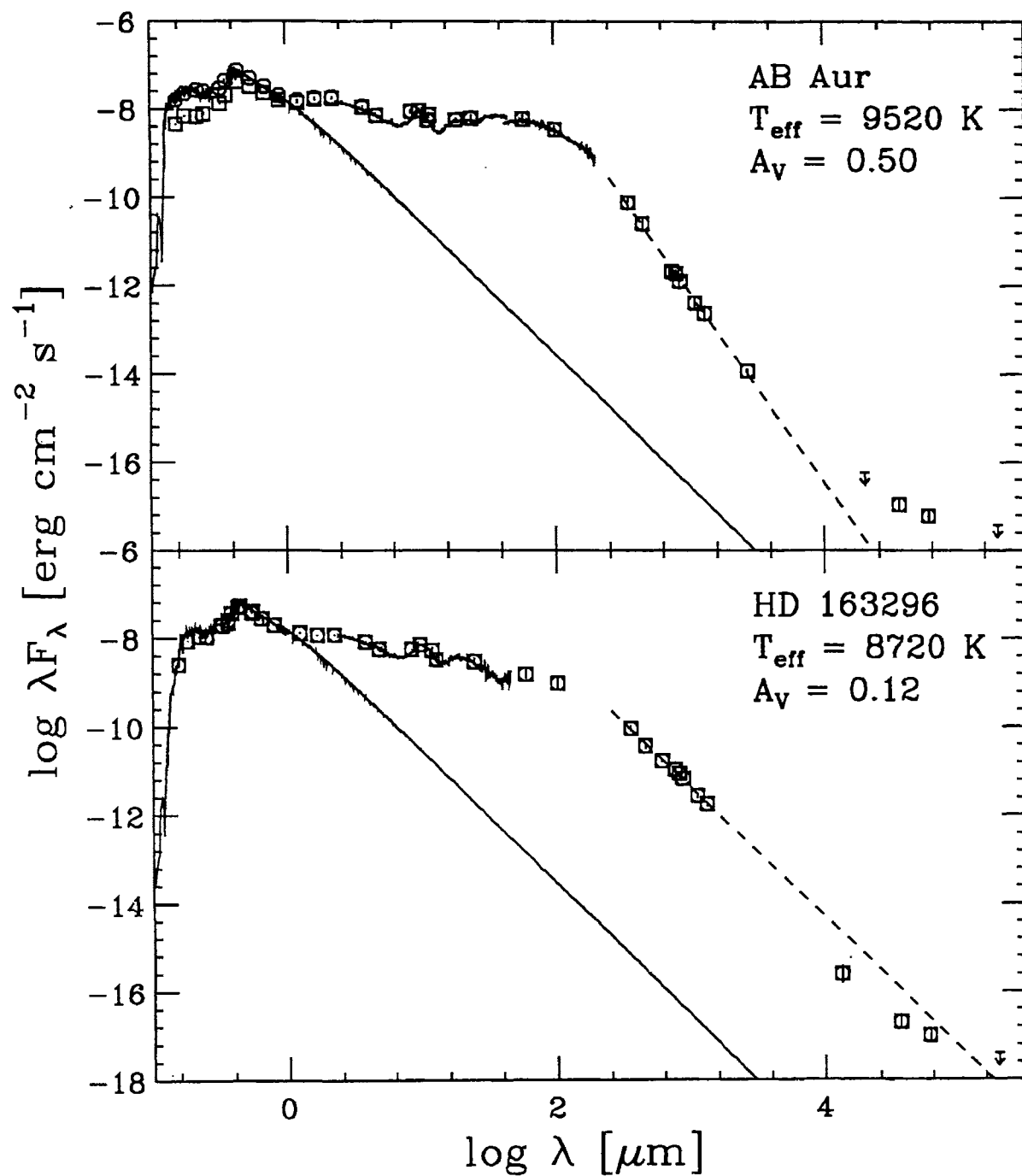


Figure 1.2: Spectral energy distributions of AB Aur (top) and HD 163296 (bottom). Open squares and circles indicate observed and extinction corrected fluxes from literature. The solid lines show Kurucz models for the stellar photospheres of AB Aur and HD 163296. The dashed lines show linear fits to the submm data points for comparison with the slope of the Rayleigh-Jeans tail of the Kurucz model (from van den Ancker et al. (2000)).

It has long been known that the pre-main sequence stars show excess emission above that expected from their photospheres at wavelengths longer than $2\mu m$. The earliest evidence for the presence of attendant circumstellar material around young stars came from the spectral energy distribution which showed significant excess emission at longer wavelengths. Spectral energy distributions of two Herbig Ae stars are shown in Figure 1.2 as an example where excess emission from infrared to mm wavelengths can be seen. Most of the excess emission in pre-main sequence stars from mid-infrared to millimeter wavelengths is due to the thermal emission from dust at a range of temperatures in the circumstellar disks. At near-infrared wavelengths the excess is from the hot gas and dust in the inner disk ($< 0.1 AU$). Disk heating responsible for the excess emission in pre-main sequence stars is caused by the dissipation of viscous energy due to accretion and radiant heating of the disk surface by the central stellar object. The shape of the disks affects its temperature profile and, therefore, its spectral energy distribution. Flared disks intercept a larger fraction of the stellar radiation at large radii than flat disks, so that their SED is flatter. (Kenyon & Hartmann 1987; Chiang & Goldreich 1997; Beckwith 1999). Most pre-main sequence stars have SEDs typical of flared disks (e.g., Chiang et al. 2001).

Observations at sub-mm and mm wavelengths where the dust emission from the disks are optically thin have been used to obtain the masses of the pre-main sequence disks. The dust mass in the disk is related to the continuum flux density at millimeter wavelength by the relation,

$$M_{dust} = D^2 \frac{F_\nu}{\kappa_\nu B_\nu(T_{dust})}$$

where D is the distance, F_ν the observed flux density, κ_ν the dust opacity at the observed wavelength and T_{dust} the dust temperature. From the dust masses obtained, disk masses are derived assuming a gas-to-dust ratio of 100 which is typical of the interstellar medium. The major uncertainty in the mass estimates is in κ_ν , which can vary substantially with changes in particle composition and to some extent with particle size and shape. A commonly adopted value is $\kappa_{1.3mm} = 0.5 - 1 cm^2 g^{-1}$ (e.g., Natta 2003). The disk masses derived this way are found to range from 0.003 to $0.3 M_\odot$. Figure 1.3 shows the distribution of disk masses derived from millimeter

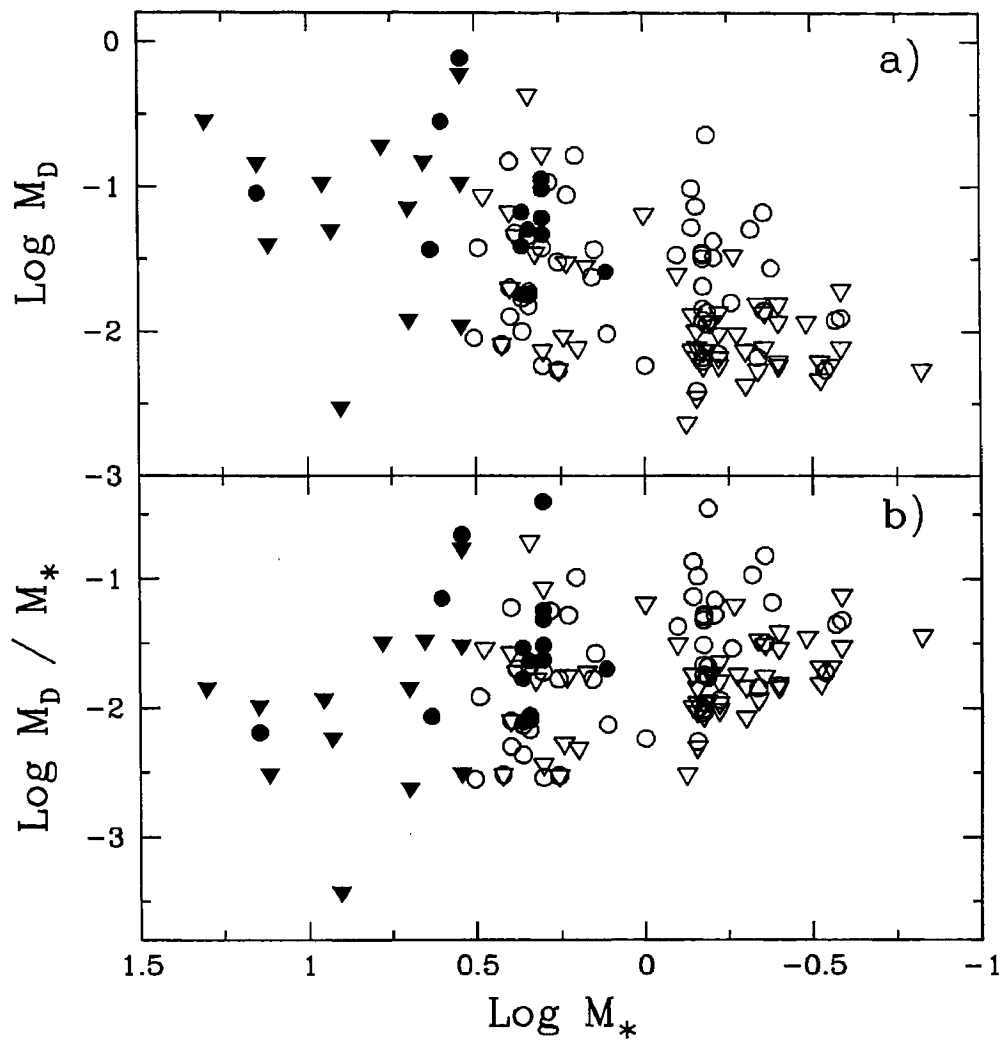


Figure 1.3: Top panel: disk masses in the units of solar masses (gas+dust, assuming a gas-to-dust mass ratio of 100) derived from millimeter fluxes are plotted as function of the stellar mass. Triangles are upper limits, dots detections; filled symbols are interferometer data, open symbols are single-dish measurements. The lower panel plots the ratio of the disk to the stellar mass. (*from Natta (2003)*).

observations as a function of stellar mass. It can be seen from the figure that there is a large spread in the disk masses even for stars of similar masses. Most stars in Figure 1.3 have disk masses greater than $0.01M_{\odot}$, which is the minimum mass required to create solar system-like planetary systems. There is enough mass in a typical disk to make a planetary system like our own.

1.3 Debris disks around main sequence stars

The existence of dusty disks around main sequence stars have been known for two decades now. Such dusty disks were discovered by Infrared Astronomical Satellite in 1983 when it detected large infrared excesses at wavelengths longward of 12μ from otherwise normal main sequence stars *Vega*, *β Pic*, *Fomalhaut* and *ϵ Eridani* (Aumann et al. 1984; Gillett 1986; Backman & Paresce 1993). The infrared excess is thought to be due to emission from circumstellar dust, in thermal equilibrium with the stellar radiation from the central star, distributed in a shell or disk, several tens to hundred AU in extent. The orbiting dust grains are at temperatures of about 50-150K (Backman & Paresce 1993). Since then, a large number of main-sequence stars have been found to have similar infrared excesses in the IRAS wavebands and are called Vega-like stars (see e.g. Backman & Paresce 1993; Vidal-Madjar & Ferlet 1994; Lagrange-Henri 1995; Mannings & Barlow 1998; Lagrange et al. 2000; Silverstone 2000; Song 2000). About 15% of nearby main sequence field stars of types A-K are found to harbour such dusty disks (Lagrange et al. 2000).

The ‘Vega-like’ disks are optically thin and gas poor ($M_{gas} \ll 10 M_{dust}$) where the dust dynamics are not controlled by gas (Lagrange et al. 2000). Fractional dust luminosities $f_d \equiv L_{dust}/L_{\star}$, where L_{dust} is the luminosity of thermal emission from dust in the far infrared and L_{\star} is the stellar bolometric luminosity, of these stars have been found to range from 10^{-6} to 10^{-2} . The dust grains found around these main sequence stars are argued to be of ‘second generation’ because of the old ages of the stars compared to the grain destruction time scales. Grain removal processes acting in such disks like radiation pressure ‘blow out’ from the central star, Poynting-Robertson drag and collisional destruction have typical timescales of 10^5 to 10^6 yr,

whereas most of the Vega-like stars have ages of a few $100Myr$ or more. Dust that we observe around these stars is continuously being replenished by collisions between planetesimals and comets that are themselves stirred by gravitational interactions with larger bodies. The presence of second generation dust around a star indicates the existence not only of planetesimals but also of larger masses capable of sending small bodies into fragmenting collisions and star-grazing orbits. It has been suggested that planet formation is well underway in Vega-like systems and that the dust debris that we detect around them are the signposts of recent planet formation (Kenyon & Bromley 2002).

1.4 Evolution of circumstellar disks

It is clear from the preceding discussion that the circumstellar disks surrounding young stellar objects are analogous in their bulk properties like size and mass to protosolar nebula and that planetary systems can form out of such disks. However, whether all such disks form planets depends on the details of the disk evolution. For instance, if disks are dissipated on much shorter timescale than what it takes to build planets predicted by planet formation theories then most of these disks will not end up as planetary systems. On the contrary, if disks survive much longer than typical planet formation timescale then planetary systems may be as common as disks around stars. A detailed knowledge of various factors affecting the disks evolution and dissipation timescales is necessary to understand the incidence and frequency of planet formation in such disks. Following the evolution of the circumstellar disks from the early pre-main sequence phase to late main sequence phase is a necessary pre-requisite for such an understanding.

As the pre-main sequence star evolves, the disk surrounding it ages and eventually gets dissipated due to planet formation process and other dispersal mechanisms. A variety of processes can cause the dispersal of the young circumstellar disks. Processes which are intrinsic to the disk which cause the depletion of material in it are the viscous accretion of the dusty and gaseous material from the disk onto the central star and the growth of sub-micron sized grains to rocky planetesimals which brings

down the disk opacity. The interaction of the disk with the ultraviolet radiation and mechanical wind from the central star can also cause disk dispersal. The immediate environment of the star is known to affect disk dissipation. For example, a nearby massive star can evaporate the disks or destroy it by tidal interactions. Stellar encounters in a crowded cluster environment and dynamical interactions with disk and possible companion stars can also cause disk disruption.

After the collapse of the cloud core and the initial infall and accretion is over, the young star plus disk system emerges out of the cloud core as an optically visible pre-main sequence star. Material from the disk is still getting accreted onto the central star at this phase. Observational diagnostics of this accretion include presence of emission lines in the spectra and excess emission at near-infrared wavelengths from the inner disk. During the pre-main sequence evolution the accretion rate is expected to gradually come down. This decay in accretion rate can be followed using the observational tracers of accretion activity like emission lines and near-infrared excess. A study of the temporal evolution of emission line activity and the strength of near-infrared excess in pre-main sequence stars should help us constrain the timescales for the cessation of accretion and inner disk dissipation.

At some stage accretion onto the central star is terminated and the emission line activity stops. How soon the entire disk gets dissipated is not clear at the moment. However, there is evidence for inner disk dissipation occurring in a timescale as short as ~ 5 Myr or less. Planet building is believed to take place during this phase. According to the planet formation theories grain growth in the disk mid-plane would have already taken place in such systems. There is evidence for the growth of grains in young disks to sizes larger than that of the interstellar dust (Gorti & Bhatt 1993; Thé 1994; Beckwith et al. 2000; Calvet et al. 2002; Natta 2003). The depletion of smaller grains in the disk is expected to bring down the optical thickness of the disks because of the reduction in the surface area of the dust offered to stellar radiation. Thus during the pre-main sequence evolution the optically thick disk gradually evolves into an optically thin disk. Young stars in this 'transition phase' showing no emission lines, and relatively low near-infrared excess due to the disruption of inner disks are important for the study of disk evolution. Transition from optically thick disks to

thin disks is believed to take place sometime during this phase. However, very few such stars are known currently. Based on this perceived lack of ‘transition objects’, it has been argued that the timescale for the process of evolution from optically thick to thin disks is probably $\lesssim 10^6$ yr (e.g., Skrutskie et al. 1990; Wolk & Walter 1996; Nordh et al. 1996). Identifying young stars in the transitional stage of evolution and studying the circumstellar environment around such stars is critical to our overall understanding of disk evolution and planet formation.

The planet formation process which has already begun in the ‘primordial’ disks gradually dissipates the disks. The multi-stage accumulation process involving dust settling and sticking and then the runaway accretion of solids which leads to the formation of large planetesimals and proto-planetary bodies render the disk optically thin. The large ($\sim 100M_{\oplus}$) rocky cores can accrete gas from the disk to form giant planets. Gravitational interactions of these large planets can stir the planetesimals in the disk and send them into highly eccentric orbits. Collisions between these planetesimals can produce the so called ‘second generation’ dust in the disk. These grains which are warmed by the central starlight, emit thermally at far-infrared wavelengths. Such optically thin ‘debris disks’ have been observed around several nearby main sequence stars, some of which are as old as ~ 1 Gyr.

The dust grains in the debris disks are being continuously removed from the system by mechanisms such as radiation pressure ‘blow-out’, Poynting-Robertson drag and collisional destruction, the timescales of which in typical Vega-like systems are $< 10^6$ yr. The very existence of debris disks then suggest that the grains will have to be continuously replenished from the ‘collisional cascade’ of planetesimals or from comets over the lifetimes of the stars. One would expect the amount of dust in Vega-like systems to go down with the age as the larger bodies which replenishes the disk are also getting depleted as the planetary system evolves. A study of the evolution of debris disks can thus give us insight into the dynamical evolution of the system towards the end stages of the planet formation process.

1.5 Outline of the Thesis

This thesis aims to study some aspects of the evolution of circumstellar disks around intermediate-mass ($2 \leq M/M_{\odot} \leq 8$) young stars. We follow the evolution of the disks from the early pre-main sequence phase of the star to well into the main sequence phase, during which a variety of physical processes modify the disk evolution.

In Chapter 2, we study the evolution of emission line activity in the pre-main sequence Herbig Ae/Be stars. We estimate the ages of these stars by placing them on the HR diagram and comparing with the theoretical pre-main sequence evolutionary tracks. Temporal evolution of the emission line strength is then discussed. We also study the evolution of the near-infrared excess emission shown by Herbig Ae/Be stars.

Young intermediate-mass stars with disks in which accretion has terminated and the inner disks have begun to dissipate are discussed in Chapter 3. Emission lines are not present in these stars. Near-infrared excess emission is seen at low levels. The transition from optically thick disks to optically thin disks is believed to take place during this stage of evolution. We identify a few such ‘transition objects’ and study the properties of circumstellar environment around them in this Chapter.

Chapter 4 discusses the polarization properties of main sequence stars with debris disks. These are the Vega-like stars. Optical polarization measurements of Vega-like stars made at the Vainu Bappu Observatory, Kavalur, India are presented. We also compile polarization data on additional Vega-like stars from the literature. The polarization properties of Vega-like stars are then compared with that of the normal field stars. We also study the correlation between thermal emission from the debris disks and polarization.

The temporal evolution of the dust disks around main sequence stars is investigated in Chapter 5. Using velocity dispersion as an age indicator, we constrain the ages of main sequence stars with debris disks. Evolution of the fractional dust luminosity of main sequence dust disks with age is discussed.

Finally, in Chapter 6, we study the disk frequency and lifetimes in nearby OB associations. We look for evidence for the presence of disks around the known members

of 12 OB associations whose ages are in the range of 5 to 50 Myr. We then estimate the disk fractions in these associations and study its behaviour as a function of the mean age of the association.

The strength of circumstellar activity as measured by $H\alpha$ emission line equivalent widths, near and far-infrared excesses and polarization is found to generally decline with age, initially rapidly on a timescale of $\lesssim 3$ Myr, in the pre-main sequence phase and the second generation debris disks survive as long as $\sim 10^9$ yr in the main sequence phase. Chapter 7 of the thesis summarizes the results obtained in this investigation.

Chapter 2

Evolution of emission line activity in Herbig Ae/Be Stars

2.1 Introduction

Herbig Ae/Be stars are pre-main sequence objects of intermediate mass ($2 \leq M/M_{\odot} \leq 8$). These stars were first discussed as a group by Herbig (1960), who identified “Be and Ae stars associated with nebulosity” based on the following membership criteria: (1) spectral type earlier than F0, (2) presence of emission lines, (3) located in an obscured region and (4) illuminating a fairly bright nebulosity in its immediate vicinity. Herbig (1960) listed 26 objects belonging to this class. The original list was further extended by Finkenzeller & Mundt (1984) and Herbig & Bell (1988). Recent catalog by Thé et al. (1994), adopting a more extended definition, lists 109 Herbig Ae/Be (hereafter HAeBe) stars and a number of candidates that include stars with later spectral types (G0 or earlier) and those found relatively isolated from star forming clouds. The authors proposed the presence of near or far-infrared excess as a necessary criterion for the membership of the HAeBe group while relaxing some of Herbig’s original membership criteria. Recently, Vieira et al. (2003) have presented a new catalog of 108 HAeBe stars identified in the Pico dos Dias Survey (PDS).

The pre-main sequence nature of HAeBe stars is now well established, based on their positions in the Hertzsprung-Russell (HR) diagram and comparison with theoretical evolutionary tracks (Strom et al. 1972; Cohen & Kuhi 1979; van den Ancker et al. 1998; Palla & Stahler 1993). Also, the upper envelope of the distribution of HAeBe stars in the HR diagram is found to match well with the theoretical birthline derived by Palla & Stahler (1993) for an accretion rate \dot{M}_{acc} of $10^{-5} M_{\odot} yr^{-1}$. The birthline is the locus along which young objects first appear as optically visible stars (Stahler 1983; Palla 1999). The pre-main sequence evolution starts at the birthline and ends at the zero-age main sequence. During the pre-main sequence evolution HAeBe stars of different masses contract quasi-statically along the respective radiative tracks in the HR diagram towards the main sequence.

HAeBe stars are associated with rich and diverse circumstellar environment. Infra-red, sub-millimeter and millimeter measurements have shown that HAeBe stars are associated with significant amounts of circumstellar dust emitting excess radiation, over that produced by stellar photosphere, at these wavelengths (e.g., Cohen & Kuhi 1979; Hillenbrand et al. 1992; Mannings & Sargent 1997; Malfait et al. 1998; Waters & Waelkens 1998; Henning et al. 1998; Mannings & Sargent 2000; Natta et al. 2000). The existence of circumstellar dust is also supported by the relatively large values of intrinsic polarization observed for these objects (e.g., Breger 1974; Garrison & Anderson 1978; Vrba et al. 1979; Jain et al. 1990; Jain & Bhatt 1995; Yudin & Evans 1998; Yudin 2000) which is generally ascribed to the presence of circumstellar dust grains (e.g., Bastien 1987). Also, from interferometric observations of molecular emission lines presence of cold gas around HAeBe stars has been inferred (Mannings & Sargent 1997; Mannings et al. 1997).

While the existence of circumstellar gas and dust around HAeBe stars is well established, the geometrical distribution of the circumstellar material is not yet fully clear. Based on the similarity of the spectral energy distribution (SED) of HAeBe stars to those of T Tauri stars, Hillenbrand et al. (1992) proposed the presence of geometrically thin, optically thick accretion disks around HAeBe stars. Several teams of authors, on the other hand, have tried to explain the SEDs of HAeBe stars with models of spherically symmetric envelopes of various optical depths and density pro-

files (Berrilli et al. 1992; Miroschnichenko et al. 1997; Pezzuto et al. 1997). Natta et al. (1993) proposed that both disks and envelopes contribute to the observed SEDs with the disk emission dominating in the near and mid-infrared and the envelope emission in the far-infrared. Recently, Meeus et al. (2001) and Natta et al. (2001) have been able to model the infrared and millimeter emission from HAeBe stars as arising from a passive reprocessing disk. The detection of compact emission on scales of 1-2 arcsec from millimeter interferometric observations (Natta et al. 2000; Mannings & Sargent 1997, 2000; Piétu et al. 2003; Eisner et al. 2003) suggests strongly that the emitting dust is in a disk rather than in a spherical envelope, as spherical distribution implies extinctions at visible and infrared wavelengths much higher than actually observed. Thus most evidence support the hypothesis that gas and dust around HAeBe stars lie in a massive ($\sim 0.01 M_{\odot}$) circumstellar disk (Natta et al. 2000).

One of the prominent observational features of HAeBe stellar group and that which distinguishes these stars from the normal main sequence stars is, by definition, the presence of emission lines in the spectra. Apart from the $H\alpha$ line which is almost always in emission, the other emission lines that are often observed in the optical spectra of HAeBe stars are HeI ($\lambda 5876\text{\AA}$ & $\lambda 6678\text{\AA}$), OI ($\lambda 7774\text{\AA}$ & $\lambda 8446\text{\AA}$) and CaII triplet ($\lambda\lambda 8498, 8542, 8662\text{\AA}$) (Herbig 1960; Cohen & Kuhl 1979; Finkenzeller & Mundt 1984; Hamann & Persson 1992; Böhm & Catala 1995). Forbidden emission lines such as [OI] ($\lambda 6300$ and $\lambda 6364$) are seen in some of the HAeBe stars (Herbig 1960; Cohen & Kuhl 1979; Hamann 1994; Böhm & Catala 1994; Böhm & Hirth 1997; Corcoran & Ray 1998; Vieira et al. 2003). Most of the emission lines seen in the spectra of HAeBe stars are thought to be arising in a stellar wind or from the surface layers of circumstellar disks as is the case for forbidden lines. However, what drives such winds in HAeBe stars has been a matter of long debate. On the one hand it has been argued, in analogy with T Tauri stars, that it is the accretion of matter from the disk onto the central star that is responsible for the emission line activity in HAeBe stars (Hamann & Persson 1992). Strength of $H\alpha$ line has often been taken as a measure of accretion rate in this scenario (Hillenbrand et al. 1992). Using the luminosity of [OI] $\lambda 6300$ emission line as an indirect measure of mass loss \dot{M}_{wind} and the IR excess luminosity over 0.7-10.2 μm as a measure of accretion \dot{M}_{acc} , Corcoran &

Ray (1998) find a strong correlation between accretion and mass loss suggesting that accretion drives the winds in HAeBe stars. These models postulate an external origin for the winds and emission line activity in HAeBe stars, invoking an accretion disk (Grinin & Rostopchina 1996). On the other hand Catala & Kunasz (1987), Catala (1988) and Bouret & Catala (1998) have been able to reproduce observed $H\alpha$ line and $MgII$ & CIV resonance lines in terms of a chromospheric-wind model. From an analysis of activity tracers like $H\alpha$, CaII IR triplet and HeI 5876Å line, Böhm & Catala (1995) have found that with models of chromospheres and winds they could explain emission line phenomena in HAeBe stars without necessitating the presence of accretion disks. They further suggest that the ultimate source of energy for the activity is linked to the star itself, rather than to a circumstellar environment.

In the emission line activity and the infrared and sub-mm excesses observed, HAeBe stars display considerable variety and range. Not all emission lines discussed above are seen in all the stars. For instance, OI and CaII triplet lines are present in emission in some stars while they are found in absorption in others (Hamann & Persson 1992). $H\alpha$ line is found in varying intensity in HAeBe stars (e.g., Finkenzeller & Mundt 1984; Herbig & Bell 1988; Corcoran & Ray 1998). The infrared and sub-mm excesses in HAeBe stars also show a large range of values (Hillenbrand et al. 1992; Corcoran & Ray 1998). The disk masses derived from millimeter interferometric measurements of HAeBe stars are found to range by two orders of magnitude (Natta et al. 2000). Vieira et al. (2003) have noted that very few stars of HAeBe stellar group satisfy all the defining criteria. These differences in the observational properties of HAeBe stars could be due to several factors. It could depend on the environment of site of formation of HAeBe stars. Different geometry for the distribution of circumstellar matter and inhomogeneity in the circumstellar environment can also provide such a variety. Hillenbrand et al. (1992), have suggested, within the frame work of optically thick accreting disks, that the large range seen in the infrared excess and $H\alpha$ emission line intensity is due to different and variable accretion rates.

Although there are other factors which influence the observed properties of HAeBe stars, evolution of the central star and the circumstellar matter around it could be of critical importance. There have been suggestions in the literature of evolution

among the HAeBe group (van den Ancker et al. 1997; Natta et al. 2000; Vieira et al. 2003). Hillenbrand et al. (1992) have noted that the HAeBe stars belonging to the three groups that they constructed based on the spectral energy distribution have different evolutionary status. Malfait et al. (1998), based on the circumstellar energy distribution, have suggested that HAeBe stars span a large range of evolutionary stages. Such an evolutionary sequence has also been found by van den Ancker et al. (1997). Moreover, the locations of HAeBe stars in the HR Diagram (see Figure 2.1) show quite a large spread. There are stars which are right on the birthline and stars which are very close to the main sequence. Other HAeBe stars occupy positions in between these two extremes. Thus it is fairly certain that HAeBe stars are in different stages of their pre-main sequence evolution and that an evolutionary trend could be expected in the observational properties of these stars.

In this chapter we study the temporal evolution of emission line activity in HAeBe stars. We estimate the ages of about 60 HAeBe stars by placing them in the HR diagram and comparing with the theoretical pre-main sequence evolutionary tracks. We have made optical spectroscopic observations of 33 HAeBe stars from our sample to measure the $H\alpha$ equivalent width. We have also compiled $H\alpha$ equivalent width information of our sample stars available from the literature. Using the strength of $H\alpha$ line as a measure we examine the evolution of emission line activity in HAeBe stars and look for any possible evolutionary trend. We also study the behaviour of near-infrared excess with ages of these stars. In section 2.2 we describe our sample and discuss the age determination of HAeBe stars. Our observations and analysis of data is discussed in section 2.3. In section 2.4 and section 2.5 we present the data and discuss the evolution of emission line activity and near infra-red excess. Results of this study and its relevance and implications are discussed in section 2.6. A summary of the chapter is provided in section 2.7.

2.2 The Sample

In order to study the the evolution of emission line activity and near-infrared excess, we compiled a sample of HAeBe stars which can be placed in the HR diagram and

for which the ages could be determined using the pre-main sequence evolutionary tracks. There have been a number of attempts to estimate ages of HAeBe stars and such studies give the effective temperatures T_{eff} and bolometric luminosity L_* of these stars (e.g., Hillenbrand et al. 1992; van den Ancker et al. 1998; Testi et al. 1998; Natta et al. 2000). We have compiled T_{eff} and L_* for several HAeBe stars from literature and estimate the ages of these stars from the pre-main sequence evolutionary tracks of Palla & Stahler (1993). Effective temperatures and bolometric luminosities taken from the literature and ages estimated using evolutionary tracks for 45 HAeBe stars are given in Table 2.1 where object name is listed in column 1, spectral type in column 2, visual extinction in column 4 and T_{eff} and L_* in columns 6 and 7 respectively. The references for spectral type and A_V are listed in columns 3 and 5 and in column 8 references for T_{eff} and L_* is listed. Estimated ages and stellar masses are listed in columns 9 and 10 respectively.

For those HAeBe stars for which T_{eff} and L_* are not found in the literature we have computed these astrophysical parameters using distances to these stars given in literature. We list 14 such stars in Table 2.2, together with ages determined from evolutionary tracks. Column 1 of Table 2.2 lists object name and column 2 & 3 the spectral type and the reference. Distances to these stars and extinction are given in columns 4 & 5 and the references to these in column 6. The computed values of T_{eff} and L_* and the estimated age and stellar mass are listed in columns 7 - 10.

In Figure 2.1 we present the HR diagram for the 59 HAeBe stars of Table 2.1 and Table 2.2. Also plotted are the theoretical evolutionary tracks (Palla & Stahler 1993) for different masses. It can be seen from Figure 2.1 that a few stars fall above the birthline. We have ascribed an upper limit age of < 0.1 Myr for these stars. There are also a few stars which are below the main sequence in Figure 2.1. We have assumed those stars to be on the main sequence in determining the age. Altogether, our sample consists of 59 HAeBe stars with estimated ages which are listed in Table 2.1 and Table 2.2.

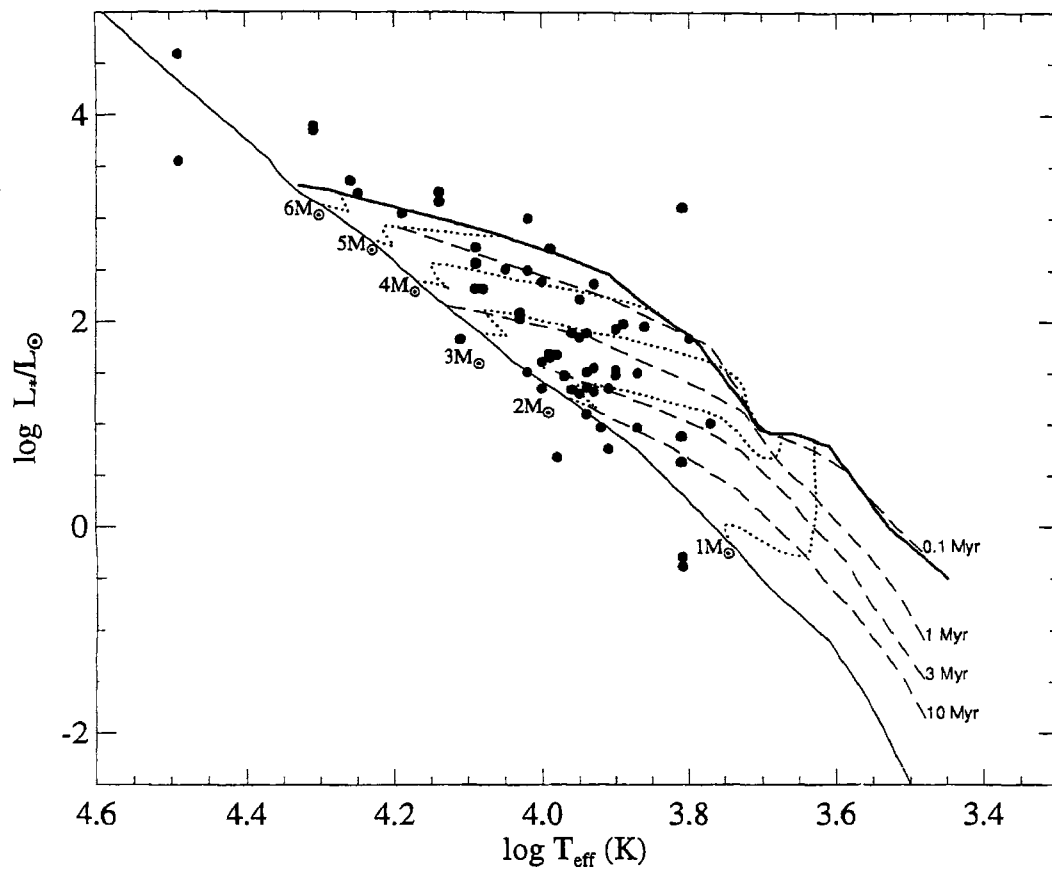


Figure 2.1: The HR diagram for Herbig Ae/Be stars. The pre-main sequence evolutionary tracks for different masses (dotted lines) and isochrones for different ages (dashed lines) are from Palla & Stahler (1993). The thick solid line represents the birthline for an accretion rate \dot{M}_{acc} of $10^{-5} M_\odot \text{ yr}^{-1}$.

Table 2.1: Ages of Herbig Ae/Be stars

Object	Sp. Type	ref	A_V mag	ref	$\log T_{eff}$	$\log L_*/L_\odot$	ref	Age (Myr)	M_* (M_\odot)
MWC 1080	B0	2	5.30	2	4.49	4.59	2	< 0.1	–
BD+40 4124	B2	2	3.00	2	4.31	3.85	2	< 0.1	–
HD 200775	B2.5IVe	1	1.92	1	4.31	3.89	1	< 0.1	–
HD 259431	B5	3	1.61	3	4.14	3.16	3	< 0.1	–
LkHa 234	B3	2	3.40	2	4.25	3.24	2	< 0.1	–
V1686 Cyg	B5	2	4.80	2	4.14	3.25	2	< 0.1	–
BD+46 3471	A0	6	1.00	1	3.99	2.71	6	0.1	4.5
RR Tau	A4	3	1.10	2	3.93	2.37	3	0.1	4.2
LkHa 215	B5	2	2.10	2	4.09	2.72	2	0.1	4.8
V376 Cas	B5	5	2.90	2	4.19	3.05	5	0.1	5.0
HD 142527	F7IIIe	1	1.49	1	3.80	1.84	1	0.2	3.5
HD 179218	B9e	1	1.27	1	4.02	2.50	1	0.2	4.3
51 Oph	B9.5Vne	1	0.15	1	4.00	2.39	1	0.3	4.0
BD+61 154	B8	3	2.10	2	4.05	2.51	3	0.3	4.0
LkHa 25	B7	3	0.60	2	4.09	2.56	3	0.4	4.0
LkHa 198	B8	5	2.50	2	4.08	2.32	5	0.5	3.5
HD 250550	B7	3	0.71	3	4.09	2.32	3	0.7	3.5
UX Ori	A2	3	0.37	3	3.96	1.89	3	1.0	3.0
LkHa 208	A3	3	1.70	2	3.94	1.89	3	1.0	3.0
T Ori	A3	3	1.70	2	3.94	1.89	3	1.0	3.0
HR 5999	A5-7III/IV	1	0.47	1	3.90	1.93	1	1.0	3.2
LkHa 218	B9	2	1.50	2	4.03	2.09	2	1.2	3.0
V380 Ori	B9	3	1.70	2	4.03	2.07	3	1.2	3.0
VV Ser	B9	2	3.00	2	4.03	2.03	2	1.2	3.0
XY Per	A2II+B6e	1	2.26	1	4.11	1.83	3	2.0	3.0

continued on next page

continued from previous page

Object	Sp. Type	ref	A_V mag	ref	$\log T_{eff}$	$\log L_*/L_\odot$	ref	Age (Myr)	M_* (M_\odot)
AB Aur	A0Ve+sh	1	0.50	1	3.98	1.68	1	2.5	2.4
HD 97048	B9-A0ep+sh	1	1.24	1	4.00	1.61	1	3.0	2.5
BF Ori	A7	3	0.26	3	3.90	1.53	3	3.0	2.3
NX Pup	A0	2	1.50	2	3.99	1.65	2	3.0	2.4
HD 104237	A4IVe+sh	1	0.31	1	3.93	1.55	1	3.4	2.3
LkHa 233	A5	2	2.60	2	3.90	1.48	2	3.8	2.2
HD 31648	A3ep+sh	1	0.25	1	3.94	1.51	1	4.0	2.2
HD 150193	A1Ve	1	1.61	1	3.97	1.47	1	5.0	2.3
HD 163296	A1Ve	1	0.25	1	3.97	1.48	1	5.0	2.3
HD 36112	A5IVe	1	0.22	1	3.91	1.35	1	5.0	2.0
IP Per	A3	3	1.01	3	3.94	1.36	3	5.2	2.0
HD 245185	A2	3	0.10	2	3.96	1.34	3	5.5	2.0
HD 100546	B9Vne	1	0.28	1	4.02	1.51	1	6.0	2.3
HD 34282	A0e	1	0.59	1	3.98	0.68	1	6.3	2.1
HD 141569	B9.5e	1	0.47	1	4.00	1.35	1	7.0	2.2
Ty CrA	A5	2	1.00	2	3.92	0.97	2	10.0	1.8
KK Oph	A6	2	1.60	2	3.91	0.76	2	> 10.0	1.7
AK Sco	F5+F5IVe	1	0.62	1	3.81	0.88	1	10.3	1.5
HD 35187	A7+A2e	4	0.43	4	3.94	1.10	4	12.0	1.8
T CrA	F5	2	2.10	2	3.81	-0.29	2	> 13.0	1.3

References:

1. van den Ancker et al. (1998); 2. Hillenbrand et al. (1992); 3. Testi et al. (1998)
4. Dunkin & Crawford (1998); 5. Natta et al. (2000); 6. Fuente et al. (2002)

Table 2.2: Ages of Herbig Ae/Be stars

Object	Sp. Type	ref	distance (pc)	A_V mag	ref	$\log T_{eff}$	$\log L_*/L_\odot$	Age (Myr)	M_* (M_\odot)
HD 98922	B9Ve	1	540	0.34	1	4.02	3.00	< 0.1	–
Z CMa	F6IIIe	1	1150	2.42	1	3.81	3.11	< 0.1	–
V361 Cep	B3ne	1	1250	1.89	1	4.26	3.36	< 0.1	–
HD 35929	F0IIIe	1	360	0.40	1	3.86	1.96	0.2	3.5
HD 37806	A2Vpe	1	500	0.03	1	3.95	2.22	0.3	3.8
HD 85567	B7-8Ve	1	480	0.81	1	4.09	2.57	0.4	4.0
V351 Ori	A7IIIe	1	500	0.50	1	3.89	1.98	0.5	3.3
V1295 Aql	A2IVe	1	290	0.19	1	3.95	1.85	1.5	2.8
HD 38120	A0	4	420	0.14	4	3.99	1.69	2.5	2.5
HD 144432	A9IVe	3	200	0.56	1	3.87	1.50	3.0	2.3
HK Ori	G1Ve	3	460	1.20	2	3.77	1.01	3.8	2.0
V346 Ori	A2IV	3	400	0.43	1	3.95	1.30	7.6	2.0
CO Ori	F7Ve	3	120	1.83	1	3.81	0.63	> 10.0	1.3
HD 100453	A9V	4	111	0.14	4	3.87	0.97	> 10.0	1.7

References:

1. van den Ancker et al. (1998); 2. Hillenbrand et al. (1992); 3. Mora et al. (2001)
4. Hipparcos

2.3 Observations and Analysis

Optical CCD spectra were obtained with resolution ($\lambda/\Delta\lambda$) ranging from 1000 – 3000 for 33 stars in our sample with the Optomechanics Research (OMR) spectrograph on the 2.34 meter Vainu Bappu Telescope (VBT) at the Vainu Bappu Observatory, Kavalur, India and with the Hanle Faint Object Spectrograph (HFOSC) on the 2 meter Himalayan Chandra Telescope at the Indian Astronomical Observatory, Hanle, India. Log of spectroscopic observations is given in the Appendix A.

All spectra were bias subtracted, flat-field corrected, extracted and wavelength calibrated in the standard manner using the IRAF¹ reduction package. The spectra which are normalized to the continuum are presented in the Appendix A.

2.4 Evolution of $H\alpha$ equivalent width with age

The most prominent emission feature in HAeBe stars is the $H\alpha$ line. It is found in varying intensity in HAeBe stars. In this Section we study the temporal evolution of $H\alpha$ emission strength in HAeBe stars. To this end, we measured the equivalent widths of the emission component of the $H\alpha$ line in HAeBe stars for which we have spectra. The observed equivalent widths are tabulated in Table 2.3. We have also compiled equivalent widths of $H\alpha$ for HAeBe stars available from the literature. These are also presented in Table 2.3. Table 2.3 contains $H\alpha$ equivalent widths for 51 HAeBe stars obtained from our observations and compiled from the literature.

Table 2.3: $H\alpha$ equivalent widths of Herbig Ae/Be stars

Object	$H\alpha$ equivalent width [†] (Å)			Object	$H\alpha$ equivalent width (Å)		
	This work	hb88	cr98		This work	hb88	cr98
MWC 1080	...	-75.0	-94.2	V380 Ori	...	-81.0	-71.0
BD+40 4124	-120.0	-94.0	-31.8	LkHa 218	...	-22.0	-31.9
HD 200775	-61.0	-35.0	-17.7	VV Ser	-50.0	-22.0	-31.8
HD 259431	-62.0	-55.0	-52.9	V1295 Aql	-29.3
LkHa 234	...	-44.0	-52.1	XY Per	-6.5
HD 98922	-27.0	HD 38120	-24.0
Z CMa	-106.0	-10.0	-24.8	AB Aur	-44.0	-27.0	-26.3
V361 Cep	...	-36.0	...	NX Pup	-44.0	...	-44.2
BD+46 3471	-21.1	-20.0	...	HD 97048	...	-30.0	-51.1
RR Tau	...	-33.0	...	HD 144432	-4.3

continued on next page

¹IRAF is distributed by National Optical Astronomy Observatories, USA.

continued from previous page							
Object	$H\alpha$ equivalent width			Object	$H\alpha$ equivalent width		
	This work	hb88	cr98		This work	hb88	cr98
LkHa 215	...	-25.0	-26.7	BF Ori	...	-10.0	-3.7
V376 Cas	...	-37.0	-33.4	LkHa 233	...	-18.0	...
HD 142527	-10.0	HK Ori	...	-56.0	-63.1
HD 179218	-13.0	HD 31648	-23.0
HD 35929	-2.4	HD 150193	-11.1	...	-7.8
51 Oph	-1.6	HD 36112	-14.3
BD+61 154	-68.0	-78.0	-44.1	HD 163296	-13.7	...	-22.5
HD 37806	-25.4	IP Per	-16.6
LkHa 25	...	-47.0	-58.2	HD 34282	-4.0
HD 85567	-41.0	HD 141569	-4.0
LkHa 198	...	-85.0	-40.5	CO Ori	...	-10.0	...
HD 250550	...	-40.0	...	KK Oph	-57.0	-22.0	-44.9
T Ori	...	-16.0	...	HD 100453	-1.0
LkHa 208	...	-8.0	...	AK Sco	-4.3
UX Ori	-5.1	-20.0	...	HD 35187	-5.1
HR 5999	-5.7	-7.0	...				

† negative values of $W(H\alpha)$ indicates $H\alpha$ in emission

References:

hb88: Herbig & Bell (1988); cr98: Corcoran & Ray (1998)

We plot equivalent widths of $H\alpha$ emission line $W(H\alpha)$ of HAeBe stars against the stellar ages to look for possible evolutionary trend. Whenever more than one measurement of $W(H\alpha)$ are available we have plotted the mean value of those measurements. The plot of $W(H\alpha)$ against ages is presented in Figure 2.2. The error bars plotted for $W(H\alpha)$ represent the dispersion in different measurements and are a measure of variability of $H\alpha$ emission strength. It is seen from Figure 2.2 that there is an overall decrease in $W(H\alpha)$ with age though at small ages there is a large spread in the $H\alpha$ equivalent widths. Out of 11 stars with ages ≥ 5 Myr, only one has

$W(H\alpha) > 20$ in Figure 2.2. Thus, while young HAeBe stars show both very strong ($W(H\alpha) > 80\text{\AA}$ e.g., MWC 1080 & BD+40 4124) and weak ($W(H\alpha) < 5\text{\AA}$ e.g., 51 Oph & HD 35929) emission and an entire range between these two extremes, older stars systematically show low emission line activity ($W(H\alpha) < 20\text{\AA}$). The dashed line shown in the figure acts as an upper envelope to the distribution of $W(H\alpha)$ with age of HAeBe stars. It is of the functional form $W = W(0)e^{-age/\tau}$ with $W(0) = -100$ and $\tau = 3\text{Myr}$. More than 80% of the data points fall below the line indicating that the strength of $H\alpha$ emission in HAeBe stars decline rapidly. Equivalent width of $H\alpha$ emission in HAeBe stars, seems to decline on a timescale of about 3 Myr.

2.5 K-band excess and age

The fact that HAeBe stars show excess emission at near-infrared wavelengths has been well documented in the literature (e.g., Lada & Adams 1992; Hillenbrand et al. 1992; Malfait et al. 1998). In this Section we look for possible correlation between the magnitude of K-band excess shown by HAeBe stars and the ages of these stars. In order to study the evolutionary trend in the near-infrared excess shown by HAeBe stars we have compiled the J, H, and K_s magnitudes for our sample stars from the 2MASS All-Sky Point Source Catalogue. In Table 2.4 we list the near-infrared data for 46 HAeBe stars. We list only those sources for which the 2MASS catalogue gives the optical association with a Tycho-2 star. Also we have excluded sources which have extended source contamination flag set to 2 in the 2MASS catalogue. Sources so indicated are often foreground stars superimposed on background galaxies, or sometimes extractions of pieces of the galaxy or nebula. The point source photometry for these sources is probably contaminated by the surrounding structured extended emission. Further, stars with only upper limit measurements for H and K_s magnitudes in 2MASS are also not listed in Table 2.4. Columns 1 and 2 of Table 2.4 give object name and the 2MASS designation of the object. Columns 3-8 list J, H, & K_s magnitudes and quoted errors in the magnitudes.

As a measure of K-band excess of the stars we use the quantity $\Delta(H - K)$ which

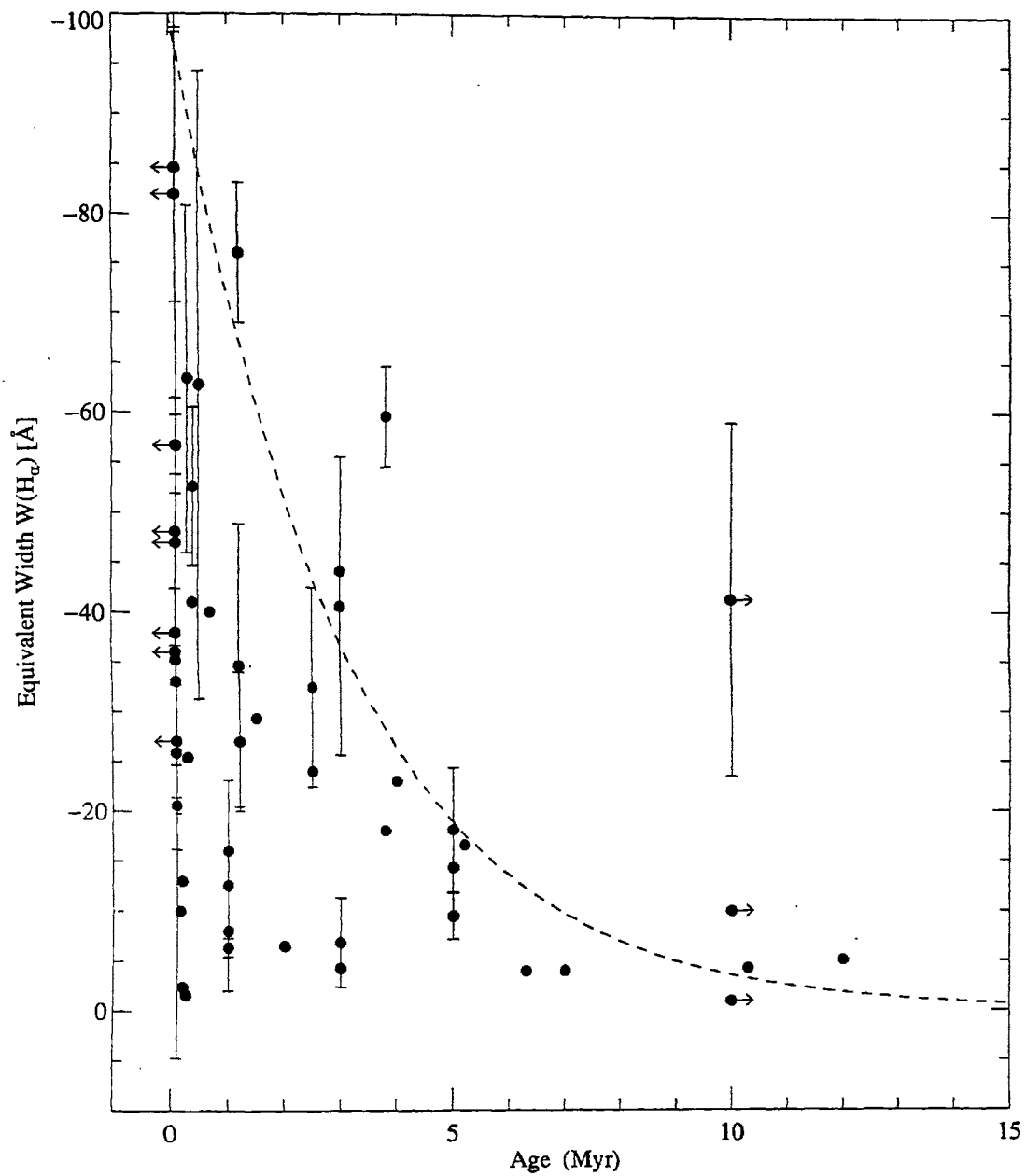


Figure 2.2: $H\alpha$ equivalent widths of Herbig Ae/Be stars plotted against derived stellar ages. Error bars in $W(H\alpha)$ represents the dispersion in the equivalent width measurements given in Table 2.3. The dashed line is of the functional form $W = W(0)e^{-age/\tau}$ with $W(0) = -100$ and $\tau = 3Myr$.

is defined as

$$\Delta(H - K) = (H - K) - (H - K)_o - 0.0645 \times A_V$$

where $(H - K)$ is the observed color, $(H - K)_o$ the intrinsic color corresponding to the spectral type of the star and A_V is the visual extinction towards the star. To compute $\Delta(H - K)$ we first converted observed 2MASS colors $(H - K_s)$ to the Koornneef (1983) system following the color transformations given in Carpenter (2001). The intrinsic colors of the stars and average reddening law used in computing $\Delta(H - K)$ are from Koornneef (1983). The extinction values used are the ones listed in Table 2.1 and Table 2.2. The $\Delta(H - K)$ values thus obtained are listed in column 9 of Table 2.4 and estimated errors in $\Delta(H - K)$ in column 10.

Table 2.4: 2MASS magnitudes of Herbig Ae/Be stars

Object	2MASS Designation	J mag	e_J mag	H mag	e_H mag	K_s mag	e_{K_s} mag	$\Delta(H - K)$ mag	$e_{\Delta(H - K)}$ mag
MWC 1080	23172558+6050436	7.461	0.030	5.980	0.038	4.826	0.018	1.13	0.11
BD+40 4124	20202825+4121514	7.904	0.023	6.792	0.018	5.766	0.016	1.11	0.04
HD 259431	06330519+1019199	7.454	0.026	6.666	0.034	5.726	0.020	1.07	0.05
HD 98922	11223166-5322114	6.004	0.020	5.226	0.029	4.280	0.036	1.15	0.06
Z CMa	07034316-1133062	6.543	0.019	5.216	0.027	3.766	0.178	1.58	0.23
RR Tau	05393051+2622269	9.685	0.020	8.416	0.016	7.389	0.023	1.17	0.06
HD 142527	15564188-4219232	6.503	0.029	5.715	0.031	4.980	0.020	0.74	0.05
HD 179218	19111124+1547155	6.994	0.020	6.645	0.026	5.995	0.018	0.71	0.04
HD 35929	05274279-0819386	7.211	0.023	6.974	0.034	6.673	0.026	0.28	0.05
51 Oph	17312497-2357453	4.900	0.186	4.712	0.206	4.296	0.029	0.49	0.26
BD+61 154	00431825+6154402	8.137	0.019	6.917	0.024	5.896	0.016	1.13	0.04
HD 37806	05410229-0243006	7.115	0.020	6.252	0.033	5.400	0.029	1.03	0.06
HD 85567	09502853-6058029	7.472	0.024	6.680	0.031	5.774	0.023	1.08	0.05
V351 Ori	05441880+0008403	7.950	0.020	7.504	0.040	6.846	0.026	0.74	0.06
HD 250550	06015998+1630567	8.475	0.020	7.528	0.026	6.635	0.018	1.07	0.04
HR 5999	16083427-3906181	5.907	0.018	5.220	0.027	4.386	0.036	0.97	0.06
T Ori	05355043-0528349	8.271	0.021	7.236	0.047	6.216	0.023	1.13	0.08
LkHa 208	06074953+1839264	10.254	0.020	9.834	0.023	9.245	0.021	0.59	0.05
UX Ori	05042998-0347142	8.707	0.021	8.044	0.034	7.214	0.020	0.98	0.05
V380 Ori	05362543-0642577	8.107	0.026	6.964	0.027	5.947	0.024	1.15	0.05
V1295 Aql	20030250+0544166	7.194	0.019	6.647	0.017	5.855	0.027	0.94	0.04
XY Per	03493638+3858556	7.654	0.018	6.917	0.017	6.092	0.018	0.85	0.03
AB Aur	04554582+3033043	5.936	0.018	5.062	0.020	4.230	0.016	0.98	0.03
HD 38120	05431188-0459499	8.432	0.027	7.847	0.086	7.156	0.018	0.83	0.11
NX Pup	07192826-4435114	8.579	0.030	7.285	0.042	6.080	0.031	1.39	0.07

continued on next page

continued from previous page									
Object	2MASS Designation	J mag	e_J mag	H mag	e_H mag	K_s mag	e_{K_s} mag	$\Delta(H - K)$ mag	$e_{\Delta(H - K)}$ mag
HD 97048	11080329-7739174	7.267	0.023	6.665	0.049	5.941	0.029	0.81	0.07
HD 144432	16065795-2743094	7.095	0.032	6.538	0.067	5.888	0.018	0.71	0.09
BF Ori	05371326-0635005	9.113	0.024	8.565	0.040	7.897	0.029	0.77	0.06
HD 104237	12000511-7811346	5.813	0.023	5.246	0.059	4.585	0.018	0.76	0.08
HK Ori	05312805+1209102	9.408	0.020	8.311	0.023	7.341	0.031	1.04	0.06
HD 31648	04584626+2950370	6.865	0.021	6.262	0.033	5.527	0.021	0.87	0.05
HD 163296	17562128-2157218	6.195	0.021	5.531	0.036	4.779	0.018	0.90	0.05
HD 150193	16401792-2353452	6.947	0.020	6.214	0.020	5.476	0.017	0.79	0.03
HD 36112	05302753+2519571	7.221	0.026	6.560	0.024	5.804	0.023	0.89	0.04
IP Per	03404696+3231537	9.139	0.020	8.409	0.018	7.589	0.016	0.93	0.03
HD 245185	05350960+1001515	9.291	0.030	8.764	0.053	8.020	0.036	0.89	0.08
HD 100546	11332542-7011412	6.425	0.020	5.962	0.031	5.418	0.023	0.64	0.05
HD 34282	05160047-0948353	9.256	0.026	8.475	0.033	7.678	0.023	0.93	0.05
HD 141569	15495775-0355162	6.872	0.027	6.861	0.040	6.821	0.026	-0.00	0.06
V346 Ori	05244279+0143482	9.699	0.023	9.188	0.024	8.561	0.019	0.72	0.04
Ty CrA	19014081-3652337	7.486	0.024	6.970	0.026	6.673	0.023	0.26	0.05
CO Ori	05273833+1125389	7.983	0.023	7.213	0.038	6.508	0.020	0.68	0.07
KK Oph	17100811-2715190	9.072	0.027	7.233	0.040	5.795	0.026	1.66	0.07
HD 100453	11330559-5419285	6.945	0.026	6.390	0.038	5.600	0.021	0.91	0.06
AK Sco	16544485-3653185	7.676	0.026	7.059	0.033	6.503	0.020	0.57	0.05
HD 35187	05240118+2457370	6.953	0.021	6.480	0.018	5.911	0.017	0.64	0.03

To study the behaviour of the K-band excess of HAeBe stars with age we plot $\Delta(H - K)$ listed in Table 2.4 against the ages of HAeBe stars estimated from pre-main sequence evolutionary tracks. The plot is shown in Figure 2.3 where for most HAeBe stars the values of $\Delta(H - K)$ are found to be in a narrow range of 0.5-1.2 mag. Nevertheless, it can be seen from the figure that the younger stars have relatively large values of intrinsic K-band excess and the older stars preferentially have lower values. Thus, although the variation in $\Delta(H - K)$ is small, a general decline of K-band excess with stellar age is perceptible. The observed trend is consistent with the magnitude of K-band excess in HAeBe stars decreasing systematically with time during the pre-main sequence phase.

From the preceding discussion it is clear that $W(H\alpha)$ and the K-band excess in HAeBe stars display clear evolutionary trends. Both the $H\alpha$ equivalent width and the magnitude of K-band excess decrease with increasing pre-main sequence age of the star. It is of interest to see how well these two quantities are correlated. A correlation

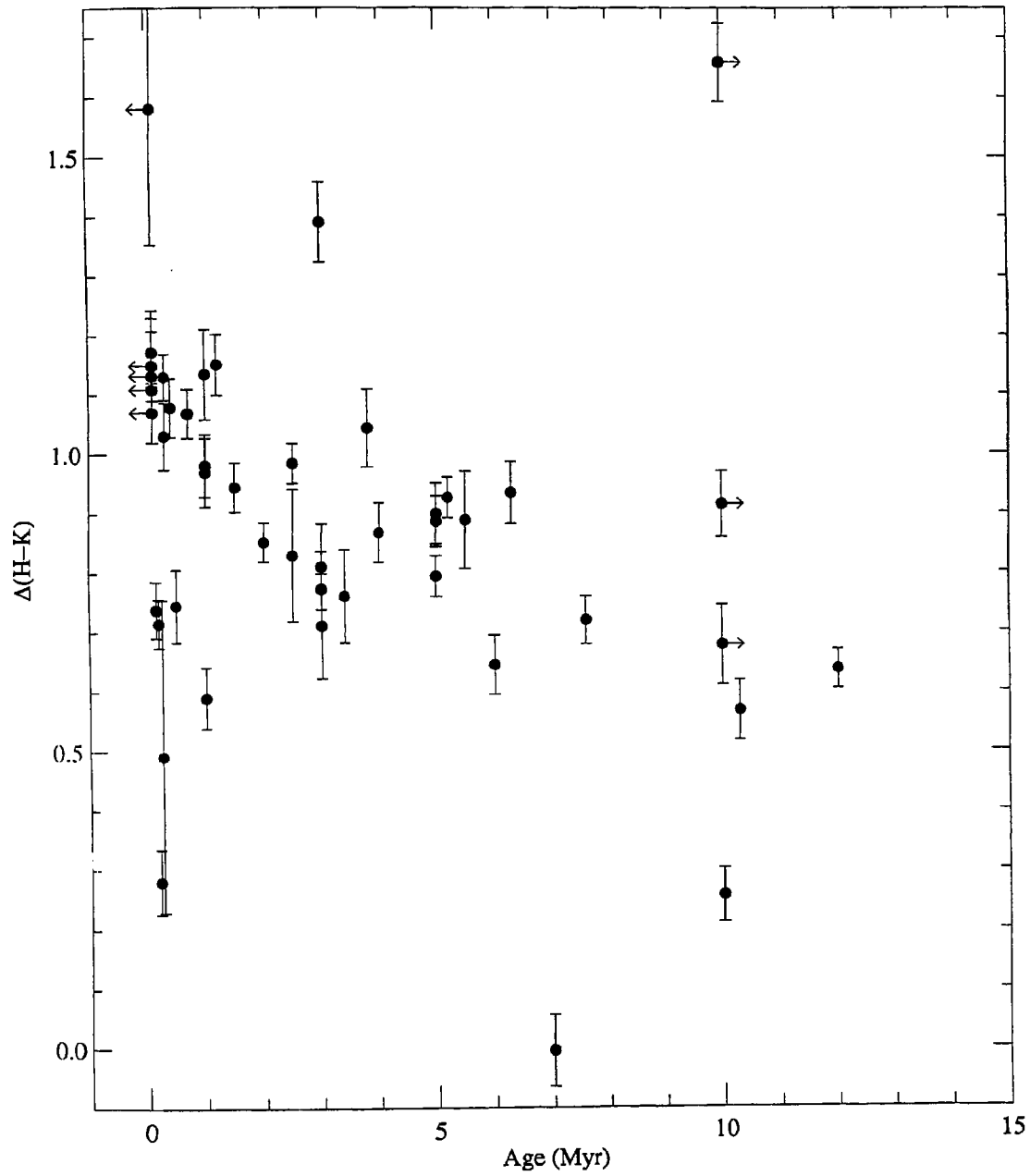


Figure 2.3: K-band excess $\Delta(H - K)$ of Herbig Ae/Be stars plotted against the stellar age.

between $H\alpha$ line strength and near-infrared excess is expected if HAeBe stars harbour accretion disks and if the emission line activity is powered by accretion. In fact such a correlation has been found for classical T Tauri stars (CTTS) (Cabrit et al. 1990), around which the existence of accretion disks has been adequately established. In HAeBe stars Corcoran & Ray (1998) have found a correlation between $H\alpha$ line equivalent width and near infrared colors. In Figure 2.4 we present the plot between absolute values of $W(H\alpha)$ and $\Delta(H - K)$ for 40 of our sample stars. Error bars plotted in $W(H\alpha)$ are the same as that in Figure 2.2. A tight correlation between $H\alpha$ equivalent width and the K-band excess is evident from the figure.

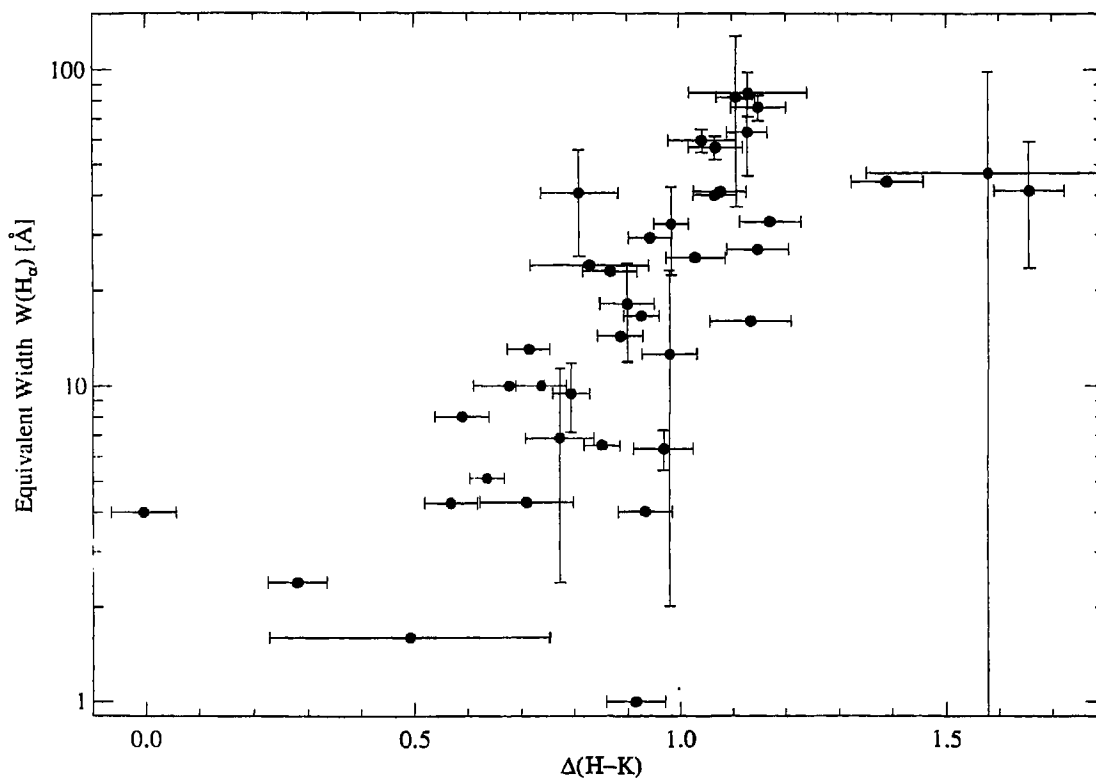


Figure 2.4: Absolute values of $H\alpha$ equivalent widths plotted against K-band excess.

2.6 Discussion

Using the ages estimated for a large sample of HAeBe stars we have studied the temporal evolution of $H\alpha$ emission and K-band excess shown by HAeBe stars. Strength

of emission line activity and the magnitude of K-band excess in HAeBe stars are found to decrease with increasing pre-main sequence age of the star. Further, the line equivalent width of $H\alpha$ and the near-infrared excess $\Delta(H - K)$ are found to be strongly correlated.

As discussed in the introduction, the origin of emission lines in HAeBe stars is not clearly understood. Some authors suggest that the HAeBe winds are accretion driven (Hillenbrand et al. 1992; Corcoran & Ray 1998) while others maintain that it is stellar in origin (Catala 1988; Bouret & Catala 1998; Nisini et al. 1995). In the accretion disk scenario, invoked in analogy with T Tauri stars, the emission is thought to be powered by accretion and the strength of $H\alpha$ emission is taken as a measure of accretion rate (e.g., Hillenbrand et al. 1992). Our result that the $H\alpha$ emission strength decreases with increasing pre-main sequence age of the star would then imply an evolution in accretion with accretion rates dropping off with increasing pre-main sequence age of the star on a timescale of ~ 3 Myr. On the other hand if the winds are stellar in origin, $H\alpha$ line is a measure of the strength of the stellar wind and may be used to compute mass loss rates (Catala & Kunasz 1987; Catala 1988; Nisini et al. 1995). Our result, in this case indicates declining mass loss rates with age. Irrespective of the driving mechanism, there is clear evidence for an evolutionary trend in the emission line activity of HAeBe stars during the pre-main sequence phase.

Apart from the overall trend of decreasing emission line strength with increasing pre-main sequence age of HAeBe stars, what is striking in Figure 2.2 is the short timescales in which the $H\alpha$ equivalent width fall substantially. The emission line strength decrease by a factor of more than 2 in as short a timescale as ~ 3 Myr. This timescale is quite similar to the disk lifetimes derived for pre-main sequence stars from the studies of disk frequencies in clusters and associations (Haisch et al. 2001; Hillenbrand 2002). Hillenbrand (2002), based on their study of inner disk frequency in a large number of young open clusters and associations, have found that the median lifetimes of inner optically thick accretion disks seen around young stars may be as short as $< 2 - 3$ Myr. The fact that emission line strength and inner disks in young stars show identical timescales of evolution argue for a possible physical connection between the origin of both phenomena. The presence of accretion disks around HAeBe

stars would naturally explain such a connection between accretion and strength of emission line activity.

The most important evidence for the existence of optically thick inner disks around HAeBe stars comes from the relatively high values of K-band excess shown by these stars. The excess $(H - K)$ color derived for HAeBe stars in Section 2.5 range from 0.5 to 1.2 mag. The near-infrared excess color $\Delta(H - K)$ has two components contributing to it: one from the reprocessed starlight by the disk and the other from the heating of the disk by viscous accretion. If the activity in HAeBe stars were to be entirely stellar in origin one cannot explain the high values of K-band excess seen in these stars. For example, in classical Be stars, where the emission line activity is entirely due to the star and the emission line spectra of which resemble that of HAeBe stars, also show K-band excess due to free-free emission from the ionized equatorial wind. But the magnitude of this excess is much smaller than that found for HAeBe stars (Lada & Adams 1992). Thus the relatively high values of $\Delta(H - K)$ in HAeBe stars argues strongly for the presence of optically thick inner disks, either passively reprocessing the central starlight or actively accreting or both. From our analysis we find a trend of decreasing $\Delta(H - K)$ with increasing pre-main sequence age of HAeBe stars. This should clearly suggest an evolution of inner disks in intermediate mass stars during the pre-main sequence phase. The accretion rate drops and the inner disks gradually get disrupted during the pre-main sequence phase and completely disappear, perhaps much before the star reaches the main sequence phase. The relatively rapid evolution of $H\alpha$ emission line strength on similar timescales as that of inner disk evolution clearly argues for a connection between the two and supports the scenario in which HAeBe stars are surrounded by accretion disks which also reprocess the central star light. The evolutionary trend that we find in both emission line activity and K-band excess further argue for a drop in the level of accretion activity and gradual disruption of the inner disk with increasing pre-main sequence age of the star.

The tight correlation found between $\Delta(H - K)$ and $W(H\alpha)$ in Figure 2.4 strongly suggests a connection between the presence of inner disks and emission line activity in HAeBe stars. The $H\alpha$ equivalent width is well correlated with K-band excess over two orders of magnitude. It is difficult to explain such a correlation if emission line

activity is solely due to the central star. The observed correlation is quite possible if there is an intimate connection between the presence of inner accretion disks and emission line activity. In T Tauri stars where presence of accretion can be established independently (e.g., optical veiling) a correlation between $H\alpha$ emission strength and near-infrared excess has been found to exist (Cabrit et al. 1990). Corcoran & Ray (1998) have shown that this correlation extends to higher mass HAeBe stars as well. All these evidence support the accretion disk scenario postulated for HAeBe star where the central star is surrounded by an accretion disk and the emission line activity in these stars are powered by accretion.

The evolutionary trend that we find in the emission line strength and the K-band excess, therefore, indicates an evolution in accretion rate. The level of accretion activity in HAeBe stars generally declines during the pre-main sequence evolution of the star. The accretion rate falls relatively rapidly during the first 2-4 Myr of the pre-main sequence evolution in most of the HAeBe stars. The inner disk may get disrupted completely on such timescales. In some HAeBe stars the disk is disrupted on much smaller timescales than the average as can be seen from the large scatter in $H\alpha$ emission line strength at ages of ~ 1 Myr. Also, a few HAeBe stars may retain inner disks and continue to have residual accretion for a few Myr longer than the average.

2.7 Summary

In this chapter we have studied the temporal evolution of emission line activity in HAeBe stars. Placing these stars in the HR diagram, we determined the ages of the stars from the theoretical pre-main sequence evolutionary tracks. Using the observed equivalent widths of $H\alpha$ line as a measure of emission line activity, we looked for possible evolutionary trend in the activity level of these stars. We also studied the behaviour of near-infrared excess of HAeBe stars with pre-main sequence age. Conclusions of this study are summarized below.

- We find an evolutionary trend of decreasing $H\alpha$ equivalent width with increas-

ing pre-main sequence age of HAeBe stars. The level of emission line activity gradually drops during the pre-main sequence evolution of intermediate mass stars.

- The $H\alpha$ line strength in HAeBe stars falls by more than a factor of two on timescales as short as ~ 3 Myr. This timescale is comparable to the inner disks lifetimes of pre-main sequence stars.
- The magnitude of K-band excess in HAeBe stars is found to decrease with increasing pre-main sequence age of the star. The accretion rate falls and the inner disk gradually gets disrupted during the pre-main sequence evolution of the star.
- We find a strong correlation between $H\alpha$ equivalent width and the K-band excess $\Delta(H - K)$ of HAeBe stars. This clearly suggests a connection between emission line activity and presence of accretion disks in these stars.

Chapter 3

Transition objects: Non-emission line young stars

3.1 Introduction

As discussed in the previous chapter, Herbig Ae/Be (HAeBe) stars which are intermediate mass ($2 \lesssim M/M_{\odot} \lesssim 8$) pre-main sequence stars, are very active and are associated with rich circumstellar environment. These stars exhibit a variety of observational signatures like presence of emission lines in the spectra, near and far-infrared excess emission, variability and intrinsic polarization of starlight. Most of the main sequence stars, on the other hand, do not show any of these features. Therefore, the circumstellar matter and its observational manifestations seen in young stars should be lost sometime during the pre-main sequence and early main sequence evolution. When the star evolves along its pre-main sequence evolutionary track in the HR diagram, the circumstellar matter around it also must evolve and more or less disperse by the time the star reaches the main sequence. Infact, such evolution of circumstellar

This chapter is partly based on the paper *Manoj P., Maheswar, G., & H. C. Bhatt, MNRAS, 334, 419 (2002)*

material has been found around several young stars. Gorti & Bhatt (1993) and Thé (1994) have discussed evidence for grain growth in the disks around HAeBe stars. Weakening of emission lines in the spectra, disappearance of near-infrared excess and a general decline of the dust content in the disk are some of the expected trends during the pre-main sequence evolution of the central star. However, several questions regarding the evolution of the young star and the attendant circumstellar material remain to be answered. What is the exact nature of the evolution of circumstellar environment around young stars? What are the mechanisms and time scales of this evolution? There have been suggestions in the literature that HAeBe stars evolve into Vega-like stars (eg. Malfait et al. 1998; Waters & Waelkens 1998). Vega-like stars are characterized by substantial far-infrared excess due to cool dust, relatively low near-infrared excess, low polarization and lack of emission lines in the spectra. The dust masses found around them are a few orders of magnitudes lower than that of HAeBes. Also, Vega-like disks in general are gas depleted (Lagrange et al. 2000). Do all HAeBe stars pass through a Vega-like phase with gas depleted disks? These questions are critical to our understanding of the nature of the pre-main sequence and main sequence evolution of the intermediate mass stars and that of the evolution of the circumstellar environment associated with these stars. One of the ways to address these issues is to identify and study young stars that are in the final stages of pre-main sequence evolution or have just reached the main sequence.

In this chapter we identify and study some young stars which are in an intermediate stage of evolution between the very active pre-main sequence phase and the main sequence phase. These stars do not show emission lines or any other signatures of activity. Near-infrared excesses are absent or, if present, are at relatively low levels, indicating the absence of hot inner disks. However, cold and extended dust disks may be present as the stars show substantial far-infrared excesses.

3.2 Non-emission line young stars of intermediate mass

In Table 5 of their catalogue, Thé et al. (1994) have listed 14 early type stars whose evolutionary status is uncertain and which have not been identified to belong to any specific group. Typical pre-main sequence properties are less clearly seen in these stars. One of them, β Pic, is a bonafide Vega-like star; it is a young main sequence star with an extended and cold dust disk. We identify 7 of the remaining stars to be in an intermediate stage of evolution between pre-main sequence and main sequence phase. In the following we present optical spectra for these stars and discuss the properties of their circumstellar environment in relation with their evolutionary status.

3.2.1 Observations

Object	Date of Observation	Exposure Time
HD 36917	27 February 2002	600s
HD 36939	11 February 2001	900s
HD 36982	27 February 2002	600s
MR Ori	26 February 2002	600s
HD 37062	26 February 2002	300s
HD 158352	11 April 2002	180s
HD 176386	11 April 2002	600s

Table 3.1: Log of spectroscopic observations of stars from Table 5 of Thé et al. (1994)

Optical CCD spectra were obtained with resolution ($\lambda/\Delta\lambda$) ranging from 1000 – 3000 for all the stars in Table 3.1 with the Optomechanics Research (OMR) spectrograph on the 2.34 meter Vainu Bappu Telescope (VBT) at the Vainu Bappu Observatory, Kavalur, India. Log of spectroscopic observations is given in Table 3.1.

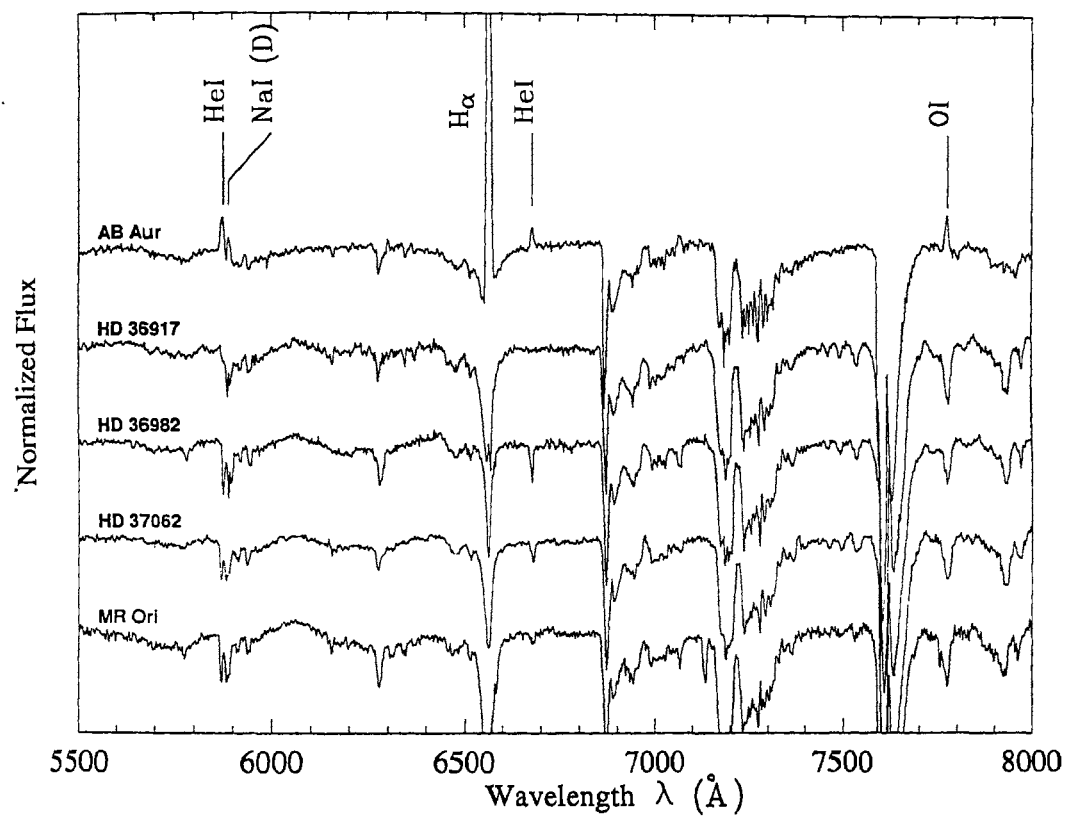


Figure 3.1: Spectra of HD 36917, HD 36982, HD 37062 and MR Ori obtained at a dispersion of $2.4 \text{\AA}/\text{pixel}$. A spectrum of prototype Herbig Ae star *AB Aur* is also shown.

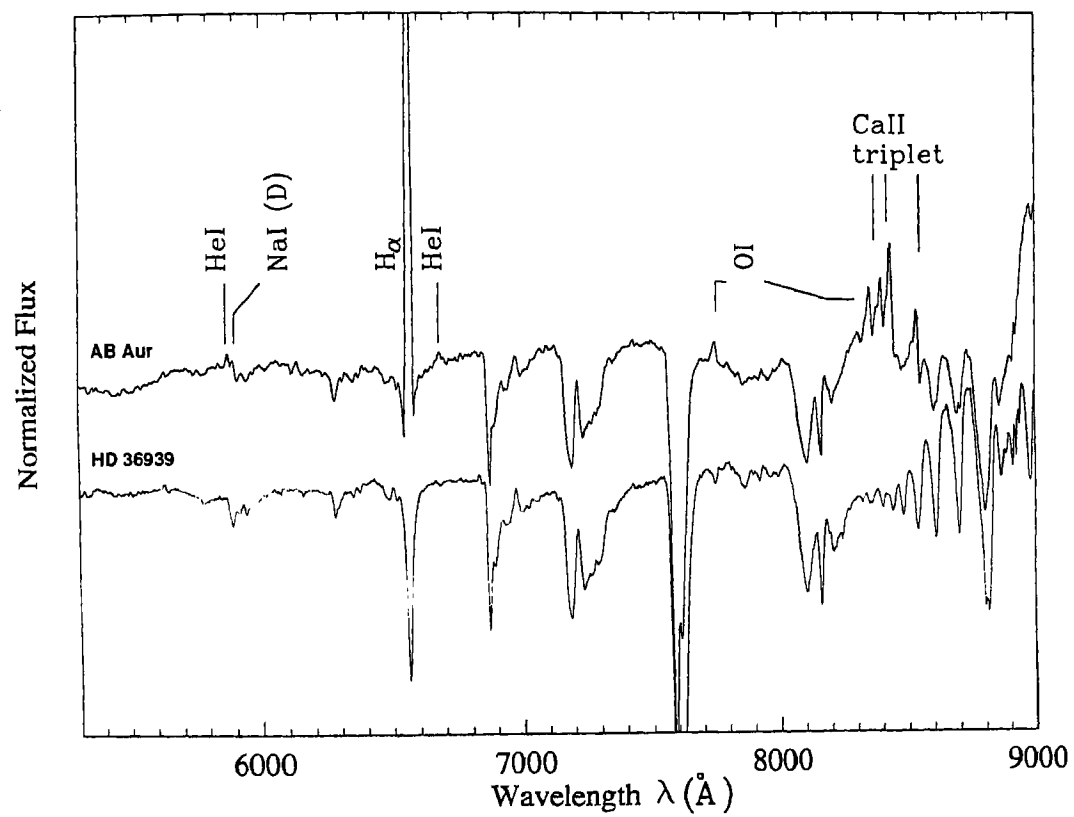


Figure 3.2: Spectra of HD 36939 obtained at a dispersion of $4.8\text{\AA}/\text{pixel}$. A spectrum of *ABAur* at similar resolution is also shown.

Object	Sp. Type	B mag	V mag	$E(B - V)$ mag	A_V mag
HD 36917	B9.5V+A0	8.18	8.05	0.200	1.00
HD 36939	B8.5V	9.00	9.04	0.066	0.13
HD 36982	B2V	8.47	8.44	0.264	1.47
† MR Ori	A2V:var	10.89	10.55	0.290	1.56
† HD 37062	B5V	7.80	8.24	0.000	0.92
HD 158352	A8V	5.64	5.41	0.000	0.00
HD 176386	B9IV	7.44	7.33	0.180	0.56

Table 3.2: Basic data for stars from Table 5 of Thé et al. (1994)

† Stars with no *Tycho* measurements

All spectra were bias subtracted, flat-field corrected, extracted and wavelength calibrated in the standard manner using the IRAF* reduction package. Reduced spectra of HD 36917, HD 36982, HD 37062 and MR Ori are presented in Figure 3.1. A spectrum of the prototype Herbig Ae star *AB Aur*, observed with the same instrumental set up, is also included in Figure 3.1 for comparison. All spectra in Figure 3.1 have been normalized by fitting a continuum. Each spectrum spans a wavelength range of $\sim 2500\text{\AA}$, centered roughly at $H\alpha$ ($\lambda \sim 6563\text{\AA}$). In Figure 3.2 we present the normalized spectrum of HD 36939 at a slightly lower resolution together with a spectrum of *AB Aur* obtained with the same instrumental setting. The spectra in Figure 3.2 range in wavelength from $5000 - 9000\text{\AA}$. In Figure 3.3 we present optical spectra of HD 158352 and HD 176386 obtained at a dispersion of $1.2\text{\AA}/\text{pixel}$ centered roughly at $H\alpha$. Both the spectra in Figure 3.3 have been normalized to the continuum.

3.2.2 Data compiled from literature

In Table 3.2 we present the basic data on the stars from Table 5 of Thé et al. (1994) for which we have obtained the optical spectra. Spectral types listed in column 2

*IRAF is distributed by National Optical Astronomy Observatories, USA.

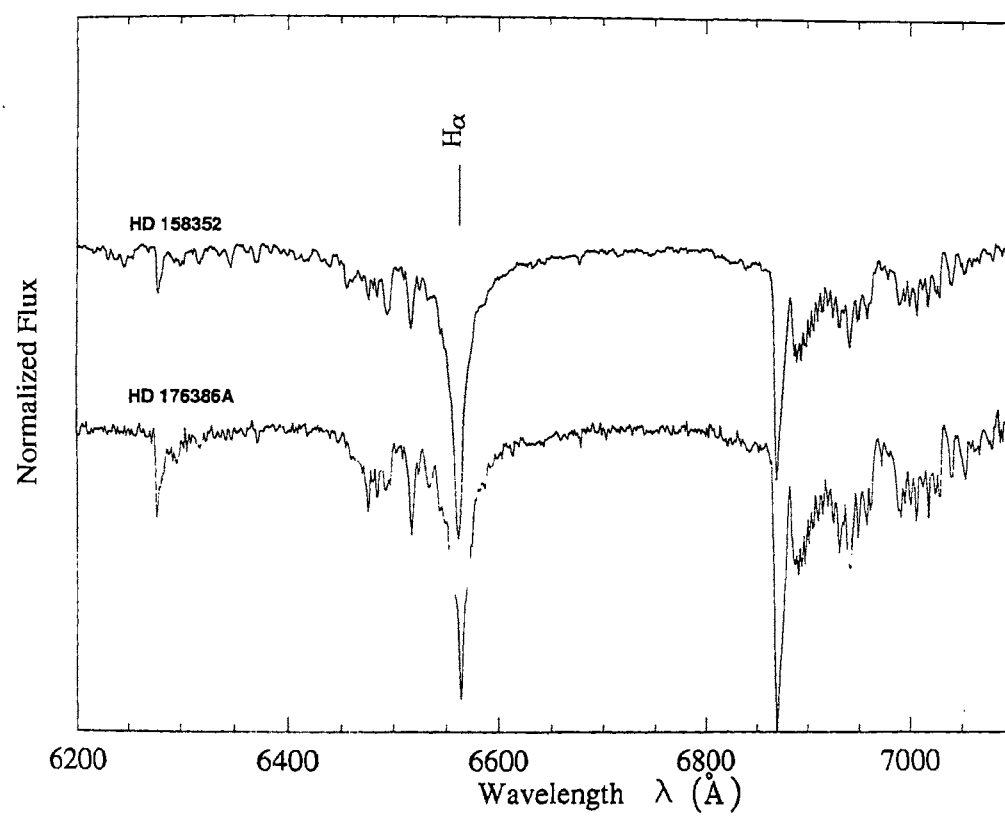


Figure 3.3: Spectra of HD 158352 and HD 176386 obtained at a dispersion of $1.2\text{\AA}/\text{pixel}$, centered at $H\alpha$.

Object	2MASS Designation	J mag	e_J mag	H mag	e_H mag	K_s mag	e_{K_s} mag
HD 36917	05344698-0534145	7.221	0.019	6.964	0.034	6.641	0.018
HD 36939	05345529-0530220	8.851	0.021	8.857	0.031	8.843	0.021
HD 36982	05350983-0527532	7.743	0.024	7.636	0.047	7.472	0.020
MR Ori	05351697-0521452	9.242	0.030	8.978	0.037	8.863	0.029
HD 37062	05353142-0525162	7.794	0.020	7.640	0.029	7.542	0.016
HD 158352	17284965+0019502	4.813	0.037	4.883	0.018	4.805	0.021
HD 176386A	19013892-3653264	6.847	0.020	6.809	0.031	6.690	0.024
HD 176386B	19013912-3653292	7.603	—	7.490	0.090	7.138	0.078

Table 3.3: 2MASS measurements for stars from Table 5 of Thé et al. (1994)

are from Levato & Abt (1976) for HD 36917, HD 36939, HD 36982 & HD 37062; from SIMBAD for MR Ori and as given in *Hipparcos* for HD 158352 & HD 176386. The optical B and V magnitudes of the stars, listed in column 3 and column 4 respectively are derived from *Tycho* magnitudes B_T and V_T whenever available or taken from SIMBAD when *Tycho* measurements do not exist. Reddening, $E(B - V)$ estimated from spectral types and photometric magnitudes is listed in column 5. Negative values of $E(B - V)$ have been called zero in the table. The visual extinction given in column 6 is from Hillenbrand (1997) for the first five stars and for the last two it is obtained from $E(B - V)$, using the average relation $A_V/E(B - V) = 3.1$.

In Table 3.3 we compile the near-infrared observations for the stars from the 2MASS catalogue. In columns 1 & 2 we list the names and the 2MASS designations of the objects. Columns 3-8 give J , H , K_s magnitudes and the corresponding errors in the magnitudes.

We have constructed near-infrared color-color ($(J - H) - (H - K_s)$) diagram from the 2MASS magnitudes for our program stars which is shown in Figure 3.4. Along with our program stars, HAeBe stars and main sequence stars are also plotted in the diagram. The colours for the main sequence stars are from Koornneef (1983)

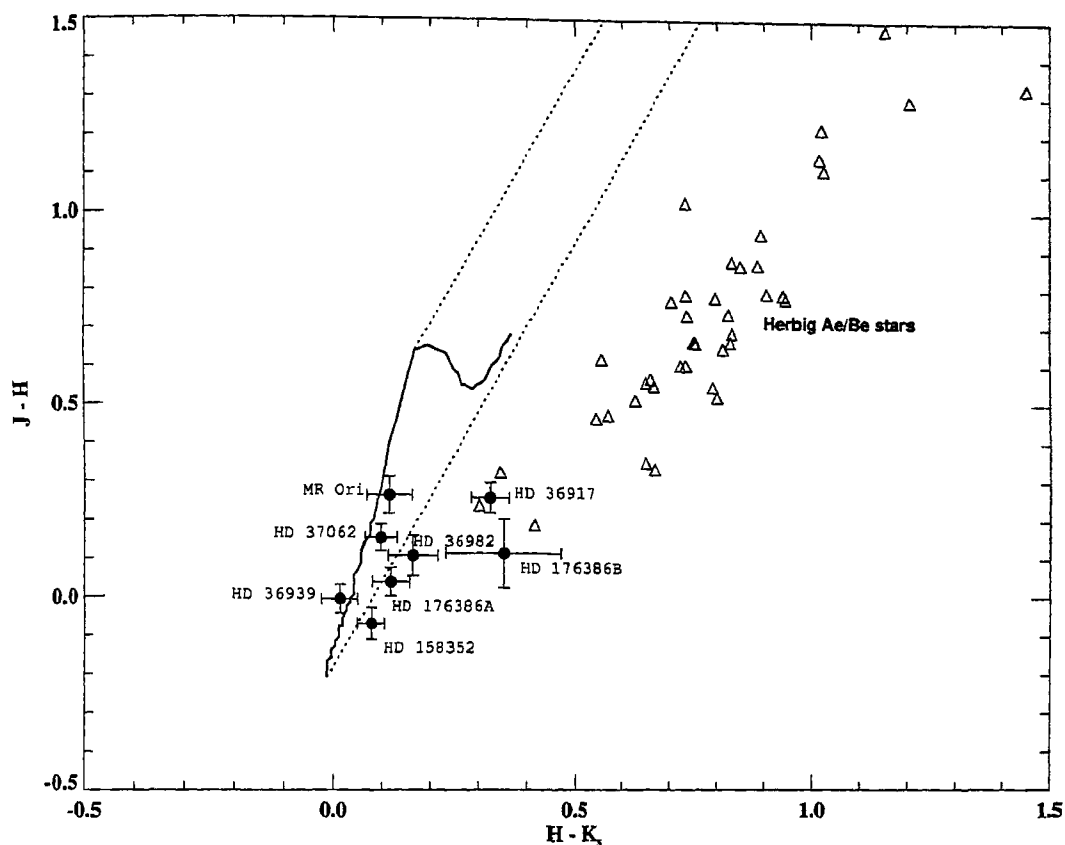


Figure 3.4: Near-infrared color-color diagram for stars from Table 5 of Thé et al. (1994). Filled circles denote program stars and the open triangles Herbig Ae/Be stars. The solid line represents main sequence dwarfs. The dotted lines define the reddening band between them.

which are then converted into 2MASS system following Carpenter (2001). HAeBe stars are taken from Thé et al. (1994) and van den Ancker et al. (1998) and their colours are derived from the 2MASS magnitudes. The two parallel dotted lines form the reddening band for normal stellar photospheres. These lines are parallel to the reddening vector and bound the range in the color-color diagram within which stars with purely reddened normal stellar photospheres can fall (Lada & Adams 1992).

Three of the program stars have *IRAS* sources associated with them. In Table 3.4 we present the *IRAS* data and quantities estimated from them. Columns 1 & 2 of Table 3.4 give name of the object and the *IRAS* source associated with it. In columns 3-6 we list the excess flux above the stellar photospheric flux in each of the

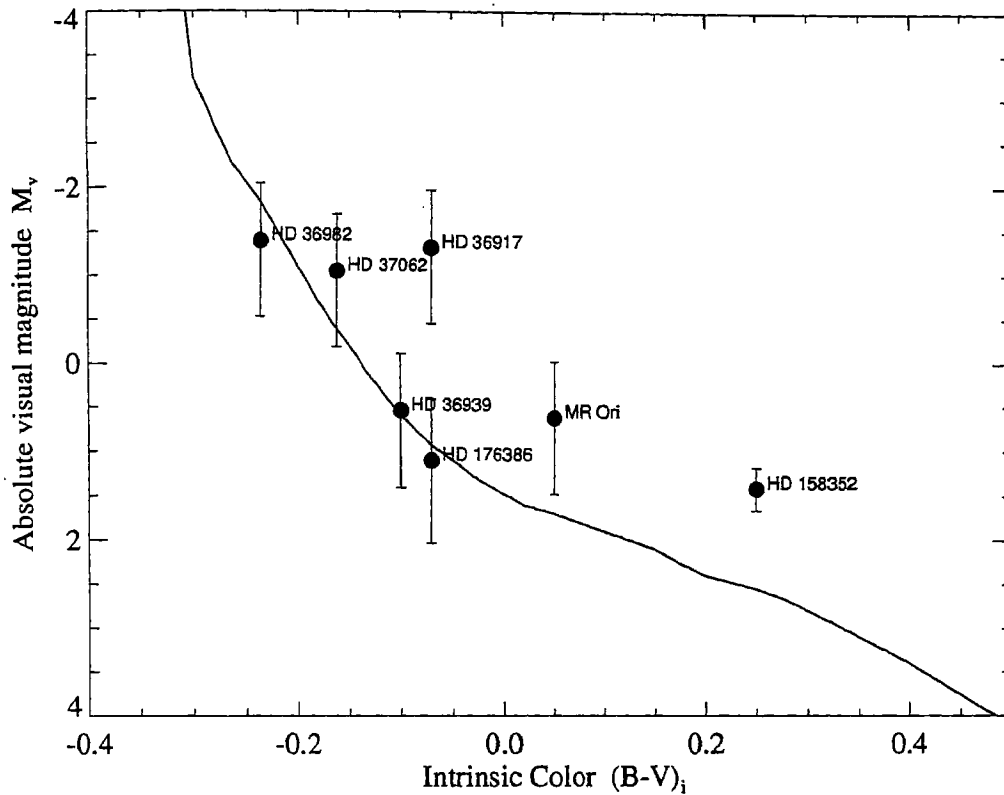


Figure 3.5: The color-magnitude diagram (CMD) for stars from Table 5 of Thé et al. (1994). Solid line represents the main sequence.

IRAS bands and in column 7, the fractional dust luminosity $f_d \equiv L_{dust}/L_*$ is listed. The excesses and f_d listed in Table 3.4 have been computed as discussed in Chapter 5. The *IRAS* flux densities quoted do represent emission from these sources and are not due to other sources in the *IRAS* beam. The association of HD 158352 with the *IRAS* source 17262+0022 has been discussed in the literature (Jaschek et al. 1991). We note that *IRAS* point sources 05323-0536, 05327-0529 have positional coincidences with HD 36917 and HD 36982 to within 4" and 2" respectively. The surface density of *IRAS* point sources in this region is $\sim 10^{-2}$ sources/(arcmin)². Therefore, for a given star, in the 12 and 25 μ bands, the probability that an unrelated *IRAS* point source is in the *IRAS* beam (0.75' \times 4.5') is only $\sim 3\%$.

A color-absolute magnitude diagram (CMD) constructed for all the program stars is shown in Figure 3.5. The zero-age main sequence data is taken from Schmidt-

Object	IRAS Source Name	Excesses at <i>IRAS</i> wavebands (Jy)				$f_d \equiv L_{dust}/L_*$
		$e_{12\mu}$	$e_{25\mu}$	$e_{60\mu}$	$e_{100\mu}$	
HD 36917	05323-0536	5.7e+00	3.4e+00	2.3e-02
HD 36982	05327-0529	3.4e+01	3.7e+02	4.8e+03	...	7.1e-01
HD 158352	17262+0022	0	1.2e-01	4.8e-05

Table 3.4: IRAS sources associated with the program stars

Kaler (1982). For the ONC member stars (see below) a distance of 470 *pc* is assumed and *Hipparcos* distances are used for HD 158352 and HD 176386 in computing the absolute magnitudes. Major contribution to the error bars shown in the figure results from uncertainties in the distances. The extinction values used in computing M_V are taken from Hillenbrand (1997) for ONC member stars and for HD 158352 and HD 176386 it is computed from reddening using the average interstellar relation $A_V/E(B - V) = 3.1$.

3.2.3 Stars in the Orion Nebula Cluster

We note that the stars in Figures 3.1 and 3.2, *viz.*, HD 36917, HD 36939, HD 36982, MR Ori and HD 37062 are towards the direction of the Orion Nebula and the diffuse *HII* region present there is projected on to the line of sight to these stars. Therefore a careful subtraction of the surrounding nebular emission from the observed spectra is very important (Manoj et al. 2002). This is illustrated in Figure 3.6 which presents the raw spectrum with superposed nebular lines and the reduced spectrum with surrounding nebular emission subtracted for HD 37062.

It can be seen from Figure 3.1 and 3.2 that emission lines are not present in the spectra of these stars. In Figure 3.1 & 3.2 we have also included a spectrum of *AB Aur*, a prototype Herbig Ae star, in the same wavelength range and of similar resolution as of the other spectra for comparison. Typical HAEBE emission features such as $H\alpha$, HeI ($\lambda 5876\text{\AA}$ & $\lambda 6678\text{\AA}$), OI ($\lambda 7774\text{\AA}$ & $\lambda 8446\text{\AA}$) and CaII triplet ($\lambda\lambda 8498, 8542, 8662\text{\AA}$) which are prominent in *AB Aur* are not seen in the spectra

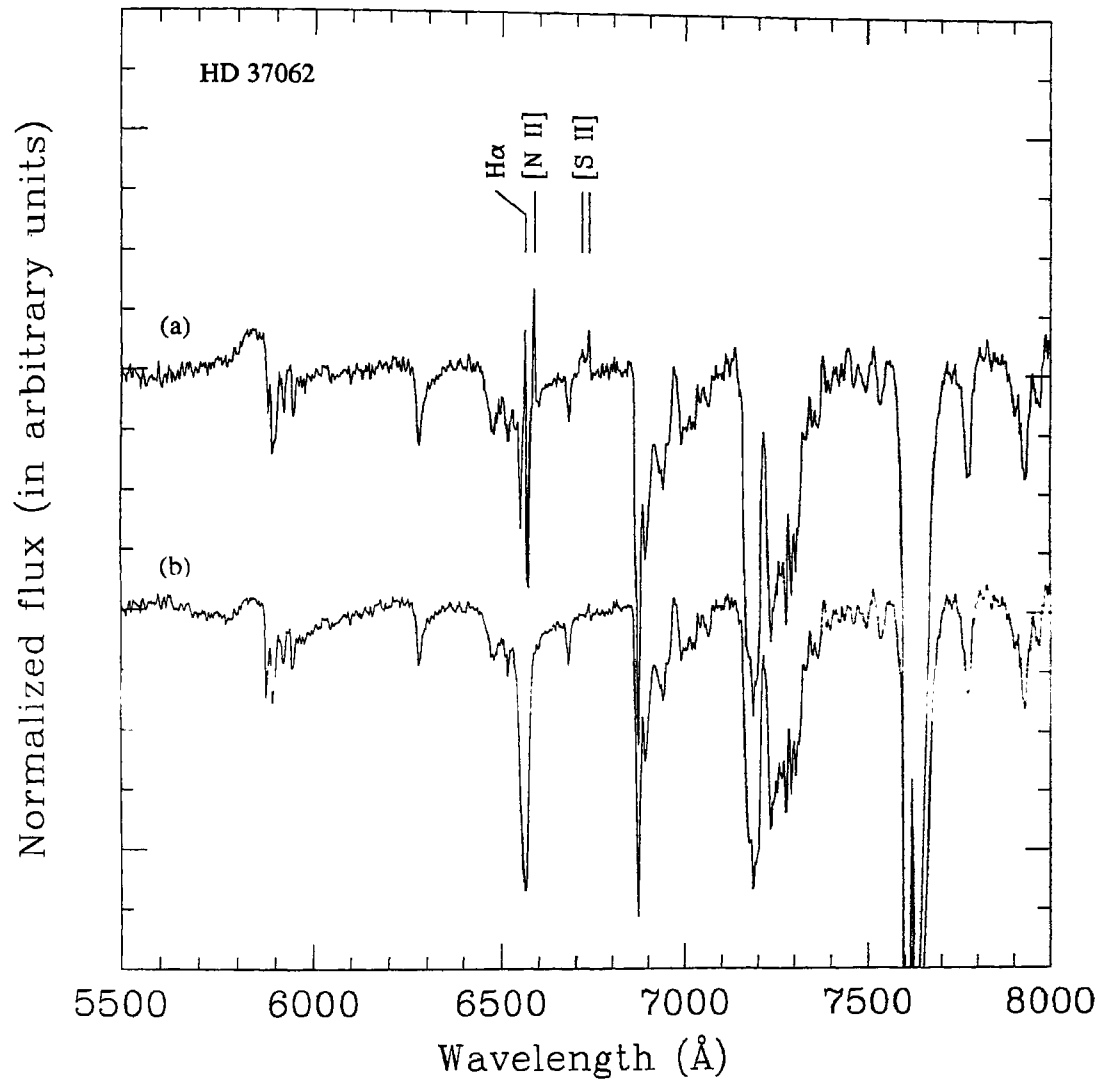


Figure 3.6: (a) The raw spectrum of HD 37062 with nebular lines superposed on it
(b) The reduced spectrum after subtraction of the surrounding nebulosity.

of HD 36917, HD 36939, HD 36982, MR Ori and HD 37062. However, all the stars have earlier been treated as HAeBe stars by different authors (e.g. Malfait et al. 1998; Yudin 2000; Valenti et al. 2000) though in the catalogue by Thé et al. (1994) these stars are identified as non-emission line stars. Spectra presented in Figure 3.1 & 3.2 show that the characteristic HAeBe emission features are conspicuously absent in these stars. The classification of these stars as HAeBe stars is, therefore, doubtful.

The stars whose spectra are presented in Figure 3.1 & Figure 3.2, *viz.*, HD 36917, HD 36939, HD 36982, MR Ori and HD 37062 are in the direction of the known *HII* region (Sharpless No. 281) towards the the Orion Nebula. From proper motion and radial velocity studies it has been established that these stars are kinematically connected with the Orion Nebula Cluster (ONC) which is at the north-western end of Orion A cloud (van Altena et al. 1988; McNamara & Huels 1983; McNamara 1976; Tian et al. 1996; Hillenbrand 1997). The stars belong to the stellar population in the inner ~ 2.5 pc of the ONC which is at a distance of 470 ± 70 pc (Genzel et al. 1981; Walker 1969; Tian et al. 1996; Hillenbrand 1997). ONC as a whole is characterized by a mean age of < 1 Myr and an age spread which is probably less than 2 Myr with an internal velocity dispersion of ~ 2 km s⁻¹ (Hillenbrand 1997; Tian et al. 1996). The kinematic association with the Orion Nebula Cluster strongly constrains the ages of these stars to within a few $\sim 10^6$ years. These are young stars of intermediate mass. The extreme youth and the absence of the emission lines in the optical spectra suggest that these stars are towards the end stages of the pre-main sequence evolution.

Next we turn to study the circumstellar dust around these stars. In the 2MASS color-color diagram given in Figure 3.4 it can be seen that all the five stars, which are members of ONC, are distinctly separated from the region occupied by HAeBe stars suggesting that the near-infrared characteristics of these stars are different from that of HAeBe stars. The near infrared excesses of all the five stars are considerably lower than that of HAeBe stars. HD 36939, HD 36982, MR Ori and HD 37062 have very little near-infrared excess, if any. HD 36917 exhibits near-infrared excess but at a much lower level than that shown by typical HAeBe stars. The near-infrared excess in HAeBe stars is attributed to a combination of accretion and reradiation from hot dust less than ~ 1 AU from the star. The low near infrared excess shown by our

program stars, then, would suggest termination of accretion and disruption of inner disk close to the stars.

Hillenbrand et al. (1998) have demonstrated that the $(J - H) - (H - K)$ diagram is less efficient than the $(V - I_C) - (I_C - K)$ diagram in picking out objects with near-infrared continuum excess, particularly in late-type systems where the temperatures of the inner circumstellar material are comparable with those of central stars for a distribution of spectral types like that in ONC. They use an index $\Delta(I_C - K)$ to identify stars with disks in ONC. The index $\Delta(I_C - K)$ derived by them for HD 36917, HD 36939, HD 36982, MR Ori and HD 37062 are 0.58, 0.12, 0.24, 0.20 and 0.24 respectively. For all the stars except HD 36917 these values are lower than the mean value $\Delta(I_C - K) = 0.36$ for the stars in ONC. Also, the value of $\Delta(I_C - K) = 0.58$ for HD 36917 is much lower than the expected excess from pole-on irradiation + accretion disks with no inner disk holes with an accretion rate of 10^{-9} (Hillenbrand et al. 1998). Thus the levels of near-infrared excess shown by HD 36917, HD 36939, HD 36982, MR Ori and HD 37062 are much lower than that found for typical HAeBe stars. It could be safely concluded that active accretion has terminated in these stars and the inner disk has probably begun to disrupt.

The fractional infrared luminosities $f_d \equiv L_{dust}/L_\star$ estimated for HD 36917 and HD 36982 (Table 3.4) are comparable to that of HAeBe stars and much higher than that found around some of the main sequence stars (Vega-like stars; see chapter 4). The dust masses computed for HD 36917 and HD 36982 are much higher than that for the prototype Vega-like stars and for “old PMS” (OPMS) and “young main sequence” (YMS) systems discussed recently by Lagrange et al. (2000) (Manoj et al. 2002). The circumstellar dust around these stars may not be the debris product as in the case of main sequence dusty systems but rather what is left over from their pre-main sequence phase.

We, now discuss the locations of these stars in the color-magnitude diagram given in Figure 3.6. It can be seen from Figure 3.6 that HD 36917 and MR Ori are above the main sequence by 2.2 and 1.1 magnitudes respectively. The fact that HD 36917

is a spectroscopic binary (B9.5 + A0.5) (Levato & Abt 1976) cannot account for this as the increase in the brightness caused by binarity would only be $\sim 0.7\text{mag}$ at the most. Thus the location of HD 36917 and MR Ori in the color - magnitude diagram is consistent with the stars being in the pre-main sequence phase and the age indicated by its kinematic association with the ONC. The positions in the CMD of the other three ONC member stars *viz.*, HD 36939, HD 36982 and HD 37062 are consistent with the stars being young main sequence stars. These three stars are of earlier spectral types and thus have shorter pre-main sequence lifetimes; the stars are physically more evolved than HD 36917 and MR Ori.

The five ONC member stars discussed above represent an evolutionary stage which is intermediate between pre-main sequence phase with emission lines and near-infrared excess and the main sequence phase. Emission lines which characterize the spectrum of typical pre-main sequence stars are not seen in these stars. Continuum near-infrared excess shown by the stars are at a very low level. These two facts taken together strongly suggests that the accretion has terminated in these stars. Two of the stars for which *IRAS* measurements are available show presence of outer disk around them, the dust content of which is comparable to that of pre-main sequence stars. The kinematic association with ONC constrains the ages of these stars to within $< 0.1 - 2\text{Myr}$. The location in the color-magnitude diagram is consistent with the stars being old pre-main sequence or young main sequence objects.

In the following we discuss the other two stars in our sample *viz.*, HD 158352 and HD 176386.

3.2.4 HD 158352

HD 158352 is a late A type star at a distance of $\sim 63\text{pc}$. Its spectrum is that of a main sequence dwarf though it has shown 'shell' characteristics in the metallic lines of *CaII* (Jaschek et al. 1986). The shell spectrum is not as pronounced as most of the other A type shell stars and the star is often described to have a very poor shell (Slettebak 1982; Jaschek et al. 1988). Variability in its shell features has also been reported (Jaschek & Andrillat 1998).

From the $(J - K) - (H - K_s)$ diagram of Figure 3.4 it can be seen that HD 158352 has little near-infrared excess suggesting the absence of heated dust within 1AU of the star. However, it shows excess emission at 25μ . The fractional dust luminosity, $f_d \equiv L_{ir}/L_*$ is computed to be 4.8×10^{-5} (see Table 3.4) which is comparable to that of Vega, a main sequence star with dust disk. A nonspherical distribution or flattened structure for the dust around the star is suggested by the linear polarization of star light seen in the V band. Percentage polarization of 0.24 ± 0.06 has been measured for the star (Bhatt 1996), a value which is comparable to that shown by Vega-like stars (see Chapter 4).

In the color-magnitude diagram of Figure 3.5 HD 158352 lies above the main sequence by 1.1 mag, suggesting a pre-main sequence evolutionary status. Hauck & Jaschek (2000) derives a surface gravity value of $\text{Log } g = 4.04$ for the star and ascribe a luminosity class of V to it. HD 158352 shows presence of circumstellar gas and dust around it, most likely distributed in a flattened disk. The dust content of the disk is comparable to that of main sequence dust disks. Location of the star in the CMD and the value derived for surface gravity taken together would indicate that HD 158352 is a young star which is towards the end of its pre-main sequence evolution.

3.2.5 HD 176386

HD 176386 is situated towards the north-west edge of the R CrA molecular cloud, roughly 1' south-east of the B8 star TY CrA. A reflection nebula surrounds TY CrA which is an eclipsing PMS binary (e.g., Vaz 2001) and HD 176386. HD 176386 is listed in SIMBAD as a pre-main sequence star. However, we do not find H_α or HeI ($\lambda 6678\text{\AA}$) in emission in the spectrum given in Figure 3.3. None of the other characteristic PMS emission lines are seen in the star (Bibo et al. 1992).

From the 2MASS $(J - H) - (H - K_s)$ diagram of Figure 3.4, it can be seen that HD 176386 has very little excess in the near-infrared. Lack of near-infrared excess was earlier demonstrated by Bibo et al. (1992) from ground based near-infrared photometry. Prusti et al. (1994) have found extended emission to be dominating in the mid-infrared observations of HD 176386. The source size derived from ISOPHOT ob-

servations at 7.3μ correspond to $\sim 1000AU$ (Siebenmorgen et al. 2000). The amount of circumstellar matter around HD 176386, estimated from the ratio of mid-infrared emission to the stellar bolometric luminosity, was found to be much smaller than that for typical Herbig Ae/Be systems (Prusti et al. 1994). Grady et al. (1993) have reported the presence of accreting gas in HD 176386 with velocities upto $+300 km/s$ in CIV and SiII lines from their analysis of the IUE spectra. They find that the values of accreting gas column densities and maximum accretion velocity are intermediate between those seen in young HAeBe systems and main sequence stars such as βPic .

HD 176386 is almost on the main sequence in the CMD given in Figure 3.5. The association with the R CrA molecular cloud argue for a young age for the star. However, characteristic pre-main sequence signatures are conspicuously absent in the star. HD 176386 clearly is in an intermediate evolutionary stage between PMS and MS phase.

The Catalogue of the Components of Double, Multiple stars (CCDM) lists this star as a binary CCDM J19017-3653AB, with a companion whose visual magnitude is 13.3. The angular separation between the components is $4.1''$, making it a visual binary. In Table 3.3 we have compiled the 2MASS magnitude of HD 176386B. It shows a clear K-band excess in the near-infrared color-color diagram. Assuming that the distance and extinction towards both the components of the binary system are the same, we derive an absolute visual magnitude of 7.1 and a spectral type of K3 or later for HD 176386B. HD 176386B is most likely a T Tauri star still in its PMS phase, contracting towards the main sequence.

3.3 Vega-like stars with high fractional dust luminosity

Since the first detection of a relatively cold dust disk around the otherwise normal main sequence star Vega by the *InfraRed Astronomical Satellite (IRAS)*, there have been several surveys to identify such disks around other stars (see Chapter 4). As a result, a large number of main sequence stars have been found to have infrared

Object	Sp. Type	B mag	V mag	$E(B - V)$ mag	<i>Parallax</i> $\pi(mas)$	$\delta\pi$ (<i>mas</i>)
HD 161489	G1V	9.82	9.25	0.000	9.5	1.8
HD 72106	A0IV	8.56	8.58	0.000	3.5	1.4
HD 155448	B9	8.77	8.72	0.128	1.7	1.9
HD 17443	B9V	9.05	8.74	0.383	2.9	1.0
HD 215592	A0	7.89	7.85	0.067	1.7	0.8
HD 113766	F3/F5V	7.94	7.55	0.014	7.6	1.8
SAO 43838	F6V	10.20	9.71	0.044	5.2	1.9
HD 109510	A7m	6.78	6.49	0.093	1.2	9.9
HD 145263	F0V	9.40	8.94	0.154	8.6	1.2

Table 3.5: Basic data for stars with high f_d

excesses similar to that of Vega in the IRAS wavebands and are called Vega-like stars (see e.g. Backman & Paresce 1993; Vidal-Madjar & Ferlet 1994; Lagrange-Henri 1995; Mannings & Barlow 1998; Lagrange et al. 2000; Silverstone 2000; Song 2000). A good measure of the ‘dustiness’ of the disks around Vega-like stars is the fractional dust luminosity $f_d \equiv L_{dust}/L_*$, which represents the optical depth offered by an orbiting dust disk to ultraviolet and visual radiation. Artymowicz (1996) have argued that the fractional dust luminosity f_d of Vega-like disks is self-limited by the dust avalanche process and that these gas-poor disks, in which gas drag is unimportant for dust dynamics, cannot be much dustier than β Pic ($f_d = 10^{-3}$). Systems with larger f_d could be disks with gas controlled dynamics and therefore younger.

We have compiled a large number of candidate Vega-like systems identified in different surveys mentioned above and have computed the fractional dust luminosity $f_d \equiv L_{dust}/L_*$ of these disks (see Chapter 5). We find a few stars with $f_d \geq 10^{-2}$ in our sample. In this section we study the disk systems with high f_d and attempt to constrain the evolutionary status of these stars.

In Table 3.5 we present the basic data for these stars. The optical B and V

Object	IRAS Source Name	Excesses at <i>IRAS</i> wavebands (Jy)				$f_d \equiv L_{dust}/L_*$
		$e_{12\mu}$	$e_{25\mu}$	$e_{60\mu}$	$e_{100\mu}$	
HD 161489	17438-2913	2.71e+00	2.18e+00	1.29e-01
HD 72106	08277-3826	2.20e+00	3.62e+00	1.88e+00	...	6.06e-02
HD 155448	17097-3210	1.55e+00	6.78e+00	6.33e+00	...	3.83e-02
HD 17443	02471+6736	3.86e-01	2.38e+00	1.45e+01	2.28e+01	3.49e-02
HD 215592	F22433+4137	3.37e-01	9.74e-01	7.45e+00	1.60e+01	2.58e-02
HD 113766	F13037-4545	1.46e+00	1.77e+00	6.17e-01	...	1.48e-02
SAO 43838	F11358+4422	...	1.72e-01	7.13e-01	8.54e-01	1.38e-02
HD 109510	F12325+1839	4.49e+00	1.04e+00	2.62e-01	...	1.32e-02
HD 145263	F16078-2523	3.95e-01	5.06e-01	1.05e-02

Table 3.6: IRAS sources associated with the high f_d stars listed in Table 3.5

magnitudes of the stars, listed in column 3 and column 4 respectively are derived from *Tycho* magnitudes B_T and V_T . Spectral type, parallax and error in parallax listed are as given in *Hipparcos* catalogue. In Table 3.6 we present the *IRAS* data and quantities estimated from them. Columns 1 & 2 of Table 3.6 give names of the object and the IRAS source associated with it. In columns 3-6 we list the excess flux above the stellar photospheric flux in each of the *IRAS* bands and in column 7, the fractional dust luminosity $f_d \equiv L_{dust}/L_*$ is listed. The excesses and f_d listed in Table 3.6 have been computed as discussed in Chapter 5.

In Table 3.7 we compile the near-infrared magnitudes of the stars from the 2MASS catalogue. In columns 1 & 2 we list the object names and the 2MASS designations of the objects. Columns 3-8 gives J , H , K_s magnitudes and the corresponding errors in the magnitudes.

We have constructed the near-infrared colour-colour ($(J-H)-(H-K_s)$) diagram from the 2MASS magnitudes of the stars which is shown in Figure 3.7. HAeBe stars and main sequence stars are also plotted in the diagram. Except HD 72106 no other star show near-infrared excess. Even in HD 72106, the magnitude of near-infrared

Object	2MASS Designation	J mag	e_J mag	H mag	e_H mag	K_s mag	e_{K_s} mag
HD 161489	17470370-2914544	8.185	0.027	7.882	0.042	7.799	0.024
HD 72106	08293488-3836214	8.425	0.023	8.279	0.036	7.915	0.020
HD 155448	17125876-3214335	8.650	–	8.508	0.044	8.534	0.044
HD 17443	02513274+6748542	8.131	0.030	8.084	0.033	7.994	0.020
HD 215592	22453812+4152585	7.670	0.020	7.712	0.023	7.668	0.017
HD 113766	13063577-4602018	6.725	0.026	6.594	0.027	6.489	0.024
SAO 43838	11383283+4405220	8.758	0.026	8.564	0.046	8.554	0.024
HD 109510	12350634+1822375	6.042	0.023	5.961	0.020	5.933	0.018
HD 145263	16105511-2531214	8.081	0.023	7.949	0.031	7.882	0.020

Table 3.7: 2MASS measurements for the stars in Table 3.5

excess is much smaller than that seen in young stars with inner accretion disks. Clearly, the inner disk accretion or irradiation from which causes the near-infrared excess, is not present in these stars. However, all the stars show far-infrared excess at *IRAS* bands indicating the presence of colder, extended dust disk. Relatively high values of f_d ($\geq 10^{-2}$) computed for the disks suggest that these disks are not gas-free (Artymowicz 1996).

In chapter 5, using velocity dispersion as an age indicator, we have found a strong correlation between fractional dust luminosity ($f_d \equiv L_{dust}/L_*$) and the ages of the stars with dust disks. The fractional dust luminosity f_d is found to fall with increasing stellar age. The relation between f_d and stellar age derived in Chapter 5 predicts ages of a few $10^7 yr$ for stars with $f_d \sim 10^{-2}$. The stars in Table 3.5 are most likely to be young main sequence stars.

In Figure 3.8 we present the colour-magnitude diagram for all the stars in Table 3.5. HD 155448 and HD 109510 are not included in the figure because of the large errors in the *Hipparcos* parallaxes of these stars. The locations of the stars in the CMD is consistent with the stars being young main sequence objects.

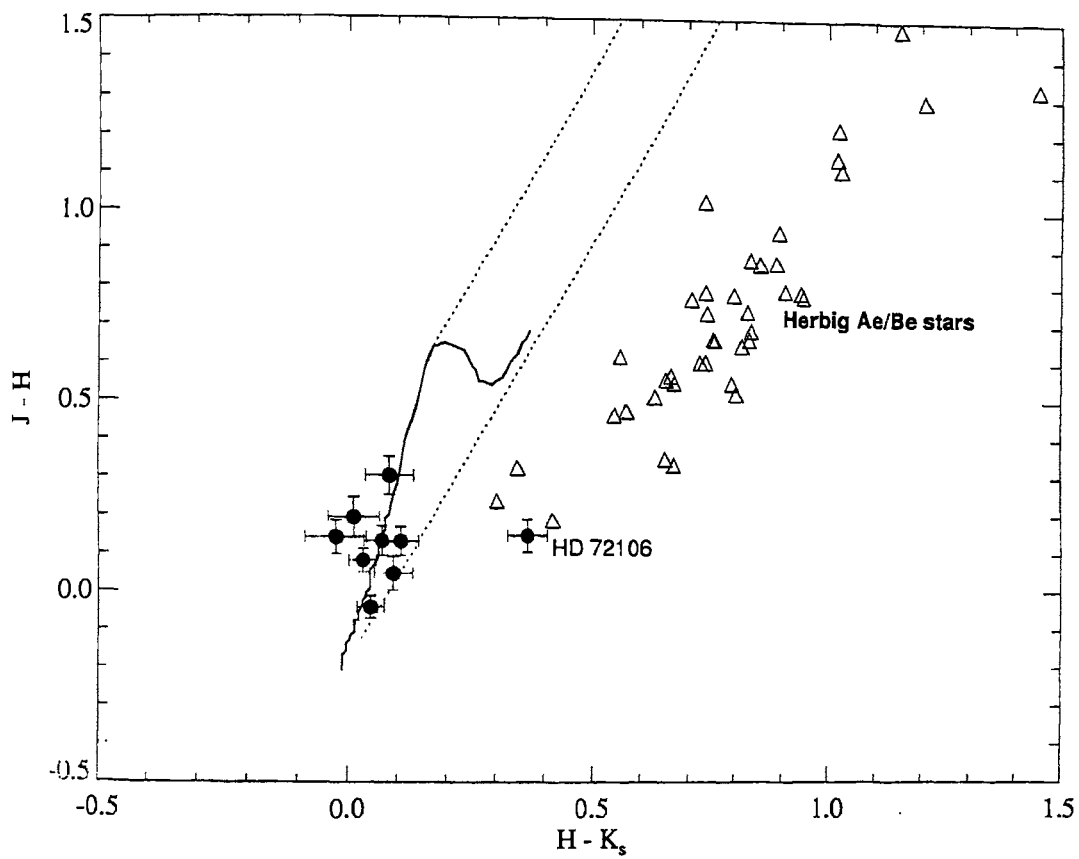


Figure 3.7: Near-infrared color-color diagram for stars with $f_d \geq 10^{-2}$ listed in Table 3.5.. Filled circles denote stars in Table 3.5 and the open triangles Herbig Ae/Be stars. The solid line represents main sequence dwarfs. The dotted lines define the reddening band between them.

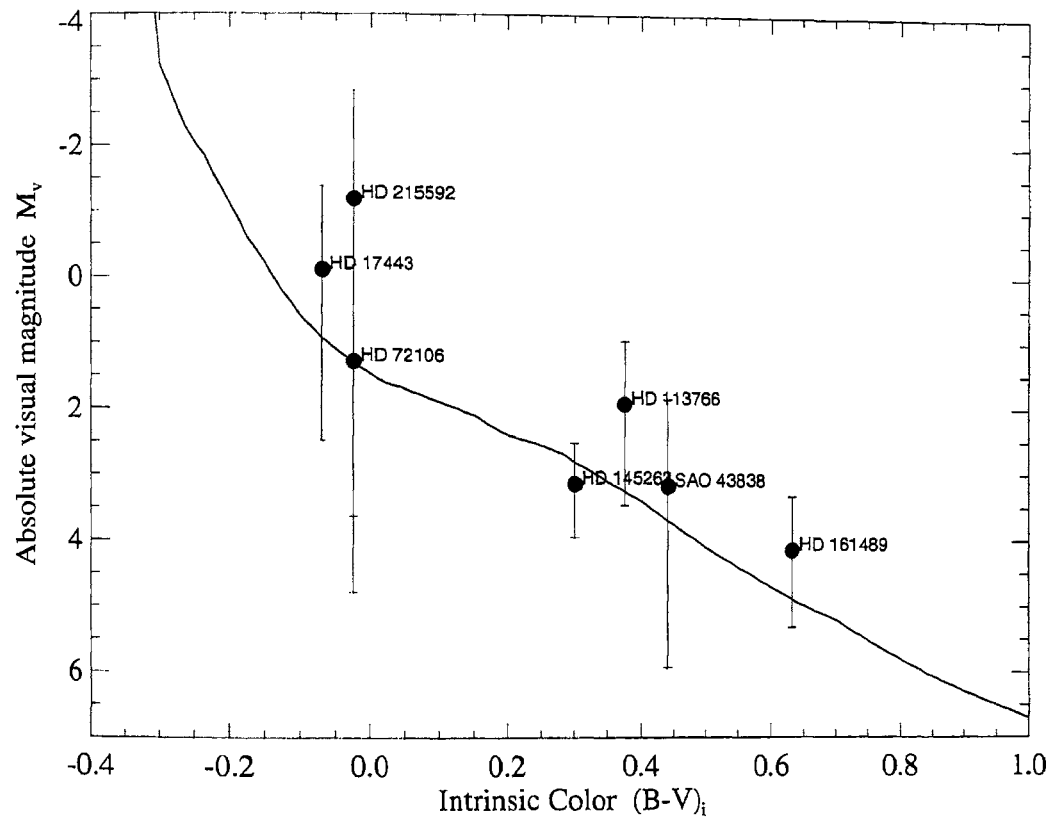


Figure 3.8: The color-magnitude diagram (CMD) for stars in Table 3.5. Solid line represents the main sequence.

3.4 Discussion

Observational properties and the nature of circumstellar environment of the transition objects discussed so far suggest an evolutionary sequence for intermediate mass pre-main sequence stars. In the early pre-main sequence phase (Herbig Ae/Be) stars show several emission lines (eg. $H\alpha$, HeI ($\lambda 5876\text{\AA}$ & $\lambda 6678\text{\AA}$), OI ($\lambda 7774\text{\AA}$ & $\lambda 8446\text{\AA}$) and CaII triplet ($\lambda\lambda 8498, 8542, 8662\text{\AA}$)), near and far-infrared excess and polarization of starlight. During the pre-main sequence evolution, timescale of which is only a few Myr for intermediate mass stars, the pre-main sequence features decrease in strength. The emission line activity weakens and eventually disappear. The near-infrared excess, which is due to both accretion and reprocessed starlight from the circumstellar disk, decreases in strength suggesting the termination of accretion and disruption of the inner disk. The far-infrared excess arising from the cold, outer disks may still persist. Such an evolutionary scenario has been suggested by a number of authors in the literature (eg. Malfait et al. 1998).

Herbig (1994) has pointed out that only a minority of pre-main sequence stars in the intermediate mass range in young clusters appear to be Herbig Ae/Be stars. A similar conclusion was reached by van den Ancker et al. (1997) from their studies of young clusters. This suggests that either the Herbig Ae/Be phenomenon is a temporary one, or that some stars in that mass range do not show it at all. However, recent studies using the measured emission above expected photospheric values in the near-infrared to infer the presence of inner accretion disks, have shown that the disk fraction is $\sim 80\%$ in clusters of ages $< 1 \text{ Myr}$ and declines steadily with time to $< 10\%$ within 3-6 Myr on the average (Hillenbrand 2002; Haisch et al. 2001; Lada 1999). It has been demonstrated in the literature that there is an empirical connection between near-infrared excess and spectroscopic signatures of accretion and outflow such as permitted and forbidden emission lines (Corcoran & Ray 1998). This observed trend indicates that though some disk evolution happens very early on for some stars before they become optically visible, most young stars have inner accretion disks and show associated spectroscopic signatures in the early pre-main sequence phase. The circumstellar environment appear to evolve relatively rapidly

during the pre-main sequence phase and most stars lose their disks within 3-6 Myr, which is comparable to the pre-main sequence lifetimes of intermediate mass stars. A small percentage of stars may retain the inner disks and show spectroscopic signatures of accretion a few times longer than the average (Hillenbrand 2002).

van den Ancker et al. (1997) have suggested that the timescale for the evolution of the central star and the circumstellar environment are probably not well coupled. They note that the timescales at which the circumstellar material is dispersed are very different for individual stars even if the initial configuration and spatial distribution of the circumstellar environment around Herbig Ae/Be stars were to be similar. This proposition is supported by Böhm & Catala (1995) who find that the strength of activity tracers like $H\alpha$, $CaII$ triplet and HeI 5876Å increase with effective temperature of the central star. The authors argue that the ultimate source of energy for the activity is linked to the star itself, rather than to a circumstellar environment.

Regardless of what drives the activity, an evolutionary sequence is seen in the spectroscopic signatures of activity and also in the observational tracers of circumstellar material during the pre-main sequence phase of the star. The emission lines decrease in strength and eventually disappear; there is a steady decline in the near-infrared excess; the far-infrared excess may persist for the entire pre-main sequence phase and beyond.

3.5 Summary

In this chapter we have discussed observational properties of a few intermediate mass stars which are likely to be transition objects. Pre-main sequence characteristics are absent or very weak in these stars. The status of being in an intermediate evolutionary stage between early pre-main sequence and main sequence phase is consistent with the locations of these stars in the CMD, the association with young clusters and star forming regions and their kinematic ages.

The properties of the transition objects identified and studied here fits well with the general evolutionary sequence proposed for the circumstellar disks found around

young stars. In the early pre-main sequence phase active accretion from the disk drives strong emission line activity. As we saw in Chapter 1, the accretion rate gradually declines with the pre-main sequence age of the star. The near-infrared excess arising from the hot inner disk also decreases in strength as the young star ages. The accretion onto the star is terminated at some point and the inner disk begins to dissipate. This results in the cessation of emission line activity and the disappearance of near-infrared excess. The stars that we have identified are likely to be in this stage of evolution. These stars show evidence for the presence of cold outer disks around them. This would suggest that the inner and outer disks are probably not dissipated on similar timescales. Moreover, the fractional dust luminosities L_{dust}/L_{\star} computed for these stars have values that are intermediate between that found for Herbig Ae/Be stars and main sequence stars with debris disks. Planet building is thought to be going on in such disks. Also, disks are believed to evolve from being optically thick to optically thin during this phase. Further studies on the grain growth and other diagnostics of disk evolution such as the gas content in these disks are necessary to understand the disks in the transitional evolutionary phase.

Chapter 4

Dust around main-sequence stars: Vega-like stars

4.1 Introduction

Infrared excess emission associated with “normal” main sequence stars was discovered by *Infrared Astronomical Satellite* (IRAS). This phenomenon was first found around the classical standard star Vega (Aumann et al. 1984) whose infrared flux at 60 and 100 μm was found to be higher by an order of magnitude than that expected from its photosphere. It was soon realized that the infrared excess emission was caused by thermal emission from grains warmed by the central star to temperatures of $\sim 100\text{K}$. It was the first time solid grains were found orbiting a main sequence star other than the Sun. Since the first detection many stars with dust disks have been found (see e.g. Backman & Paresce 1993; Vidal-Madjar & Ferlet 1994; Lagrange-Henri 1995; Mannings & Barlow 1998; Lagrange et al. 2000; Silverstone 2000; Song 2000). These stars have been named *Vega-like stars*, after the prototype Vega. A detailed discussion of Vega-like stars can be found in Section 3 of Chapter 1.

This chapter is based on the paper *Bhatt H. C. & Manoj P., A&A, 362, 978, (2000)*

4.2 Polarization studies of Vega-like stars

What is the spatial distribution of the circumstellar dust in Vega-like stars? Optical coronagraphic observations of β Pic by Smith & Terrile (1984) showed that the scattering dust in this object is distributed in a flattened disk being viewed nearly edge-on. Vega-like stars are now generally thought to have circumstellar dust distributed in disks. The disk structures in these objects may be the end products of evolution of more massive disks associated with pre-main-sequence stars and are replenished by the dust debris produced by the disruption of planetesimals due to collisional and thermal evaporation processes (e.g. Backman & Paresce 1993; Malfait et al. 1998). However, other than for β Pic, direct evidence for the flattened disk-like distribution of the circumstellar material around Vega-like stars has so far been obtained only for a handful of these objects by optical and infrared imaging (e.g. BD +31°643, Kalas & Jewitt (1997); SAO 26804, Skinner et al. (1995); HR 4796A, Jayawardhana et al. (1998) & Koerner et al. (1998); HD 98800, Koerner et al. (2000); Hen3-600, Jayawardhana et al. (1999)).

Circumstellar dust emits thermally in the infrared producing the infrared excess. It also scatters the stellar radiation giving rise to reflection nebulae. Another manifestation of scattering by dust in the circumstellar disk can be polarization of the stellar radiation. For example, the polarization observed in the light of young T Tauri stars and the Herbig Ae/Be stars is generally ascribed to dusty circumstellar disks (e.g. Bastien 1988). Therefore, it is of interest to look for polarization in Vega-like stars. In β Pic, where the disk can be resolved, imaging polarimetry in the R band shows linear polarization at the level of $\sim 17\%$ (Gledhill et al. 1991). When the disk can not be resolved, any polarization in the integrated light from the *star + disk* system will show much lower values of polarization depending on the amount of scattering dust, degree of flattening of the disk and its orientation with respect to the observer's line of sight to the star. In the observed polarization for an object, there will also be present a component of the interstellar polarization that will depend on the direction and distance to the star. Any significant intrinsic component of polarization in the observed polarization for a star will indicate the presence of circumstellar dust

with a spatial distribution around the star that is not spherically symmetric. The dust could be in a disk-like structure with the disk-plane making relatively small angles with the line of sight, because a circularly symmetric disk at right angles to the line of sight will produce no net polarization in the integrated light. Thus polarization measurements can give important information on the spatial distribution of scattering dust in Vega-like stars.

In the following we present the results of optical linear polarization measurements of about 30 Vega-like stars. We also compile polarization data on additional Vega-like stars from the literature. The Vega-like stars are then compared with normal field stars. It is found that a significant fraction of the Vega-like stars show polarization that is much larger than can be explained as due to the interstellar polarization. In *Section 4.3* we present our measurements. Comparison with field stars, the intrinsic polarization of Vega-like stars, the distribution and nature of the dust grains is discussed in *Section 4.4*. The conclusions are summarized in *Section 4.5*.

4.3 Observations

Optical linear polarization measurements were made with a fast star-and-sky chopping polarimeter (Jain & Srinivasulu 1991) coupled at the $f/13$ Cassegrain focus of the 1-m telescope at the Vainu Bappu Observatory, Kavalur of the Indian Institute of Astrophysics. A dry-ice cooled R943-02 Hamamatsu photomultiplier tube was used as the detector. All measurements were made in the V band with an aperture of 15 *arcsec*. Observations were made during the period of January to May 1999. The instrumental polarization was determined by observing unpolarized standard stars from Serkowski (1974). It was found to be $\sim 0.1\%$, and has been subtracted vectorially from the observed polarization of the programme stars. The zero of the polarization position angle was determined by observing the polarized standard stars from Hsu & Breger (1982). The position angle is measured from the celestial north, increasing eastward. The Vega-like stars selected for observations were taken from the lists of Vega-like objects in Backman & Paresce (1993), Coulson et al. (1997), Mannings & Barlow (1998), Song (2000) and Silverstone (2000).

Table 4.1: Polarization measurements of Vega-like stars

HD No.	Date of observation (1999)	Sp. Type	V (mag)	$E(B - V)$ (mag)	d (pc)	$P(\%)$	$e_P(\%)$	$PA(^{\circ})$	$e_{PA(^{\circ})}$	$f_d \equiv L_{dust}/L_{\star}$
9672	17Jan	A1V	5.6	0.05	61	0.17	0.05	12	8	7.4e-04
17206	17Jan	F5/F6V	4.5	0.04	13	0.10	0.03	88	5	<1.0e-06
17443	17Jan	B9V	8.7	0.38	341	1.10	0.17	139	5	3.5e-02
32509	16Jan	A2	7.5	0.15	150	0.95	0.09	51	3	7.5e-03
34700	17Jan	G0	9.2	0.00	1162	0.11	0.12	37	19	1.9e-01
37389 [†]	17Jan	A0	8.3	0.00	250	0.46	0.12	15	8	9.5e-02
53300 [†]	16Jan	A0	8.0	0.31	140	1.00	0.13	81	3	4.5e-03
93331	8Apr	B9.5V	7.3	0.09	151	0.24	0.06	175	5	1.2e-03
98800	13Mar	K4V	8.9	0.08	46	0.54	0.13	89	6	9.8e-02
99211	8Apr	A9V	4.1	0.00	25	0.06	0.06	175	5	4.2e-06
102647	7Apr	A3Vvar	2.1	0.01	11	0.15	0.05	50	6	1.7e-05
109085	8May	F2V	4.3	0.04	18	0.38	0.04	147	5	5.0e-05
115892	8Apr	A2V	2.8	0.02	17	0.18	0.06	164	6	<1.0e-06
121847	8May	B8V	5.2	0.02	104	0.53	0.04	172	2	2.4e-04
123247	8May	B9V	6.4	0.07	101	0.21	0.06	57	5	7.3e-05
131885	8Apr	A0V	6.9	0.03	121	0.57	0.07	13	3	4.8e-04
135344 [†]	11Mar	A0V	8.6	0.48	145	0.07	0.11	108	15	5.1e-02
139614 [†]	10Mar	A7V	8.2	0.03	138	0.65	0.10	38	5	2.1e-01
139664	12Mar	F5IV-V	4.6	0.00	17	0.76	0.07	165	5	1.2e-04
142096	6May	B3V	5.0	0.18	128	0.42	0.04	173	2	3.2e-05
142114	8May	B2.5Vn	4.6	0.17	132	0.45	0.05	14	2	7.7e-05
142165	6May	B5V	5.4	0.16	127	0.75	0.06	3	2	2.4e-05
142666 [†]	11Mar	A8V	8.8	0.27	121	0.80	0.12	72	4	1.7e-01
143006 [†]	8Apr	G6/G8	10.2	0.03	96	0.69	0.08	7	3	2.7e-01
145482	8may	B2V	4.6	0.07	143	0.50	0.05	117	4	4.3e-05
149914	11Mar	B9.5IV	6.7	0.32	165	2.54	0.07	66	1	2.2e-03
233517 [†]	10Mar	K2	9.7	0.40	27	1.8	0.21	177	4	5.1e-02

[†] - Stars which do not have *HIPPARCOS* data

The results of our polarization measurements are presented in Table 4.1. We observed 27 Vega-like stars. In Table 4.1, the HD numbers of the stars observed are given in Column 1, the date of observation in Column 2, spectral type in Column 3, V magnitude in Column 4, colour excess $E(B - V)$ in Column 5 and the distance d in Column 6. For most of the stars the stellar parameters and the distance are taken from the *HIPPARCOS* catalogue. Stars for which *HIPPARCOS* distances are not available, the distance is estimated from spectral type and photometric magnitudes. Intrinsic colours and absolute magnitudes are taken from Schmidt-Kaler (1982). The distance has been corrected for extinction by using a value of 3.0 for the ratio of total to selective extinction $A_V/E(B - V)$. The extinction values are generally quite small. Negative values of $E(B - V)$ in Column 5 have been called zero to derive the corrected magnitudes of the stars. The observed degree of polarization $P(\%)$ and the position angle $PA(^{\circ})$ are given in Columns 7 and 9, while the probable errors in the measurements of polarization $e_P(\%)$ and the position angle e_{PA} are given in Columns 8 and 10. In column 11 we list fractional dust luminosity f_d (L_{dust}/L_*) computed for these stars from their *IRAS* flux densities (see Section 4.4).

4.4 Discussion

It can be seen from Table 4.1 that the degree of polarization for the Vega-like stars varies from small values of $\sim 0.06\%$ (for HD 99211) to values as large as $\sim 2.5\%$ (for HD 149914). Most of the Vega-like stars are nearby objects within $\sim 100 pc$ and are at large galactic latitudes ($|b|$ generally $> 10^{\circ}$, due to a selection effect in making the searches for stars with excess far-infrared fluxes in the *IRAS* catalogue). At such short distances the contribution of the interstellar polarization to the observed polarization is expected to be small $\sim 0.1\%$. A significant fraction (about 2/3) of the Vega-like stars have polarization values $> 0.3\%$. As discussed below, such large values indicate intrinsic polarization being caused by the circumstellar dust around the Vega-like stars.

As most of the known Vega-like stars are relatively bright objects, a number of them are likely to have been observed earlier as part of other polarimetric programmes.

Therefore, to supplement our observations, we have made a search for polarization measurements of additional Vega-like stars in the *SIMBAD* data base at *CDS*, Strasbourg. We found polarization measurements for 81 additional Vega-like stars in the catalogue of stellar polarization by Heiles (2000). In a manner similar to Table 4.1, we list data for these stars from Heiles (2000) in Table 4.2. Altogether, in Tables 4.1 and 4.2, we now have 108 Vega-like stars with polarization measurements. In the following we compare the polarimetric behaviour of the Vega-like stars with normal field stars.

Table 4.2: Polarization data for additional Vega-like stars from literature

HD No.	Sp. Type	V (mag)	$E(B - V)$ (mag)	d (pc)	$P(\%)$	$e_P(\%)$	$PA(^{\circ})$	$e_{PA}(^{\circ})$	$f_d \equiv L_{dust}/L_{\star}$
3003	A0V	5.1	0.06	46	0.03	0.01	127	9	4.8e-05
3191	B1IV:n	8.6	0.72	540	2.40	0.20	53	2	4.0e-04
6343	B8	7.3	0.21	251	1.66	0.20	98	3	2.4e-03
6811	B7III	4.3	0.15	225	1.00	0.12	90	3	3.3e-05
9826	F8V	4.1	0.02	13	0.02	0.12	26	71	< 1.0e-06
10472	F2IV/V	7.6	0.07	66	0.02	0.01	78	6	2.0e-04
10476	K1V	5.2	0.00	7	0.05	0.04	178	19	3.4e-05
10647	F8V	5.5	0.03	17	0.04	0.04	20	23	2.9e-04
11241	B1.5V	5.5	0.10	315	0.60	0.04	107	1	9.3e-05
13161	A5III	3.0	0.00	38	0.05	0.12	137	50	1.5e-05
14055	A1Vnn	4.0	0.00	36	0.03	0.12	18	63	7.5e-05
16157	K7V	8.9	0.12	11	0.13	0.05	170	10	2.4e-03
17081	B7IV	4.2	0.02	135	0.37	0.20	3	15	1.1e-04
18978	A4V	4.1	0.04	26	0.01	0.01	10	26	< 1.0e-06
20010	F8V	3.8	0.02	14	0.01	0.01	115	36	< 1.0e-06
21455	B7V	6.2	0.27	176	0.55	0.32	105	16	1.8e-04
21856	B1V	5.9	0.19	502	0.78	0.20	66	7	2.3e-05
22049	K2V	3.7	0.00	3	0.01	0.01	147	35	7.3e-05
23480	B6IV	4.1	0.10	110	0.37	0.02	134	1	1.5e-04
34233	B5V	6.1	0.14	269	0.97	0.20	0	5	2.3e-05
35532	B2Vn	6.2	0.16	200	0.00	0.20	0	90	1.5e-04
36576	B2IV-V	5.7	0.22	574	0.11	0.01	75	0	1.6e-04
36695	B1V	5.4	0.10	568	0.00	0.20	0	90	1.9e-04
37795	B7IV	2.6	0.02	82	0.15	0.10	109	18	1.5e-04
38087	B5V	8.3	0.27	199	2.53	0.06	117	0	4.3e-02
38120	A0	9.1	0.06	421	0.69	0.03	170	1	4.4e-01

continued on next page

continued from previous page									
HD No.	Sp. Type	V (mag)	$E(B - V)$ (mag)	d (pc)	$P(\%)$	$e_P(\%)$	$PA(^{\circ})$	$e_{PA(^{\circ})}$	$f_d \equiv L_{dust}/L_*$
38393	F7V	3.6	0.00	8	0.57	0.04	42	1	< 1.0e-06
43955	B2/B3V	5.5	0.08	304	0.09	0.04	63	11	1.6e-05
44892	A9/F0I	6.6	0.01	160	0.57	0.05	94	2	2.5e-03
50013	B1.5IV	3.5	0.15	242	0.31	0.10	106	9	6.6e-05
56099	F8	7.6	0.05	86	0.60	0.10	71	4	8.9e-04
58715	B8Vvar	2.9	0.01	52	0.03	0.12	24	63	1.3e-04
68456	F5V	1.7	0.00	21	0.06	0.04	166	16	< 1.0e-06
69830	K0V	6.0	0.00	12	0.08	0.04	140	12	5.1e-05
71155	A0V	3.9	0.01	38	0.02	0.12	13	71	2.2e-05
73390	B3V+..	5.3	0.08	294	0.17	0.04	119	5	4.2e-05
83953	B5V	1.8	0.05	152	0.53	0.12	176	6	3.0e-04
84117	G0V	1.9	0.00	14	0.05	0.04	71	19	< 1.0e-06
95418	A1V	2.3	0.01	24	0.00	0.12	43	90	4.2e-06
97495	A2III	5.4	0.12	19	0.04	0.03	0	20	7.4e-06
104731	F6V	5.2	0.00	24	0.04	0.04	64	23	< 1.0e-06
108483	B3V	3.9	0.02	135	0.14	0.04	59	7	< 1.0e-06
110335	B6IV	1.9	0.11	317	0.46	0.04	89	2	2.4e-04
110411	A0V	1.9	0.10	36	0.02	0.12	39	71	3.8e-05
114576	A5V	6.5	0.04	112	0.22	0.04	80	4	1.8e-04
117176	G5V	5.0	0.03	18	0.02	0.12	101	71	< 1.0e-06
120136	F7V	4.5	0.02	15	0.06	0.02	31	8	< 1.0e-06
120324	B2IV-V	3.5	0.07	161	0.07	0.10	169	35	1.8e-05
124771	B4V	5.1	0.08	168	0.67	0.04	111	1	5.0e-04
125162	A0sh	1.2	0.11	29	0.03	0.01	0	0	2.3e-05
127762	A7IIIv	3.0	0.00	26	0.00	0.12	158	90	4.8e-06
127972	B1Vn	2.3	0.11	94	0.04	0.10	174	51	1.2e-05
128167	F3Vwva	1.5	0.00	15	0.09	0.12	26	33	6.7e-06
129433	B9.5V	5.7	0.08	125	0.29	0.04	77	3	3.0e-05
135379	A3V	4.1	0.01	29	0.02	0.04	66	41	1.1e-04
139006	A0V	2.2	0.05	22	0.06	0.12	29	45	8.4e-06
139129	B9V	5.4	0.08	140	0.05	0.04	71	19	3.1e-04
140775	A1V	5.6	0.02	117	0.42	0.12	108	8	1.7e-04
142860	F6V	3.9	0.01	14	0.01	0.04	62	23	9.2e-06
143894	A3V	4.8	0.00	51	0.03	0.12	82	63	2.1e-05
149630	B9Vvar	4.2	0.06	92	0.08	0.12	75	36	1.6e-05
155401	B9Vn..	6.1	0.02	167	0.03	0.04	63	30	2.3e-03
159082	B9.5V	6.4	0.06	151	0.38	0.04	97	2	3.8e-04
161868	A0V	3.8	0.06	29	0.01	0.01	33	3	5.4e-05
162917	F4IV-V	5.8	0.01	31	0.10	0.04	65	9	1.8e-05
172167	A0Vvar	0.0	0.02	7	0.02	0.12	75	71	1.4e-05
176638	A0Vn	4.7	0.00	56	0.03	0.04	13	30	6.5e-05
181296	A0Vn	5.0	0.01	17	0.04	0.04	99	23	1.4e-04
181869	B8V	4.0	0.01	52	0.01	0.04	75	60	4.9e-06

continued on next page

continued from previous page									
HD No.	Sp. Type	V (mag)	$E(B - V)$ (mag)	d (pc)	$P(\%)$	$e_P(\%)$	$PA(^{\circ})$	$e_{PA(^{\circ})}$	$f_d \equiv L_{dust}/L_*$
192685	B3V	4.8	0.03	367	0.00	0.20	0	90	6.9e-05
196740	B5IV	5.1	0.04	151	0.07	0.01	45	0	4.5e-05
209296	B6:V:n	8.3	0.38	699	0.92	0.20	22	6	2.5e-03
212097	B9III	4.8	0.06	186	0.37	0.20	125	15	4.1e-05
212150	A1Vn	6.6	0.00	289	0.36	0.05	57	4	1.1e-04
214748	B8V	4.2	0.01	228	0.09	0.10	155	29	1.0e-04
214953	G0	6.0	0.00	23	0.03	0.01	115	16	2.6e-05
216956	A3V	1.2	0.06	7	0.01	0.01	122	26	4.9e-05
219571	F1III	4.0	0.09	22	0.01	0.01	152	26	2.2e-06
224392	A1V	5.0	0.04	48	0.04	0.01	128	7	< 1.0e-06
224686	B9IV	4.5	0.00	114	0.08	0.20	86	51	9.3e-06
281159	B5V	8.5	0.86	221	1.20	0.20	154	4	2.5e-02

In order to assess the strength of the intrinsic component in the polarization of the Vega-like stars, one needs to have an estimate of the interstellar polarization. For more distant Vega-like stars the interstellar component could be relatively large, since the interstellar polarization in general increases with distance, and should be subtracted from the observed polarization. This is, however, not possible for the programme stars individually, as the interstellar polarization in the direction of these stars, as a function of distance, is generally not known. We therefore make a statistical comparison between the polarization observed for the Vega-like stars and normal field stars with similar magnitudes and distances. For the comparison, polarization measurements for normal field stars have been taken from Heiles (2000). Normal stars within $\sim 1 - 2^{\circ}$ of the Vega-like stars were chosen for comparison. Stars with any known peculiarities (like the presence of emission lines in the spectra, infrared excesses, association with nebulosities, variability etc.) were excluded. In Fig. 4.1 we plot the observed degree of polarization against the distance for the Vega-like stars as well as the normal field stars. It can be seen from Fig. 4.1 that, on an average, the Vega-like stars have polarization values generally larger than the normal field stars at comparable distances.

The average value of polarization for the Vega-like stars is 0.36% with a large dispersion of 0.51%, while the normal field stars have an average polarization of 0.23% and a smaller dispersion of 0.27%. Fig. 4.2 shows frequency distribution (as a

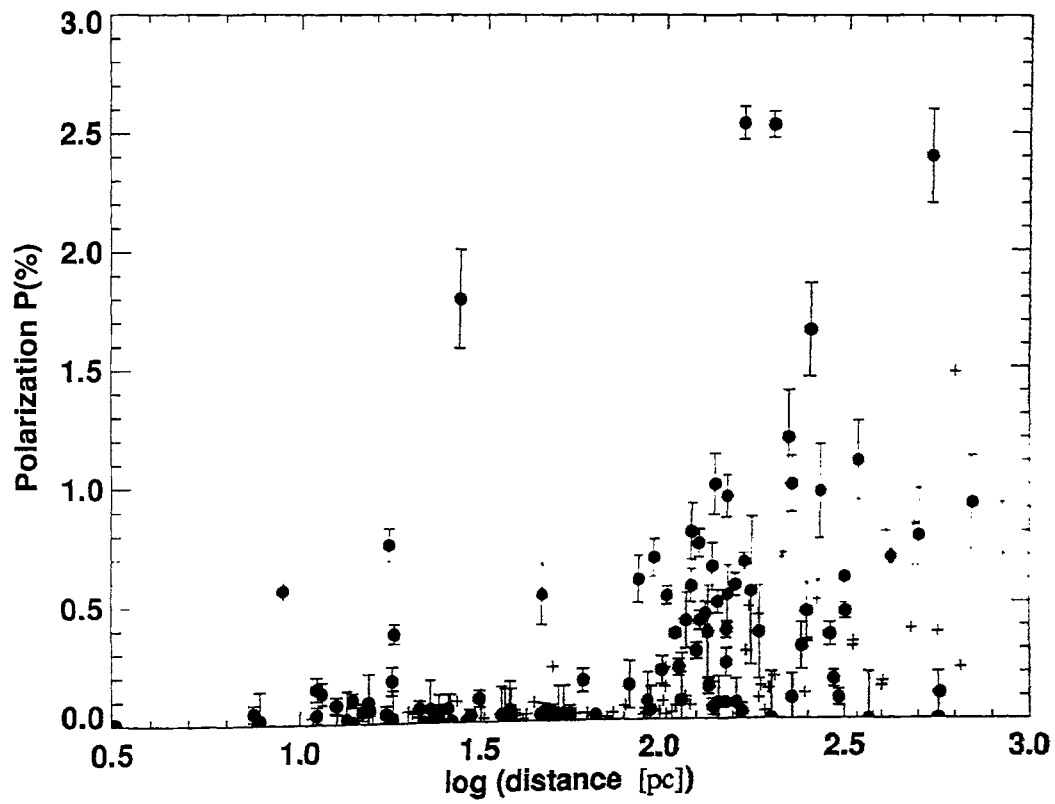


Figure 4.1: Percentage polarization plotted against distance modulus for Vega-like stars. Vega-like stars are represented by filled circles while crosses denote normal stars.

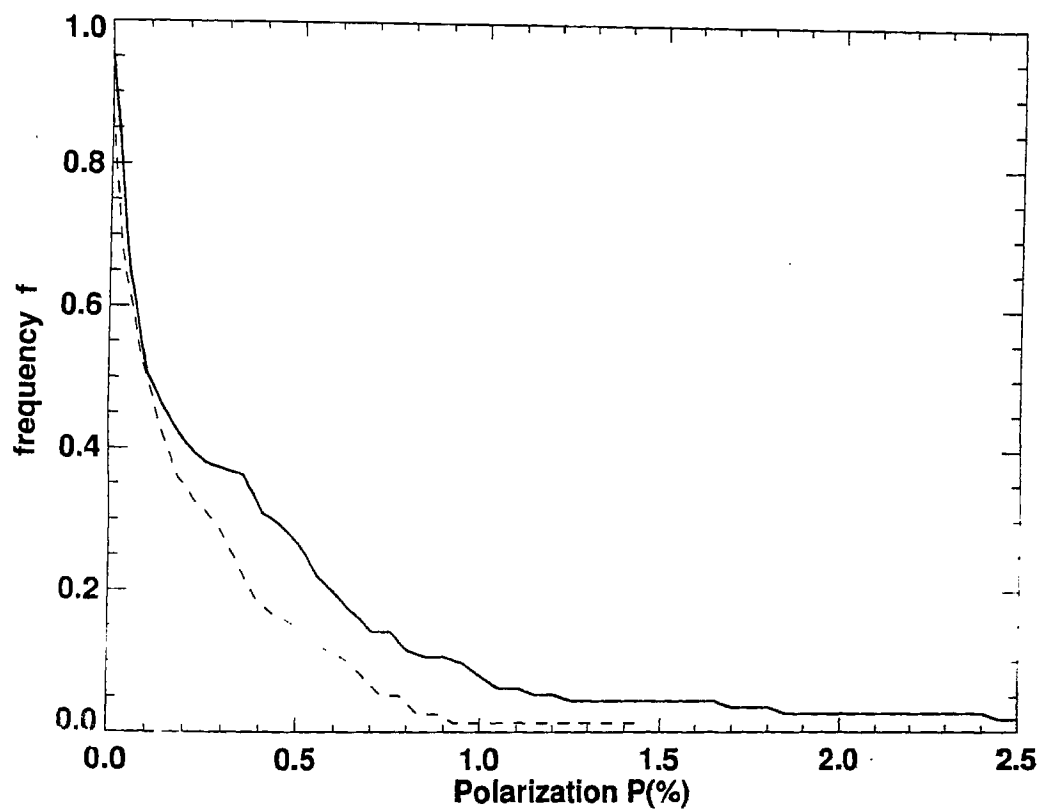


Figure 4.2: Frequency distribution of observed polarization values for Vega-like and normal field stars. f is the fractional number of stars with observed polarization larger than a given value. Solid line represents Vega-like stars and dashed line normal field stars.

fraction of the total number of stars in the two samples separately) of stars with observed polarization larger than a given value. Now the difference between the polarimetric behaviour of the two samples of stars is more clear. About 30% of the Vega-like stars show polarization values larger than 0.5%, whereas only 14% of the normal field stars show polarization values larger than 0.5%. Normal field stars with polarization values larger than 1% is $\leq 1\%$, while about 10% of the Vega-like stars show polarization values larger than 1%. For the stars plotted in Fig. 4.1 a two-sided Kolmogorov-Smirnoff test shows that the two samples (Vega-like and normal field stars) are different to 99.7%.

For the Vega-like stars that show relatively large degree of polarization, the observed polarization cannot be accounted for by normal interstellar polarization and must be circumstellar in origin. Circumstellar dust around these stars, to which the observed infrared excesses are ascribed, can cause polarization by the process of scattering of the light from the central star. In order to be able to produce a net polarization in the integrated light the dust must be distributed in a non-spherical geometry. These non-spherical distributions could be flattened disks around the stars similar to those in β Pic. The disk planes should have relatively small inclinations with the observer's line of sight. Given this constraint on the inclination of the disks, the difference between the Vega-like stars and the normal stars noticed in Fig. 4.1 becomes even more significant, because only a fraction of the stars with disks will have favourable inclinations.

The large values of polarization observed for Vega-like stars thus support the existence of dusty disks around these stars. The polarization is produced by scattering of light from the central star. In contrast, the interstellar polarization is caused by selective extinction due to nonspherical dust grains aligned by the interstellar magnetic field. The interstellar polarization shows a correlation with reddening given by the average relation: $P_V/E(B-V) = 3\%mag^{-1}$. The circumstellar dust in Vega-like stars is believed to consist of relatively large grains (a few tens of microns (Backman & Parsce 1993)) that are not expected to produce any additional reddening at optical wavelengths. Thus large values of polarization may result even with small values

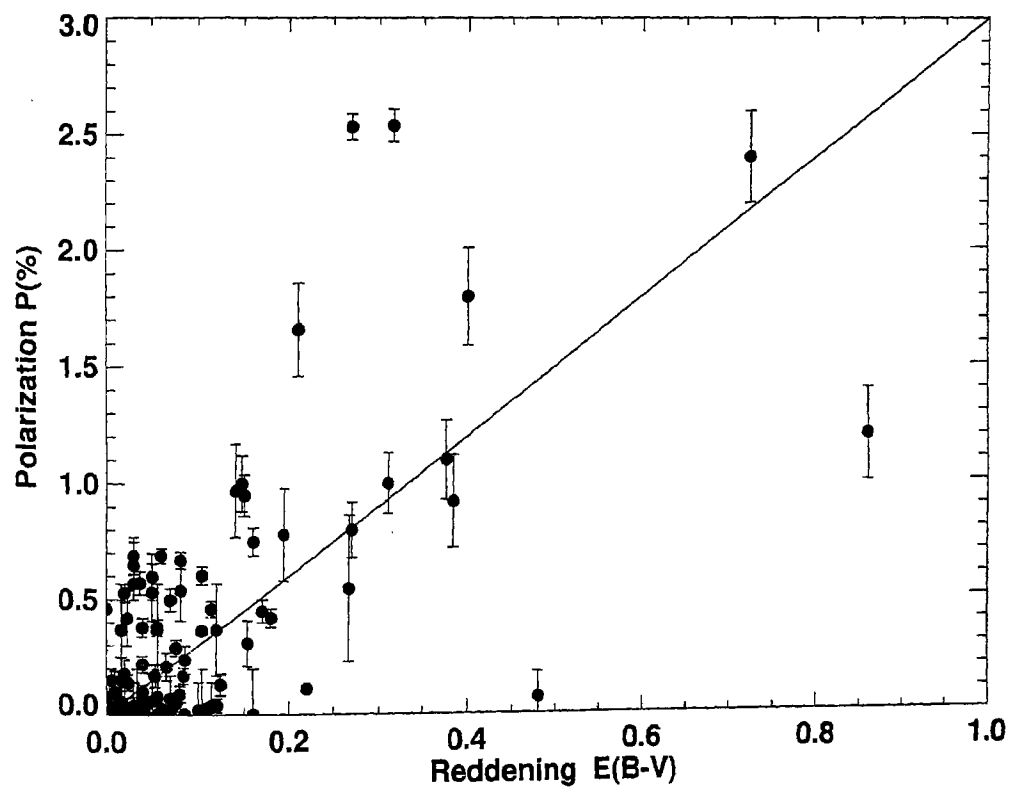


Figure 4.3: Percentage polarization against reddening for Vega-like stars. The average interstellar relation $P(\%)/E(B - V) = 3$ is shown as the solid line.

of reddening at small distances. Fig. 4.3 shows a plot of the observed polarization against reddening $E(B-V)$ for the Vega-like stars, together with the line representing the average relation followed by interstellar polarization and reddening. It can be seen that there are more stars above this line than below it. Also, there is a lack of correlation between polarization and reddening in Vega-like stars for smaller values of reddening. Only at relatively large distances when the interstellar component becomes large does the observed polarization begin to generally increase with reddening.

Circumstellar dust in Vega-like stars absorbs light from the central star and radiates thermally in the infrared. Dust also scatters starlight and produces polarization. One may therefore expect some correlation between the observed polarization in the optical and the excess infrared emission from these objects. In Fig. 4.4 we plot the observed percentage polarization against the excess infrared luminosity due to thermal emission from dust (L_{dust}) as a fraction of the total bolometric luminosity (L_*) of the star (fractional dust luminosity $f_d \equiv L_{dust}/L_*$) for the Vega-like stars. The f_d values of Vega-like stars are computed using the method described in Section 3.1 of Chapter 5.

A positive correlation is apparent from Fig. 4.4. Vega-like stars with relatively larger infrared excesses tend to have larger values of polarization in the optical. The ratio L_{dust}/L_* can be taken to be a rough measure of the dust optical depth τ in the optical where the absorption of starlight takes place. The observed values of the ratio L_{dust}/L_* imply τ in the range $\sim 10^{-6}$ - $\sim 10^{-1}$. For large dust grains (grain size $a \gg \lambda$, the wavelength of light), that are generally thought to dominate the dust disks of Vega-like stars, the absorption and scattering efficiencies can be taken to be ~ 1 . If the polarization is produced by scattering of starlight by the same dust that absorbs stellar radiation and emits thermally in the infrared, then for the observed range of the L_{dust}/L_* ratio the expected range of polarization values would be $\sim 0.0001\% \sim 10\%$. Stars with $L_{dust}/L_* \sim 10^{-2}$ would have polarization up to the level of $\sim 1\%$. Here it is assumed that the circumstellar material is optically thin so that there is single scattering only (Bastien 1987). The maximum linear polarization that can be produced in ellipsoidal models with single scattering is about 1.1% (Shaw 1975). Larger values of polarization can result if the direct light from the central star

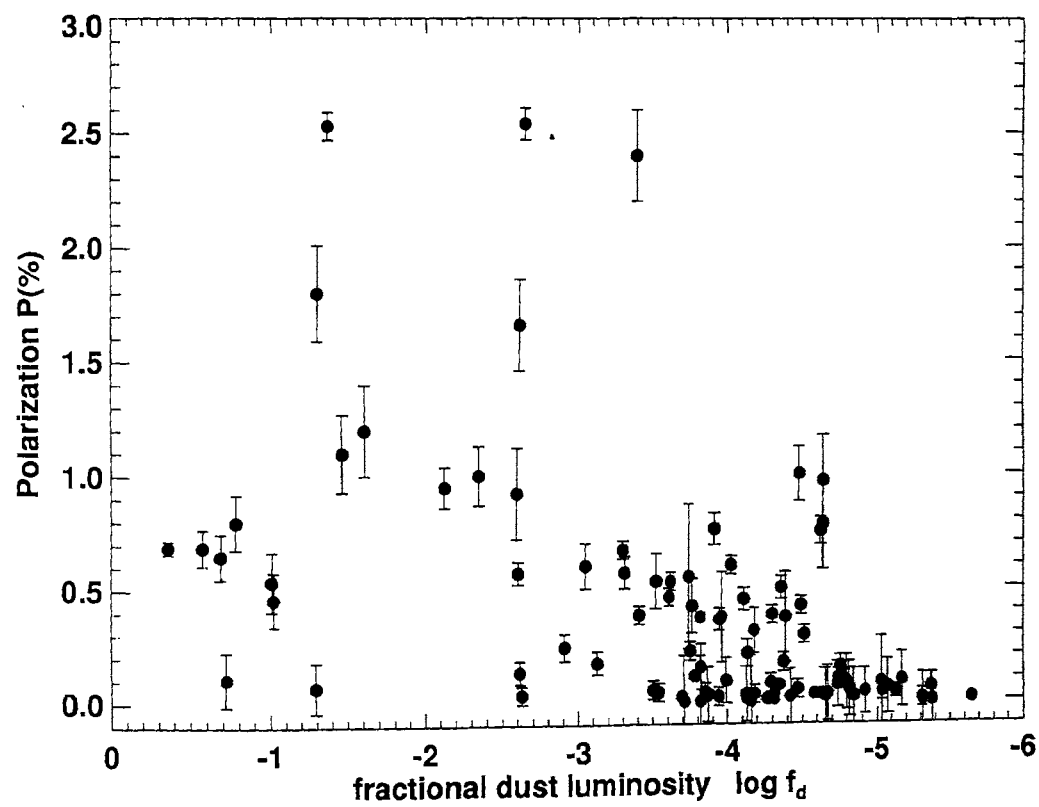


Figure 4.4: Plot of percentage polarization against the fractional infrared excess for Vega-like stars.

is extinguished by obscuring dust in front of the star. Also, the observed polarization depends on the flatness and orientation of the dust disk. It is to be noted from Fig. 4.4 that several stars with $L_{dust}/L_{\star} \sim 10^{-3}$ or less also show polarization $\sim 0.5\%$, much larger than the expected values of $\lesssim 0.1\%$. It is possible that these stars have an additional dust component with smaller grains with high albedo. This population of grains would cause relatively large polarization by scattering without producing large infrared excesses.

4.5 Conclusions

The results of the present study of the polarimetric behaviour of Vega-like stars can be summarized as follows.

- Vega-like stars generally show optical linear polarization that is much larger than that which can be ascribed to interstellar polarization along the line of sight to these relatively nearby objects.
- The anomalous polarization in Vega-like stars is caused by scattering of stellar light due to circumstellar dust distributed in non-spherically symmetric envelopes, and is fully consistent with a distribution in flattened disks.
- The absence of any excess reddening in these stars is consistent with the dust grains in their circumstellar disks being relatively large in size.
- In some Vega-like stars that show relatively small infrared excesses but large values of polarization, an additional component of dust consisting of smaller grains with high albedo may also be present.

Multiwavelength polarization measurements of Vega-like stars would be able to shed more light on the nature and distribution of the dust in their circumstellar environment.

Chapter 5

Kinematics of Vega-like stars and the temporal evolution of the dust disks

5.1 Introduction

It has been well established now that a majority of pre-main sequence stars are surrounded by circumstellar disks which are analogous in their properties to protosolar nebula before the onset of planet formation (Beckwith 1999; Mundy et al. 2000; Wilner & Lay 2000; Beckwith & Sargent 1996). Young circumstellar disks lose most of the material due to planet formation and other disk dispersal processes by the time the central stars harbouring these disks reach the main sequence. In the standard model of planet formation, the dust grains with sizes typical of interstellar dust, settle down to the disk mid-plane and stick together to grow into rocky planetesimals. The disk is depleted of smaller grains and this lowers the opacity of the reprocessing

This chapter is based on the paper *Manoj, P. & H. C. Bhatt, Astrophysics & Space Science Library, Vol. 299, p295, Kluwer Academic Publishers (2003)*

disk. Planetesimals grow further to earth-like planetary bodies by coalescence and eventually accrete gas in the outer disk to form giant planets. When the disk has become sufficiently gas-free, so that it is dominated by grain dynamics, the planetary mass objects can gravitationally perturb kilometer-sized planetesimals sending them into highly eccentric orbits. Collisions between these planetesimals then replenishes the disk with ‘second generation dust’ which are observed around many main sequence stars. These main sequence stars with debris disks, known as ‘Vega-like’ stars, were first discovered by IRAS in 1983 (Aumann et al. 1984). At least 15% of the main sequence stars are surrounded by such disks (Lagrange et al. 2000). Planet formation is well underway in main sequence dusty systems and the disks that we observe are the debris product of the planet formation process. These disks are thought to be ‘sign posts’ of planet formation. What are the lifetimes of these disks? Do disk lifetimes depend on the central star? How do these observed disks evolve in time? These questions are central to our understanding of planet formation and disk dispersal processes. A study of the lifetimes and the temporal evolution of the dust disks, therefore, should provide insight into the formation of planetary systems and disk dispersal timescales and mechanisms.

There have been a number of studies on the evolution of circumstellar disks around main sequence stars. Zuckerman & Becklin (1993) have found that the mass of dust in the disks declines as rapidly as $(time)^{-2}$ during the initial 3×10^8 yr. Similar results have been reported by Holland et al. (1998) from their recent SCUBA observations. There is general agreement now on the fact that the amount of dust retained in the disks decreases with increasing stellar age (Habing et al. 1999; Lagrange et al. 2000). However, the exact nature of this decline is not clear. Most of these studies are based on the ages of a few prototype Vega-like stars. When more stars are employed, reliable estimation of their ages pose a serious problem. It is difficult to determine the ages of main sequence stars with reasonable accuracy. There have been various attempts to estimate ages of field Vega-like stars (eg. Lachaume et al. 1999; Song 2000; Silverstone 2000), but the ages determined using different techniques are not always mutually consistent (Zuckerman 2001). Recently, Spangler et al. (2001) have carried out a survey of circumstellar disks around pre-main sequence and young

main sequence stars which are members of young open clusters of known ages using ISOPHOT. They found that the fractional dust luminosity f_d drops off with stellar age according to the power law $f_d \propto (\text{age})^{-1.76}$. This suggestion of a global power law has been contested by Decin et al. (2003) who find a spread in fractional dust luminosity at any age from the revised age estimates of their sample stars observed by ISOPHOT. Dominik & Decin (2003), based on a physical model that they developed for the dust production in Vega-like disks, have argued that collisional cascade with constant collision velocities leads to a power law decrease of the amount of dust seen in debris disk with a power law index of -1 . They add that collisional cascade with continuous stirring can produce slopes steeper than -1 .

In this chapter we study the temporal evolution of dust disks around main sequence stars. We consider the kinematics of a large sample of Vega-like stars and use the velocity dispersion as an age indicator. It has long been known that there is a strong correlation between the random velocities and ages of stars in the Galactic disk. Velocity dispersion of stars in the solar neighborhood has been found to increase with its age (Wielen 1977; Jahreiß & Wielen 1983). Observationally, velocity dispersion σ is found to grow with age at least as fast as $t^{0.3}$ and more like $t^{0.5}$ (Wielen 1977; Binney & Tremaine 1987). Dynamical origin of this effect is attributed to the encounters between the disk stars and the massive gas-clouds (Spitzer & Schwarzschild 1951, 1953) and to transient spiral waves heating up the Galactic disk (Barbanis & Woltjer 1967). Recently, using accurate *Hipparcos* parallaxes and proper motions, Binney et al. (2000) and Dehnen & Binney (1998) have shown that for a coeval group of stars the rms dispersion in transverse velocity S , which is connected to the principal velocity dispersion by the relation $S^2 = 2/3[\sigma_R^2 + \sigma_\phi^2 + \sigma_z^2]$, increases with time from 8 km.s^{-1} at birth as $t^{1/3}$. We follow this formalism and use the dispersion in transverse velocity to constrain the ages of Vega-like stars in order to study the lifetimes and temporal evolution of the dust disks.

5.2 Data

A number of recent studies give lists of Vega-like stars and candidate Vega-like stars, selected on the basis of their infrared excesses in the *IRAS* wave bands. Song (2000) lists 361 objects taken from different surveys and searches published in the literature. From a search of the *IRAS* FSC catalog, Silverstone (2000) produced a list of 191 Vega-like stars. A number of additional Vega-like objects have been discussed in Coulson et al. (1998) and Malfait et al. (1998). We first compiled a total of 486 distinct Vega-like stars taken from these lists that had many objects in common. This large sample could have some stars that are erroneously classified as Vega-like or have uncertain associations with the *IRAS* sources due to the large *IRAS* beam size. In our study we consider only those stars for which the positional offset between the optical star and the *IRAS* association is $\leq 30''$. Alternative associations have been found for some of the proposed Vega-like stars in the literature (Sylvester & Mannings 2000; Lisse et al. 2002). We have excluded such stars from our sample. We also exclude known pre-main sequence stars (eg. Herbig Ae/Be stars; Thé et al. (1994)) and other emission-line objects from our sample. Further, we consider only stars in the spectral range B9-K5: infrared excess from early B type star could be due to free-free emission (Zuckerman 2001) and K-giants are known to exhibit Vega-like excesses (e.g., Plets et al. 1997; Jura 1999). Finally, our sample contains 249 Vega-like stars for which both *Hipparcos* and *IRAS* (PSC/FSC) measurements are available.

5.3 Analysis

5.3.1 Dustiness of Vega-like Stars

A good measure of the ‘dustiness’ of the disks around Vega-like stars is the fractional dust luminosity $f_d \equiv L_{dust}/L_*$, which represents the optical depth offered by an orbiting dust disk to ultraviolet and visual radiation (Zuckerman 2001). We compute f_d from *IRAS* (PSC/FSC) fluxes for the Vega-like stars in our sample using the

relation

$$f_d = L_{dust}/L_* = \frac{10^{-4} \times [6.45e_{12} + 2.35e_{25} + 1.43e_{60} + 0.55e_{100}]}{10^{[0.4(4.75 - m_V - BC)]}}$$

(Emerson 1988). In the above equation e_{12} , e_{25} , e_{60} , e_{100} are the excess flux densities in Jy over the photospheric values in the IRAS wave bands at 12, 25, 60 and $100\mu m$ respectively, m_V is the extinction corrected visual magnitude of the star and BC the bolometric correction.

The excess flux density in each *IRAS* band was estimated as follows. The photospheric $12\mu m$ magnitude was derived from the extinction corrected V magnitude and (B-V) color of the star as discussed in Oudmaijer et al. (1992). The photospheric magnitudes at the other bands were calculated using the relations given in Oudmaijer et al. (1992). Photospheric magnitudes were then converted into flux densities in the *IRAS* bands by using the magnitude zero points listed in the *IRAS* catalogue, and then color corrected to a photospheric SED (e.g., Silverstone 2000). The photospheric estimates in the *IRAS* catalogue color convention were subtracted from the corresponding non-upper limit *IRAS* PSC/FSC flux densities to obtain the excess flux densities e_λ in each of the *IRAS* bands.

In order to account for the possible inexact approximation of the photosphere, the excesses computed are considered, as in Silverstone (2000), to be significant only if it exceeds 20% of the photospheric flux value in each of the bands. Stars with significant excess in any one of the bands are taken as ‘true’ Vega-like and their f_d is computed as described above. Fractional dust luminosities thus computed for 203 ‘true’ Vega-like systems agree well with earlier estimates in the literature (Backman & Gillett 1987; Song 2000; Silverstone 2000), generally to within 10%. We find a number of stars with excesses less than 20% of the photospheric fluxes in all the four *IRAS* bands. The excesses, if any, that these stars show are at a very low level. However, these stars have been classified as Vega-like stars in earlier studies in which excesses were inferred by different methods. We assign an upper limit value of 10^{-6} for f_d of these stars as the values of f_d computed for the ‘true’ Vega-like stars with significant excess are always $> 10^{-6}$.

5.3.2 Kinematics - Transverse Velocities of Vega-like Stars

For all the stars in our sample we have proper motions and parallaxes from *Hipparcos* catalog (ESA 1997). The transverse velocity perpendicular to the line of sight relative to the solar system barycenter is then computed using the relation $V_T = \frac{A_v \mu}{\pi}$ where $A_v = 4.740470 \text{ km yr s}^{-1}$, π is the parallax in *milliarcseconds* and $\mu = (\mu_\delta^2 + (\mu_\alpha \cos \delta)^2)^{1/2}$ with μ_δ and $\mu_\alpha \cos \delta$ being the proper motions along declination and right ascension in *milliarcseconds*. Errors in transverse velocities are estimated from the probable errors in parallaxes and proper motions given in *Hipparcos*. Transverse velocities of stars thus obtained will have solar motion reflected in them. We have corrected the velocities for solar motion using the values of $U = 10.0 \pm 0.4 \text{ km s}^{-1}$, $V = 5.2 \pm 0.6 \text{ km s}^{-1}$, $W = 7.2 \pm 0.4 \text{ km s}^{-1}$ (Binney & Merrifield 1998) for the standard solar motion. To minimize the effect of Galactic differential rotation we consider only stars within 250 pc from the Sun. Further, we include only those stars in our analysis that have fractional error in transverse velocity less than 0.5. We have, then, 174 Vega-like stars with transverse velocities and fractional dust luminosities computed for the final analysis.

5.4 Results

As mentioned earlier the velocity dispersion of a group of stars is an indicator of the average age of the group. We use velocity dispersion as an age indicator to constrain the ages of the stars with dusty disks in order to study the disk lifetimes and evolution. The velocity dispersion of all the Vega-like stars in our final sample is found to be $22.2 \pm 1.2 \text{ km/sec}$. The velocity dispersion of field stars (B9 - K5) within 250 pc and whose fractional error in transverse velocity is less than 0.5 is computed to be $37.3 \pm 0.2 \text{ km/sec}$. The smaller velocity dispersion for Vega-like stars compared to field stars indicate, at the very outset, that the main sequence dusty systems are younger than the field stars and that the debris disk lifetimes are shorter than the main sequence lifetimes of the stars. In the following we analyse the spectral type dependence of the velocity dispersion of Vega-like stars.

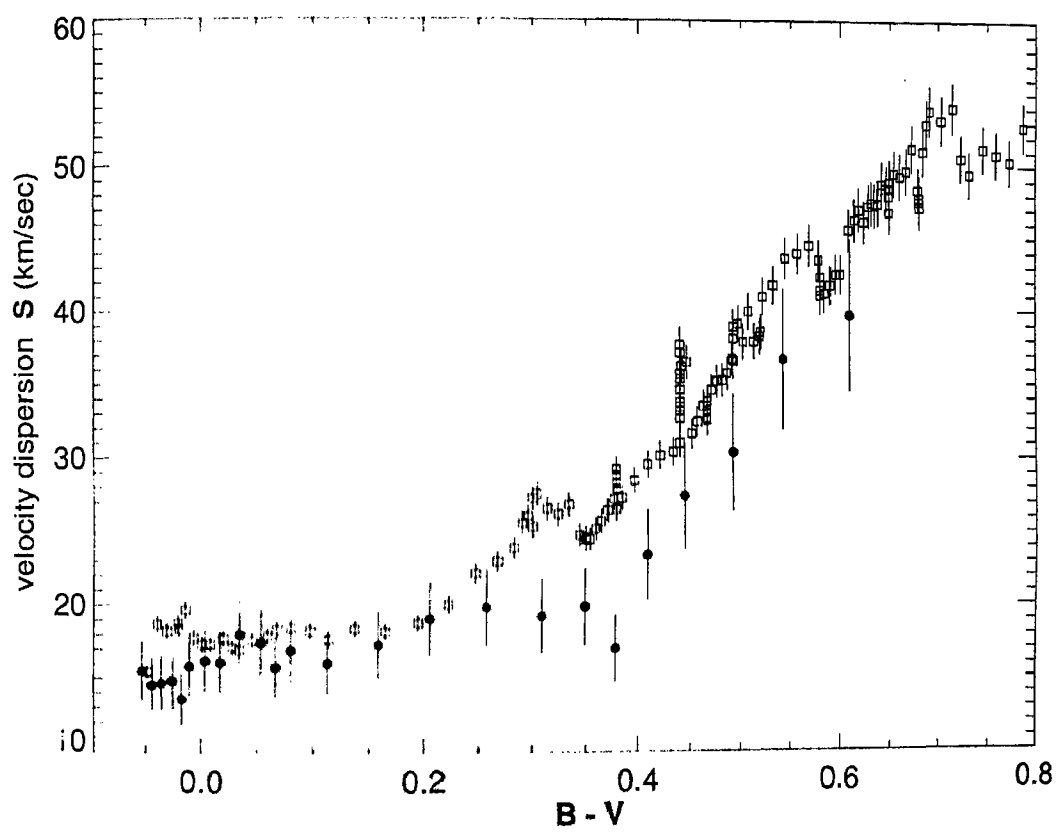


Figure 5.1: Transverse velocity dispersion S plotted against the dereddened color ($B-V$) for Vega-like stars. Filled circles represent Vega-like stars and open squares the normal field stars.

In Figure 5.1 we plot velocity dispersion against the dereddened ($B - V$) color of Vega-like stars. The values of transverse velocity dispersion S shown here are for a sliding window of 30 stars plotted against the mean ($B - V$) for each bin. A fresh point is plotted every time 6 stars have left the window. We have overplotted velocity dispersion of field stars in the figure for comparison. The values of S plotted for field stars are for bins of 500 stars with a fresh point plotted when 100 stars have left the window. The error bars plotted in S are the standard deviation of dispersion in each bin which is given by $\Delta S = S/\sqrt{(2n - 2)}$ where n is the number of stars in the bin. It can be seen that, on the average, Vega-like stars show a lower velocity dispersion than the field stars at any given ($B - V$). While this trend is clearly evident on visual inspection for stars with $B - V \geq 0.3$ (spectral type F0 or later), it is not as striking for stars of early spectral type, though, in general, their velocity dispersions are smaller than the field stars. A two-sided two dimensional Kolomogorov-Smirnov test shows that the velocity dispersion - ($B - V$) relation for Vega-like stars and field stars to be different to 99.99%. Thus, Vega-like stars have lower velocity dispersion than the that of field stars for any given spectral type. Since lower velocity dispersion indicate smaller ages, it follows that main sequence dusty systems are systematically younger than field stars of similar spectral type. In other words the detectable debris disks harboured by main sequence stars do not last for the entire lifetimes of the stars. It can also be seen from Figure 5.1 that late type Vega-like stars have larger velocity dispersion than early type Vega-like stars suggesting that statistically they are older. This would mean that the debris disks survive longer around late-type main sequence stars.

In order to quantify the disk lifetimes of Vega-like stars, we relate the velocity dispersion to the stellar age following the formalism of Binney et al. (2000) where the velocity dispersion for a coeval group of stars as a function of age is given by $S = v_{10}[(\tau + \tau_1)/(10Gyr + \tau_1)]^\beta$. In this equation τ_1 determines the random velocity of stars at birth, and v_{10} and β characterize the efficiency of stellar acceleration. Using values of $\beta = 1/3$, $v_{10} = 58kms^{-1}$ and $\tau_1 = 0.03Gyr$ (Binney et al. 2000) we translate velocity dispersion into age. In Figure 5.2 we plot the ages thus derived against ($B - V$) for Vega-like stars along with that for field stars. The vertical error bars plotted are

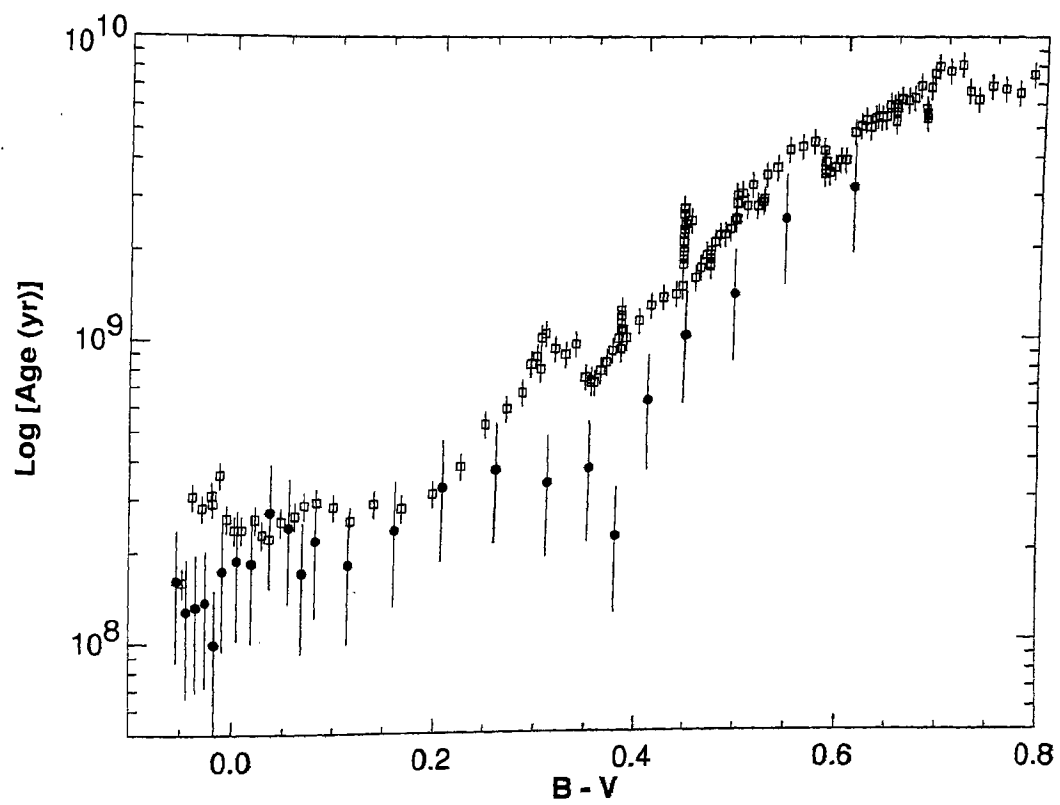


Figure 5.2: Ages derived from velocity dispersion plotted against dereddened color ($B-V$) for Vega-like stars. Filled circles are Vega-like stars and open squares are normal field stars.

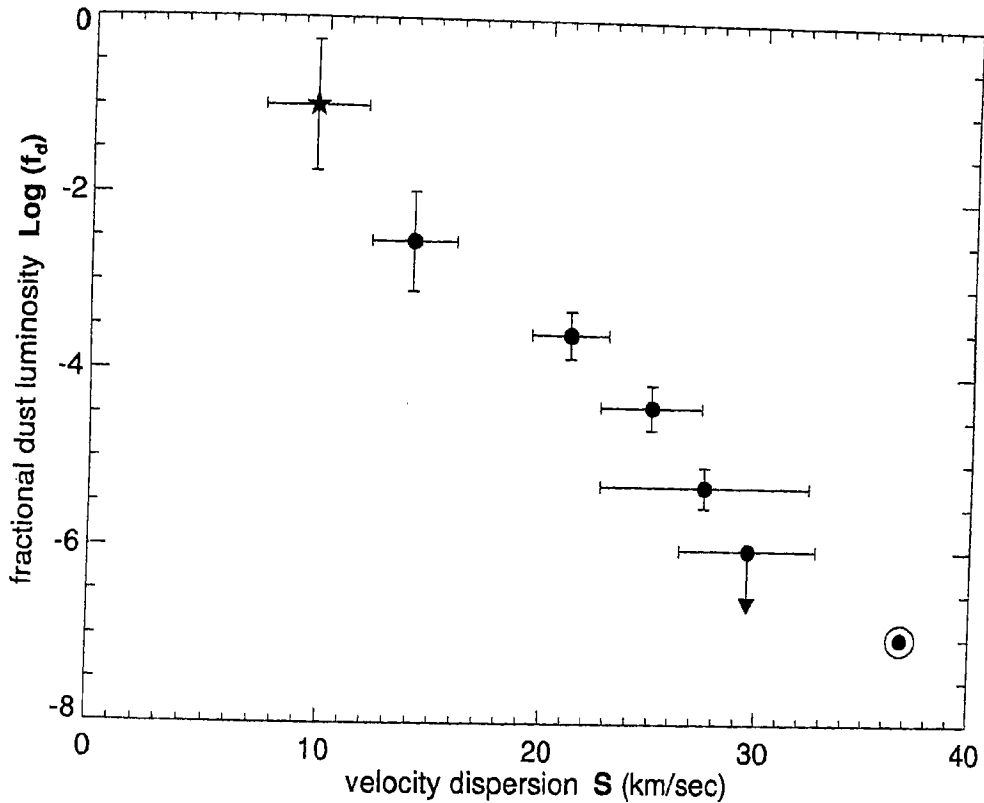


Figure 5.3: Fractional dust luminosity f_d plotted against transverse velocity dispersion S for stars with disks. Filled circles represent Vega-like stars. Herbig Ae/Be stars are also plotted, represented by the solid star symbol. The point with a downward arrow are for stars whose infrared excesses are below the significance level (see text). The open circle with a dot represents normal field stars.

the errors in S translated into errors in ages. The figure shows Vega-like stars to be systematically younger than the field stars for all values of $(B - V)$ indicating that the lifetimes of debris disks are shorter than the main sequence lifetimes of the stars which harbour them. Further, the ages of Vega-like stars is seen to range from 10^8 yr to $\sim 2 - 3 \text{ Gyr}$ with late type Vega-like stars, on the average, being older than the early type Vega-like stars. In terms of absolute ages, debris disks last longer around late type stars, a conclusion also reached by Song (2001). Though the disks can survive as long as $2 - 3 \text{ Gyr}$ around late type stars, these disks do not last for the entire main sequence lifetimes of the stars.

Next, we turn to study the evolution of the ‘dustiness’ of circumstellar disks with age. We look for a correlation between fractional dust luminosity f_d and transverse velocity dispersion S for stars of similar f_d . For this we grouped the stars into bins of a given range in dustiness (f_d). We then computed the dispersion in transverse velocities of stars in each of these bins. The mean value of f_d in each bin is then plotted against the velocity dispersion of stars in that bin as shown in Figure 5.3. Error bars for f_d represent the standard deviation from the mean in each bin. Error bars in S are obtained as discussed earlier. The point with a downward arrow represents stars which were assigned an upperlimit value for $f_d \leq 10^{-6}$. The open circle with a dot plotted in the figure represents field stars (B9-K5) which are within a distance of $250pc$ and with fractional errors in transverse velocities less than 0.5. In Figure 5.3, we also include Herbig Ae/Be stars which are pre-main sequence stars of intermediate mass and are thought to be the progenitors of Vega-like stars. We computed V_T and f_d for 44 Herbig Ae/Be stars taken from Thé et al. (1994), van den Ancker et al. (1998) and Malfait et al. (1998), and for which *Hipparcos* and *IRAS* measurements are available. As for Vega-like stars we restrict ourselves to stars within $250pc$ and with fractional errors in transverse velocities less than 0.5. We have 22 such Herbig Ae/Be stars. Their average f_d is plotted against the velocity dispersion S and is represented by the filled star symbol in Figure 5.3.

It is clear from Figure 5.3 that there is a systematic decrease in the dustiness (f_d) of the disks with increasing velocity dispersion S of stars. Herbig Ae/Be stars have velocity dispersion S smaller than the Vega-like stars indicating younger ages. As discussed earlier, the velocity dispersion S of stars, in general, is found to increase with stellar age as $S \propto t^{1/3}$ (Binney et al. 2000). The correlation between fractional dust luminosity of stars with disks and their velocity dispersion seen in Figure 5.3 clearly implies a steady decrease in the optical thickness of the disks with stellar age. This is consistent with the earlier findings that the amount of dust in the disks appears to decrease generally with system age.

We note here that the correlation that we find between f_d and velocity dispersion is not because of the spectral type dependence of velocity dispersion that we discussed above. Such a manifestation is expected if f_d has a spectral type dependence where

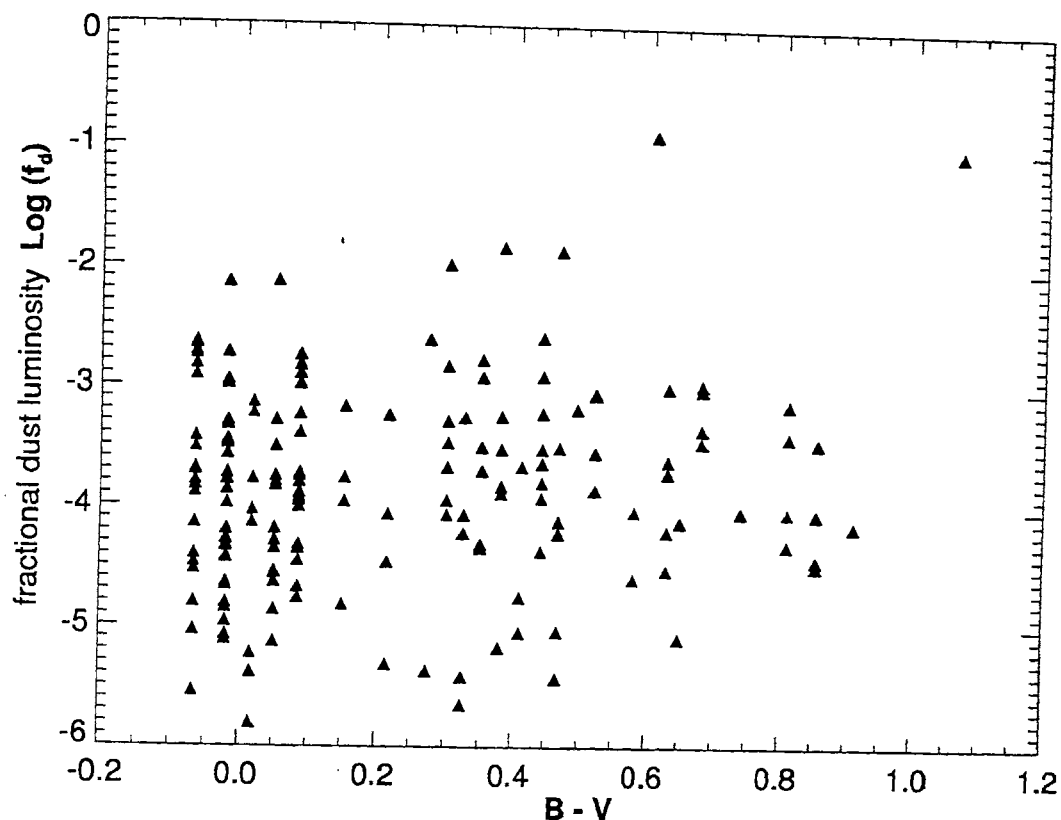


Figure 5.4: Fractional dust luminosity f_d plotted against dereddened color ($B - V$) for Vega-like stars.

the late type stars preferentially have lower values of f_d . However, for our sample stars, we find that there is no such trend of f_d with spectral type. In Figure 5.4 we present a plot of f_d against ($B - V$) where it can be seen that there are as many or more early type stars with lower values of f_d as there are late type stars.

In order to quantify the temporal evolution of the dustiness of disks around stars, we translate velocity dispersion into age using the formalism of Binney et al. (2000) as described earlier. In Figure 5.5 we plot f_d against the stellar ages thus obtained. The star symbol represent Herbig Ae/Be stars and the filled circles Vega-like stars. The point with a downward arrow represents stars which were assigned an upperlimit value for $f_d \leq 10^{-6}$. The open circle with a dot plotted in the figure represents field stars. The vertical error bars in Figure 5.5 are the same as those in Figure 5.3. Horizontal error bars represent errors in velocity dispersion translated into errors in age. The

steady drop of fractional dust luminosity with increasing stellar age is evident from Figure 5.5. There is an overall decrease in the ‘dustiness’ of the circumstellar disks from the early pre-main sequence phase to well upto the late main sequence phase. It can be seen from Figure 5.5 that the Herbig Ae/Be stars have larger values of f_d and younger ages than Vega-like stars. This is consistent with them being progenitors of Vega-like stars.

We note here that the ages that we derive from velocity dispersion are statistical in nature. They are the average ages appropriate for the velocity dispersion shown by the group of stars and are derived from the relation between velocity dispersion and age given by Binney et al. (2000). The ages obtained this way have large errors for small ages as can be readily seen from Figure 5.5. This is because of the fact that for small ages velocity dispersion S is a steeply rising function of age for the relation $S \propto t^{1/3}$.

5.5 Discussion

As discussed earlier, the primary difficulty in studying the temporal evolution of main sequence debris disks has been the problem of age determination of the individual main sequence stars. We have used velocity dispersion as an age indicator to constrain the ages of the main sequence Vega-like stars. Velocity dispersion of a group of stars is known to be a measure of the statistical age of that group. From our analysis, we have been able to study the debris disk lifetimes and its dependence on spectral type and the temporal evolution of the ‘dustiness’ of the circumstellar disks.

We find that the main sequence stars with debris disks have smaller velocity dispersion than normal field stars for all spectral types (B9-K5). This suggests that the stars with debris disks are statistically younger in age than the field stars of similar spectral type. Vega-like stars being a younger population than field stars argues for disk lifetimes that are shorter than the main sequence lifetimes of the stars. The debris disk may not survive for the entire lifetime of the central star. However, it is possible that this is a selection effect as *IRAS* will not be able to detect low luminosity

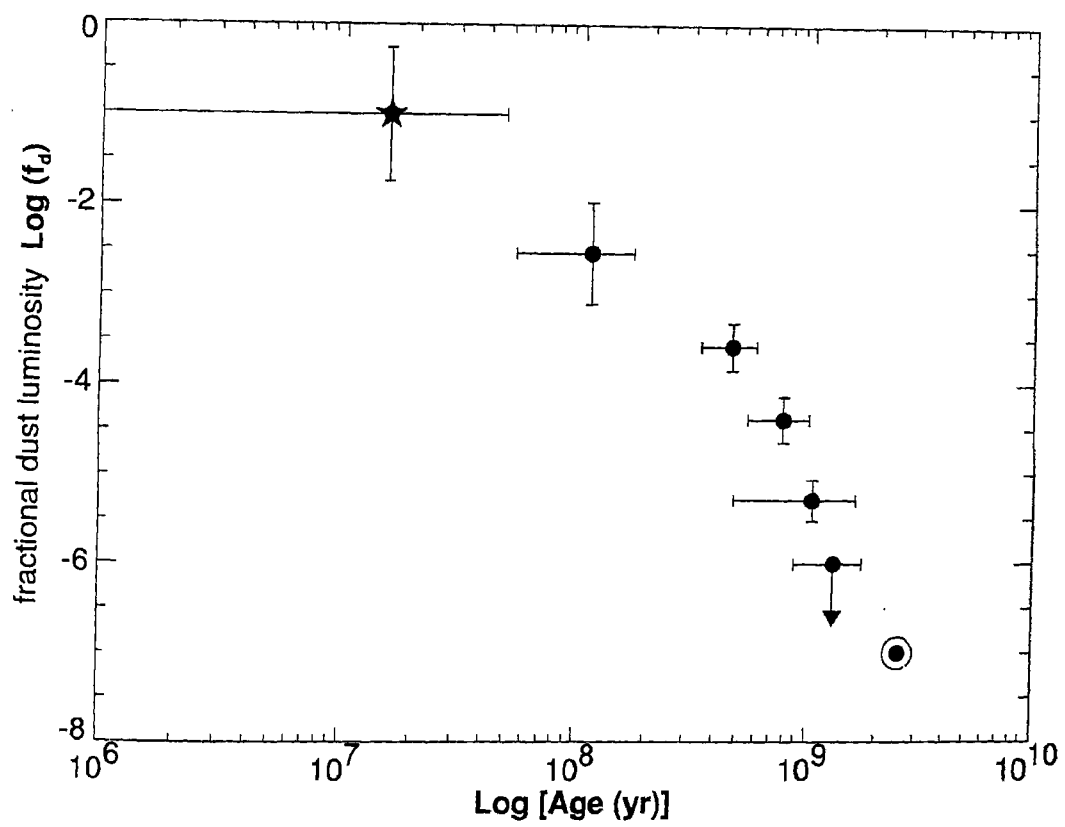


Figure 5.5: Fractional dust luminosity plotted against the average ages derived from velocity dispersion. The symbols have the same meaning as in Figure 5.3.

disks below its sensitivity limit. The luminosity of debris disks gradually go down as the central stars age and eventually fall below the limit of detection. This is expected physically as the larger bodies which replenishes the disk are getting eroded continuously and are finite in supply. We also find such a fall in fractional dust luminosity of debris disks with age as demonstrated in Figure 5.5. A dust debris of low optical depth $f_d \leq 10^{-7}$ like that around the Sun may be present over the entire lifetimes of the main sequence stars.

The ages of Vega-like stars are found to range from $10^8 yr$ to $2 - 3 Gyr$ with Vega-like stars of later spectral types being older on the average than stars of early spectral types. Ages of early type Vega-like stars span from $10^8 yr$ to $4 - 5 \times 10^8 yr$ while late type Vega-like stars can be as old as $2 - 3 Gyr$. Main sequence dusty systems of earlier spectral type being systematically younger than the late type systems strongly suggests shorter lifetimes for debris disks around early type stars. This would mean that the temporal evolution of main sequence disks is a function of the spectral type of the central star with debris disks surviving longer around late type stars. This is not surprising as the timescales for grain removal processes like radiation pressure ‘blowout’ and Poynting-Robertson drag which dominate Vega-like disks are inversely proportional to the stellar luminosity and thus are shorter for early type stars.

We further find a strong correlation between the fractional dust luminosity f_d of stars with circumstellar disks and the velocity dispersion which is a statistical measure of the average age of the stars. The fractional dust luminosity is found to steadily decrease with increasing velocity dispersion. Translating velocity dispersion into age, we obtain the behaviour of f_d with stellar age as demonstrated in Figure 5.5. There is an overall decline in the fractional dust luminosity f_d of stars with circumstellar disks with increasing stellar age. Fractional disk luminosity falls steadily from pre-main sequence disks to main sequence debris disks until the disk luminosity falls below the current detection limit ($f_d \leq 10^{-7}$).

In Figure 5.3 and Figure 5.5 we have plotted both Herbig Ae/Be stars and Vega-like stars together and have derived an overall decline in fractional dust luminosity with stellar age. We point out here that the pre-main sequence disks like that around

Herbig Ae/Be stars and the main sequence disks are physically different. Pre-main sequence disks are optically thick ($f_d \sim 0.1$) and gas-rich and are formed from the primordial cloud core from which the star itself was born. The infrared excess that the *IRAS* detect in these disks is due to the re-radiation from the first generation dust grains. On the other hand, the excess shown by Vega-like disks is due to the debris dust produced in the collisions between larger bodies. The debris disks are gas-poor and the disk evolution is dominated by dust dynamics. Moreover, the decline in the fractional dust luminosity in the pre-main sequence disks is primarily due to the grain growth by which smaller sub-micron sized grains get depleted in the disks thereby reducing the effective surface area of dust absorption/emission. In main sequence debris disks where the grains causing infrared excess are being continuously replenished, the fall in f_d is due to the decline in the collisional regeneration rate. Nevertheless, it is expected that the pre-main sequence disks gradually evolve into Vega-like disks though it is not clear at the moment when exactly the secondary dust generation begins in these disks. Recent studies suggest that in general the lifetimes of primordial disks are only a few *Myr* (Hillenbrand 2002; Haisch et al. 2001; Lada 1999). Larger bodies like kilometer-sized planetesimals and comets, which replenishes the main sequence debris disks can also be formed within a few *Myr* (eg. Beckwith et al. 2000). Thus the transition of optically thick disks to optically thin disks is expected to take place in similar timescales. The resolution of the stellar ages derived from velocity dispersion is poor and is inadequate for addressing the issue of timescale of the transition from primordial pre-main sequence disks to Vega-like disks. However, a general decline in the ‘dustiness’ of the disks with stellar ages from pre-main sequence phase to late main sequence phase is clearly seen.

The results that we obtain from our analysis are consistent with earlier studies on the disk evolution around main sequence stars. The overall decline in the dust content of the debris disks has been reported by Zuckerman & Becklin (1993). Holland et al. (1998) and Spangler et al. (2001). The conclusions of Decin et al. (2003) that there are few young stars with small excesses and Vega-like excess is more common in young stars than in old stars are consistent with our result of Vega-like stars being younger than field stars for all spectral types. Decin et al. (2003) also argue that at most ages,

there is a spread in fractional dust luminosity of Vega-like stars. While this may be true, our results strongly suggest that there is also a general decline in the f_d of the disks with stellar ages. However, it is not clear from our study if this fall of f_d is governed by a global power law as suggested by Spangler et al. (2001) and Zuckerman & Becklin (1993) who find a power law of $f_d \propto t^{-2}$. Recently, Dominik & Decin (2003) have argued in favour of a power law of index of -1 if the dust production mechanism in Vega-like disks is collisional cascade with constant collision velocities. A collisional cascade which is continuously stirred can produce slopes steeper than -1 . We are not able to fit a single power law to the fall in f_d with the average stellar ages that we derive from velocity dispersion of the stars.

5.6 Conclusions

In this chapter we have used the velocity dispersion as an age indicator to constrain the ages of a large sample of Vega-like stars. From the statistical ages derived from the velocity dispersion we have studied the disk lifetimes and the temporal evolution of the dust disks around main sequence stars. The conclusions of this study are summarized below.

- Velocity dispersion of Vega-like stars is found to be smaller than that of the main sequence field stars for all spectral types. Main sequence stars with debris disks, on the average, are younger than the field stars of similar spectral type.
- The ages of Vega-like stars derived from velocity dispersion range from 10^8 yr to $2 - 3$ Gyr.
- Vega-like stars of later spectral types are statistically older than stars of early type. Debris disks survive longer around late type stars than early type stars.
- There is a strong correlation between fractional dust luminosity and velocity dispersion of Vega-like stars. Average fractional dust luminosity f_d of stars with disks decreases monotonically with increasing velocity dispersion.

-
- Fractional dust luminosity of main sequence stars with debris disks is found to fall steadily with increasing stellar age. There is a general decline of f_d with stellar age right from early pre-main sequence phase to late main sequence phase.
 - The observed high f_d , lower velocity dispersion S and the implied younger ages for Herbig Ae/Be stars are consistent with them being progenitors of Vega-like stars.

Chapter 6

A disk census of nearby OB associations

6.1 Introduction

In Chapter 2 we found that the accretion rates in intermediate mass stars tend to fall with increasing age of the stars during the first 10 Myr of the pre-main sequence evolution. It would be instructive to see if this trend continues beyond that age range. Additionally, the transition of circumstellar disks around young stars from being optically thick to optically thin is believed to take place during the late pre-main sequence phase. Identification and detailed studies of the disks around stars in the age range of 10-50 Myr is important for our understanding of the evolution and eventual dissipation of pre-main sequence disks. Member stars of nearby OB associations which are in the age range of 5-50 Myr are best suited for such studies. Here we study the disk properties of the stars which are known members of young OB associations. First we identify stars with disks in the associations based on the near-infrared excess emission shown by these objects. We then study the disk evolution and properties of the stars thus identified.

Empirical knowledge of disk evolution can be derived and disk lifetimes deter-

mined from the study of disk frequency in young clusters and associations of varying ages. Young clusters and associations are ideal targets for such a study because of the relatively uniform distance, age, chemical composition and star formation history of their member stars. Also, the frequency of disks within a cluster or an association is directly related to the physical process of disk formation and evolution. A number of near-infrared studies of young embedded clusters have found that the initial disk frequency in a cluster can be as high as 80-85% and disk lifetimes as short as 5-6 Myr (e.g., Strom et al. 1993; Kenyon & Hartmann 1995; Lada et al. 1996; Carpenter et al. 1997; Lada 1999; Haisch et al. 2001). Observations show a rapid decline in the disk fraction with cluster age such that half the disks in a cluster being lost within 2-3 Myr (Lada & Lada 2003). Such a short timescale for disk evolution has placed stringent constraints on the timescale for building giant gaseous planets, the formation times of which is generally thought to be 10^7 yr or longer (Lissauer 2001). Recently, Hillenbrand (2002) have studied the inner disk evolution of a sample of ~ 3000 field and cluster member stars, located ~ 50 -800 pc from the Sun. Utilizing the measured emission above photospheric level at near-infrared wavelengths which probes hot gas and dust in the inner 0.05 - 0.1 AU of the disk, they find a steady decline in the fraction of stars with inner disks with time. They find the median lifetime of inner disk to be as short as 2-3 Myr. The authors further note that although most disks evolve relatively rapidly, a small fraction may retain such disks 5-10 times longer than the average.

In the studies of disk frequencies in clusters and associations discussed above, the age range that is poorly represented is 10-50 Myr. Only very few stars in this age range are known. This is primarily because of the difficulty in identifying such stars from the field population as they stand out from older field stars only with detailed observations. As mentioned earlier this age range is nevertheless important for disk evolution studies because the transition from optically thick to optically thin disks is believed to take place during this phase. OB associations, which are 'fossil' records of star formation, are excellent targets for the study of disk evolution in this age range of 5- 50 Myr.

OB associations are young (≤ 50 Myr) stellar groupings of low density containing

a significant population of B stars. They are unbound “moving groups” which can be detected kinematically because of their small internal velocity dispersion. Their projected dimension usually vary from $\sim 10 pc$ to $\sim 100 pc$ (e.g., Brown et al. 1999). The traditional astrometric membership determination by ground based proper motion studies were confined to only bright stars ($V \leq 6$) due to the large extent of nearby associations in the sky. As a result membership for many associations had been determined unambiguously only for spectral types earlier than B5. However, the *Hipparcos* catalog which contains accurate positions, proper motions and trigonometric parallaxes for $\sim 120\,000$ stars and which has a limiting magnitude of $V \sim 12$, and is complete to $V \sim 7.3$ in the Galactic plane, and to $V \sim 9$ in the polar regions, has improved the situation dramatically. Using the *Hipparcos* catalog, de Zeeuw et al. (1999) have identified astrometric members of moving groups by combining the refurbished convergent point method of de Bruijne (1999) with the “spaghetti method” of Hoogerwerf & Aguilar (1999). They list astrometric members of 12 young OB associations with ages in the range of 3 - 50 Myr, out to a distance of $\sim 650 pc$.

In this chapter we study the disk frequencies and lifetimes in 12 nearby OB associations, the *Hipparcos* members of which are listed by de Zeeuw et al. (1999). Using the 2MASS near-infrared photometry available for the members of these associations we first identify stars with disks based on the excess emission shown at near-infrared wavelengths. We then estimate the disk fractions in these associations and study its behaviour as a function of the mean age of the association. Further, we look for possible evolutionary trend between the magnitude of the excess shown by the stars with disks and the ages of the associations to which those stars belong. This chapter is organized as follows. In Section 6.2 we present the data for all the 12 associations and describe our analysis of identifying stars with inner disks. Results of the study are presented and their implications discussed in Section 6.3. We summarize our conclusions in Section 6.4.

OB Association	Age (Myr)	Mean Distance (pc)	Number of Hipparcos members
Cepheus OB2	5	615	71
Collinder121	5	592	103
Upper Scorpius	5	145	120
Perseus OB2	4-8	318	41
Lower Centaurus Crux	10	118	180
Vela OB2	10	410	93
Upper Centaurus Lupus	13	140	221
Trumpler10	15	366	23
Lacerta OB1	16	368	96
Cassiopeia-Taurus	50	210	83
Perseus OB3 (α Per)	50	177	79
Cepheus OB6	50	270	20

Table 6.1: Properties of the 12 OB associations studied

6.2 Data and analysis

The basic data on the 12 OB associations studied are given in Table 6.1 where mean distances, ages and number of *Hipparcos* members (de Zeeuw et al. 1999; Brown et al. 1999) of these associations are listed.

We use the excess emission at the near-infrared wavelengths as evidence for the presence of circumstellar disks around stars which are members of these associations. In order to pick out stars with excess emission, we compile the J , H , and K_s magnitudes of the astrometric members of the 12 OB associations from 2MASS All-Sky Point Source Catalog. As a first step in identifying stars with circumstellar disks we plot near-infrared color-color diagram for the members of all the associations. In Figure 6.1 we present the 2MASS color-color $(J - H) - (H - K_s)$ constructed for the member stars of the 12 OB associations. In the figure crosses represent stars in the associations. The solid line in the $(J - H) - (H - K_s)$ diagram represents the main

sequence. The colors for the main sequence stars are from Koornneef (1983) which are then converted into 2MASS system following Carpenter (2001). The two parallel dotted lines in the diagram form the reddening band for normal stellar photospheres. These lines are parallel to the reddening vector and bound the range in the color-color diagram within which stars with purely reddened normal stellar photospheres can fall (Lada & Adams 1992). Stars with excess emission due to circumstellar material fall to the right of the reddening band in the color-color diagram. In each of the diagrams we have also plotted Herbig Ae/Be stars, which are represented by open circles in the plots, for comparison. A visual inspection of the $(J - H) - (H - K_s)$ color-color plots shows that there are very few stars with strong near-infrared excess in these 12 associations. A few stars which show relatively high near-infrared excess in Upper Scorpius (HD 150193 & HD 145718), Lower Centaurus Crux (HD 100453 & HD 100546) and Upper Centaurus Lupus (HD 152404) are known HAeBe stars. However, the fraction of stars with circumstellar disks in these associations are relatively very low. Also, the level of excess emission shown by those stars with disks is relatively low except for the known HAeBe stars in the three associations mentioned above.

In order to quantify the near-infrared excess from the stars in the OB association we use the quantity $\Delta(H - K)$ which is defined as

$$\Delta(H - K) = (H - K) - (H - K)_o - 0.0645 \times A_V$$

where $(H - K)$ is the observed color, $(H - K)_o$ the intrinsic color corresponding to the spectral type of the star and $0.0645A_V$ represents the interstellar reddening with A_V the visual extinction towards the star. The intrinsic color excess $\Delta(H - K)$ is a measure of the strength of emission from the disks. To compute $\Delta(H - K)$ we first converted observed 2MASS colors $(H - K_s)$ to the Koornneef (1983) system following the color transformations given in Carpenter (2001). The intrinsic colors of the stars are taken from Koornneef (1983) corresponding to the spectral type listed in the *Hipparcos* catalog for the stars. We calculate the visual extinction towards the star from $E(B-V)$ using the average interstellar law $A_V = 3.1 \times E(B - V)$. The color excess $E(B-V)$ is computed from the Tycho B_T and V_T magnitudes converted to the Johnson system following Mamajek et al. (2002) and from the intrinsic $(B-V)$ colors

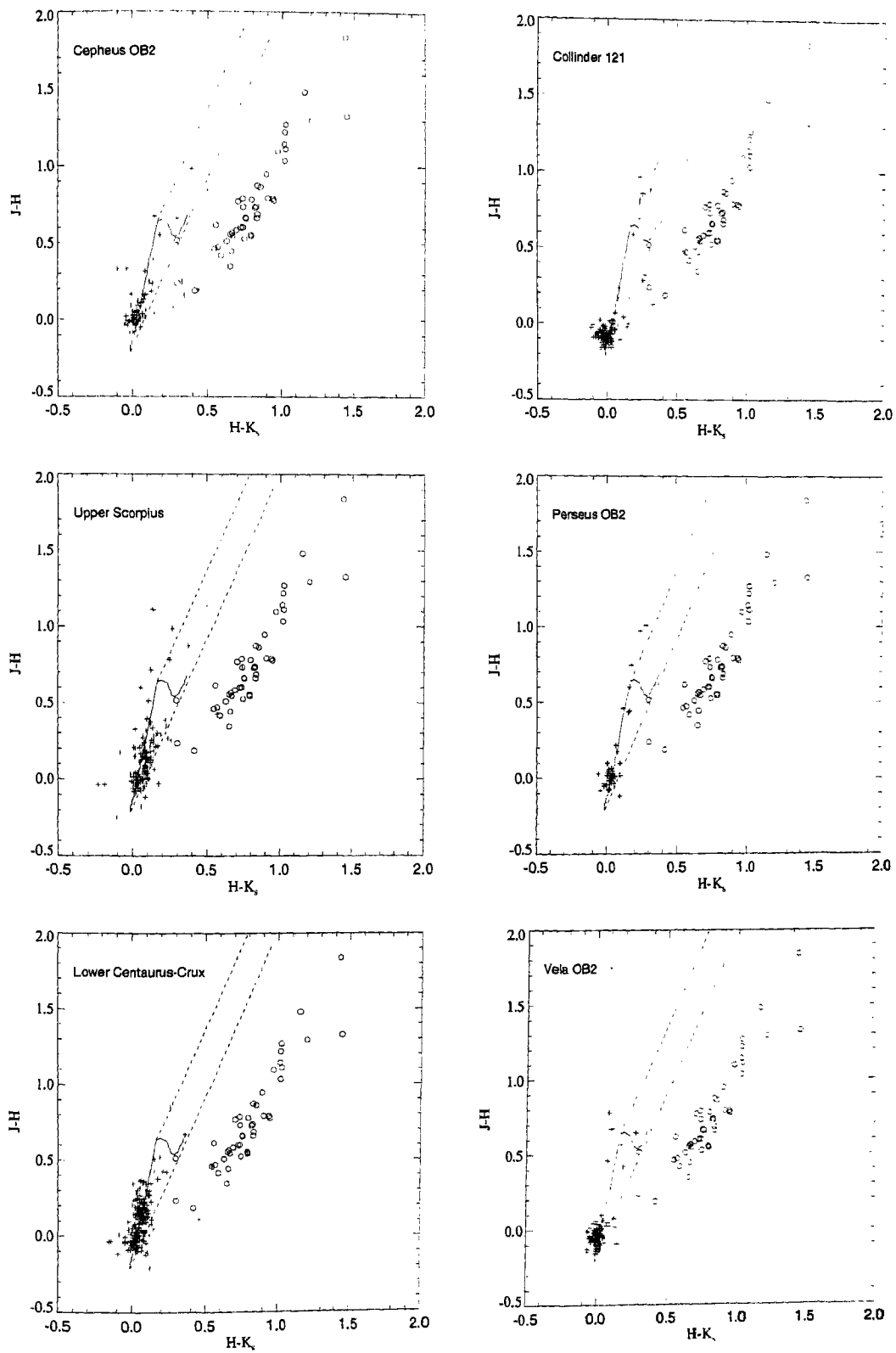


Figure 6.1: 2MASS color-color diagram for stars of OB associations. Crosses are member stars of OB association. Open circles denote H AeBe stars.

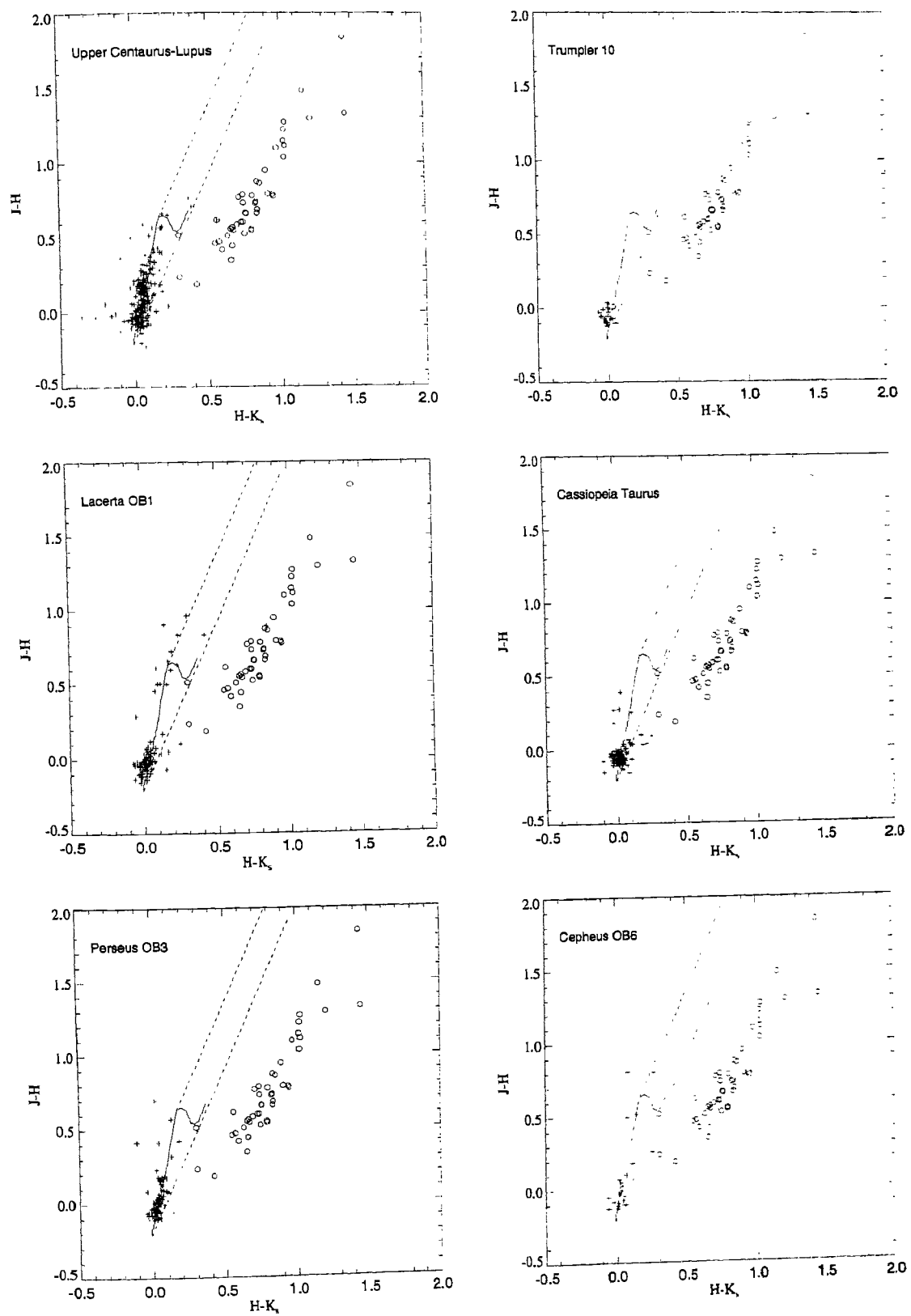


Figure 6.1: 2MASS color-color diagram for stars in the OB associations. Crosses represent OB association member stars and open circles denote HAeBe stars.

corresponding to the spectral type of the stars taken from Schmidt-Kaler (1982).

Here we note that among *Hipparcos* members of 12 OB associations listed by de Zeeuw et al. (1999) most are of spectral type B, A and F. There are also a few later type stars which are listed as association members. However, the association membership for late type stars is very incomplete. Early type stars, on the other hand, are better represented in the *Hipparcos* census. In the following we consider only stars of early spectral types (B, A and F) in our analysis of disk frequency and evolution in the OB associations.

The intrinsic color excess $\Delta(H - K)$ is used to infer the presence of inner accretion disks in stars. In the analysis that follow stars for which $\Delta(H - K) > 0.05$ and fractional error in excess $e_{\Delta(H-K)}/\Delta(H - K) < 0.5$ are considered to have inner disks. Stars of early spectral type (B, A and F) which are identified to have circumstellar disks using the above criterion in the 12 OB associations studied are listed in Table 6.2. The *Hipparcos* and HD identifiers are listed in columns 1 and 2 of the table. Spectral type and E(B-V) are given in columns 3 and 4 and $\Delta(H - K)$ and error in $\Delta(H - K)$ in the last two columns.

Table 6.2: Stars identified to have inner disks in the OB associations

HIP Number	HD Number	Spectral Type	E(B-V)	$\Delta(H - K)$	$e_{\Delta(H-K)}$
Cepheus OB2					
105699	204116	B1Ve	0.763	0.271	0.028
107164	206773	B0V:pe	0.434	0.367	0.039
111785	240010	B1:IV:	0.719	0.419	0.054
Collinder 121					
32292	48917	B2V	0.101	0.327	0.065
33673	52356	B3V(n)	0.050	0.167	0.060
33769	52597	B2/B3V	0.116	0.177	0.044
Upper Scorpius					
<i>continued on next page</i>					

<i>continued from previous page</i>					
HIP Number	HD Number	Spectral Type	E(B-V)	$\Delta(H - K)$	$e_{\Delta(H-K)}$
78207	142983	B8	0.011	0.274	0.101
79476	145718	A8III	0.183	0.619	0.038
79739	146285	B8V	0.301	0.104	0.045
80338	147648	B8II	0.729	0.112	0.037
81624	150193	A1V	0.498	0.798	0.022
Perseus OB2 – No stars with excess					
Lower Centaurus Crux					
56354	100453	A9V	0.020	0.919	0.049
56379	100546	B9Vne	0.073	0.648	0.041
59413	105874	A6V	0.017	0.518	0.045
60320	107566	A0m	0.202	0.109	0.028
61639	109808	A1/A2V	0.056	0.095	0.041
63204	112381	A0p	0.000	0.136	0.025
63945	113703	B5V	0.025	0.101	0.026
Vela OB2					
40397	69404	B3Vnne	0.038	0.142	0.054
Upper Centaurus Lupus					
69618	124367	B4Vne	0.090	0.263	0.032
79631	145880	B9.5V	0.085	0.193	0.065
82747	152404	F5V	0.315	0.545	0.042
Trumpler 10 – No stars with excess					
Lacerta OB1					
110476	0	B8	0.183	0.082	0.027
111546	214167	B1Ve	0.100	0.170	0.058
112148	215227	B5:ne	0.213	0.255	0.035
113226	216851	B3V:n	0.241	0.149	0.022
Cassiopeia-Taurus					
<i>continued on next page</i>					

<i>continued from previous page</i>					
HIP Number	HD Number	Spectral Type	E(B-V)	$\Delta(H - K)$	$e_{\Delta(H-K)}$
22109	30211	B5IV	0.016	0.200	0.096
Perseus OB3- No stars with excess					
Cepheus OB6 - No stars with excess					

6.3 Discussion

OB Association	No. of B, A & F type stars	No. of stars with $\Delta(H - K)$ excess	Fraction of stars with inner disks (%)
Cepheus OB2	67	3	4.5±2.6
Collinder121	94	3	3.2±1.8
Upper Scorpius	105	5	4.8±2.1
Perseus OB2	35	0	0
Lower Centaurus Crux	157	7	4.5±1.7
Vela OB2	86	1	1.2±1.2
Upper Centaurus Lupus	189	3	1.6±1
Trumpler10	23	0	0
Lacerta OB1	83	4	4.8±2.4
Cassiopeia-Taurus	83	1	1.2±1.2
Perseus OB3 (α Per)	75	0	0
Cepheus OB6	15	0	0

Table 6.3: Disk fraction in OB associations

From our analysis described in the previous Section we have identified stars with circumstellar disks in 12 nearby OB associations. In Table 6.3 we list the number of early type (spectral type B, A & F) stars in these associations, number of stars with inner disks inferred using the criterion discussed in the last Section, and the fraction of stars (the formal errors represent probable uncertainties resulting from

poisson statistics) with inner disks in the 12 OB associations studied. In the following we discuss two aspects of our findings: the disk frequency in OB associations and the magnitude of the near-infrared excess of the stars with circumstellar disks as a function of the mean ages of these associations.

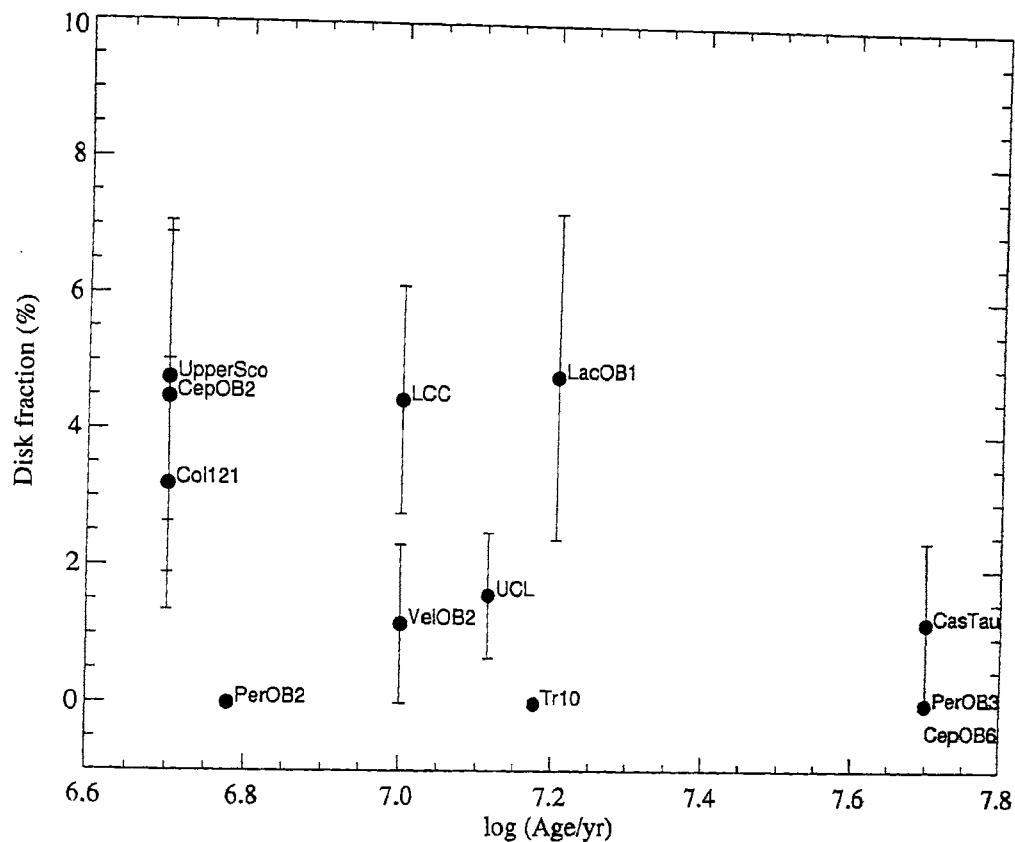


Figure 6.2: Disk fraction in the associations against the mean ages.

As can be seen from Table 6.3 the number of stars with inner circumstellar disks are very low in these associations. Disk frequencies in these associations range from 0-5%. In Figure 6.2 we plot fraction of stars with circumstellar disks in an association against the mean age of that association. The disk fraction is never higher than 5% in any of these associations. Most of the disks appear to be lost if the initial disk frequency was high and all the stars were born with disks. The OB associations studied here are in the age range of 5 to 50 Myr. The fact that only less than 5% of the stars seem to retain their disks argues for a timescale as short as < 5 Myr for most of the inner disk to be lost. This is consistent with the short disk lifetimes found for

the evolution of inner disks by Haisch et al. (2001) and Hillenbrand (2002). However, the possibility of extreme environments because of the presence O and early B type stars in OB associations affecting the nature of evolution and lifetimes of circumstellar disks in these associations cannot be ruled out.

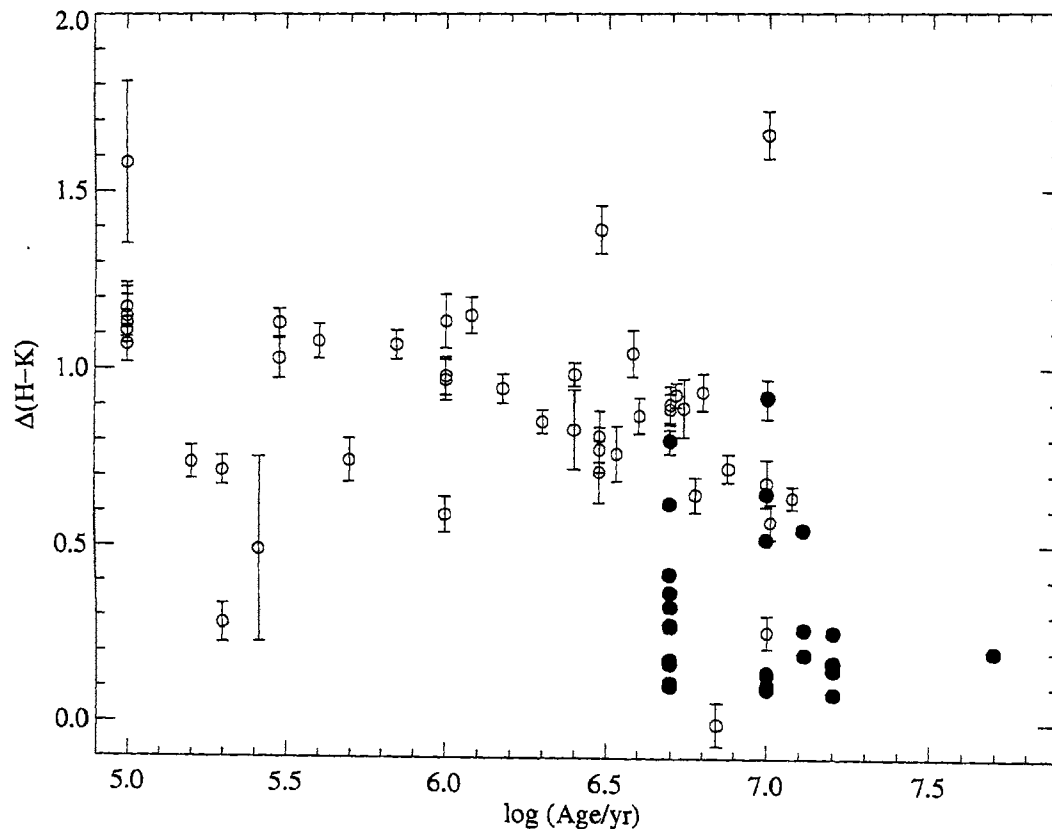


Figure 6.3: $\Delta(H - K)$ against ages for stars with disks in associations and HAeBe stars.

Next we look at the magnitude of the near-infrared color excess in stars which are identified to have circumstellar disks in the OB associations studied. As mentioned earlier, 5 stars in Upper Scorpius, Lower Centaurus Crux and Upper Centaurus Lupus are known Herbig Ae/Be stars. These stars have relatively high values of $\Delta(H - K)$ of ≥ 0.5 signifying accretion rates similar to that found for HAeBe stars. Other stars with excess have relatively small values of $\Delta(H - K)$. In Figure 6.3 we show a plot of $\Delta(H - K)$ of stars with inner disks against the mean ages of associations, together with that of HAeBe stars. The values of $\Delta(H - K)$ and ages of HAeBe stars are from Chapter 2. On an average the trend of decreasing excess

with age seen for HAeBe stars is seen to continue for stars in the associations also. Thus the drop in accretion rate with age found for HAeBe stars extends to stars in relatively old OB associations. Also, OB associations as old as 10-13 Myr appear to have stars with accretion rates comparable to that of HAeBe stars suggesting that measurable accretion can persist for more than 10 Myr in some stars. It is known that though the overall disk lifetimes can be as short as $< 5\text{Myr}$, a small percentage of stars retain disk material for factors of 5-10 longer than the average (Muzerolle et al. 2000; Hillenbrand 2002). The relatively high values of $\Delta(H - K)$ found for stars in OB associations suggest that some of the stars not only retain their disks for a longer time but also have significant accretion rates. However, the accretion rates appear to fall sharply after ~ 10 Myr as can be seen from Figure 6.2.

There is also a large spread in the values of $\Delta(H - K)$ for stars in an association of given age. First of all only a small fraction ($< 5\%$) of stars show signatures of disks. Even among the stars with disks, there are those with relatively high accretion rates similar to that of HAeBe stars and those which show low accretion. This may indicate either different evolutionary timescales for individual stars in an association or an age spread among the association members.

6.4 Summary and conclusions

In this chapter we have studied the evolution of circumstellar disks in 12 nearby OB associations which are in the age range of 5-50 Myr. We identified stars with circumstellar disks in these OB associations based on the near-infrared excess emission shown by the stars. We estimated the disk frequency of these OB associations and studied the evolution of disk frequency with mean ages of the associations. We also looked for possible evolutionary trend in the magnitude of excess shown by the stars which are identified to have disks. Our conclusions are summarized below.

- The fraction of stars with circumstellar disks in the OB associations studied, which are in the age range of 5-50 Myr, is as low as $< 5\%$. This is consistent with the disk evolution timescale being as short as < 5 Myr. Most of the disks

- around young stars are lost within this time.
- In some OB associations stars as old as 10-13 Myr show relatively high accretion rates. Though most of the disks are lost within a short timescale of < 5 Myr, a small fraction of stars retain disks longer than the average with relatively high accretion rates.
 - Among the stars that are identified to have disks in the OB associations, the magnitude of near-infrared excess emission shows a large range. The disk evolution timescales of individual stars even within an association can have a large scatter. Alternatively, this may be due to an age spread among the association members.

Chapter 7

Conclusions

Stars are formed when the dense cores in the cold and deep interiors of molecular clouds collapse gravitationally. Such a collapse of a slowly rotating cloud core leads to the formation of a central protostar surrounded by a nebular disk and an infalling envelope which rains matter on to the star/disk system. After the initial infall and accretion is over, the young star surrounded by a disk emerges out of its parental cocoon of molecular gas and dust and becomes visible as a pre-main sequence star. Circumstellar disks of gas and dust have been observed around a majority of pre-main sequence stars. As the young star evolves, a variety of processes modify and change the physical structure and properties of the disk until it is completely dispersed off. Planet formation, interaction of the disk with the radiation from the central star and the destructive environment because of the close proximity to high mass stars are some of the mechanisms that affect disk evolution and dissipation. In this thesis we have studied the evolution of such circumstellar disks around young stars of intermediate-mass. We have followed the evolution of the circumstellar disks from the early pre-main sequence phase (Herbig Ae/Be stars) to the late main sequence phase (Vega-like stars) of the star. Observational diagnostics such as emission lines in the spectra, near and far-infrared excess and polarization of starlight which probe the disks around young stars are used to follow the evolution of circumstellar disks. In this concluding chapter we summarize the main results of our study.

In the early pre-main sequence phase, young stars of intermediate-mass show strong emission line activity. In Chapter 2, we have studied the evolution of emission line activity in Herbig Ae/Be stars. We found a strong correlation between $H\alpha$ equivalent width and the age of the stars. The $H\alpha$ emission strength is found to decrease with increasing pre-main sequence age. The $H\alpha$ line strength in HAeBe stars is found to fall by more than a factor of two on timescales as short as 2-4 Myr. This timescale is comparable to the inner disk lifetimes of young stars derived from the studies of young embedded clusters (Haisch et al. 2001; Hillenbrand 2002). We also find a drop in the near-infrared excess emission from HAeBe stars with age. Further, the $H\alpha$ line strength and the near infrared excess are found to be strongly correlated, clearly suggesting a connection between emission line activity and the presence of inner disks which produce near-infrared excess emission. The connection between emission line strength and near-infrared excess emission is naturally explained if accretion from the disk onto the star drives emission line activity in Herbig Ae/Be stars. The evolutionary trends in emission line activity and near-infrared excess that we find then indicate a decrease in accretion rates with increasing pre-main sequence age. Accretion rates in young stars seem to fall substantially within the first ~ 3 Myr of pre-main sequence evolution.

At some point in time the accretion is terminated and the inner disks begin to dissipate. As a result, the emission line activity and near-infrared excess emission disappears. As noted in the preceding paragraph, the cessation of emission line activity and the termination of accretion and dissipation of inner disks appear to take place in < 5 Myr and is thought to happen during the late pre-main sequence phase or early main sequence phase. However, not many such stars which are in this intermediate phase of evolution are known. In Chapter 3, we have identified a few such stars and have studied the properties of the circumstellar environment around them in detail. Emission lines are not seen in the spectra of these stars. Near-infrared excess emission is also absent or if present is at a very low level. From various age indicators such as the location in the color-magnitude diagram, association with young clusters and starforming regions and kinematics we have been able to show that these stars are either in the late pre-main sequence phase or early main sequence phase. Though the

inner accretion disks have certainly dissipated in these stars, cool and extended outer disks may be present around some of them as inferred from the significant far-infrared excess emission observed towards them. The fractional dust luminosity L_{dust}/L_{\star} computed for these stars have values that are intermediate between that found for Herbig Ae/Be stars and main sequence stars with debris disks. These stars are possibly the 'transition objects' which are in the evolutionary stage where the transition of circumstellar disks from being optically thick to optically thin takes place. Further studies of the properties of disks around such stars like gas content of the disk, grain growth and grain size distribution and possible gaps in the disks due to the presence of giant planets, however, are essential to the detailed understanding of the processes that affect and control the transition of optically thick circumstellar disks to optically thin.

As discussed in the previous chapters, planet formation and other dispersal processes eventually dissipate the 'primordial disks'. The collisions between large planetesimals and breaking up of star-grazing comets, which are gravitationally stirred by the larger planetary bodies in the disks, replenishes the disks with smaller grains. Excess emission at the far-infrared wavelengths due to orbiting dust particles have been observed around several main sequence stars. However, direct evidence for the flattened disk-like distribution of the circumstellar material around such stars has so far been obtained only for a handful of objects. In Chapter 4, we have studied the polarization properties of Vega-like main sequence stars with dust disks. We find that Vega-like stars are intrinsically polarized, caused by the scattering of the stellar light due to circumstellar dust distributed in non-spherically symmetric envelopes, fully consistent with a distribution in flattened disks. The absence of any excess reddening in these stars is consistent with the dust grains in their circumstellar disks being relatively large in size. We also find a correlation between polarization and fractional dust luminosities of Vega-like stars which is expected as the dust grains in the disk are responsible for both scattering and thermal re-radiation of central star light. Some Vega-like stars in our sample show relatively small infrared excesses but large values of polarization which suggest the presence of an additional component of dust consisting of smaller grains with high albedo. Multiwavelength polarization

measurements of Vega-like stars would be able to shed more light on the nature and distribution of the dust in their circumstellar environment.

The debris disks around main sequence stars represents the final stages of planet formation and disk clearing phase. The grain removal processes such as radiation pressure ‘blowout’, Poynting-Robertson drag and collisional destruction acting in the relatively gas-free debris disks, can clear the dust particles off the disks on timescales as short as $< 10^6$ yr. The fact that we observe such disks around old main sequence stars implies that the disk is continuously being replenished by mechanisms discussed earlier. In Chapter 5 we have studied the lifetimes and the temporal evolution of the main sequence debris disks. We have used the velocity dispersion as an age indicator to constrain the ages of Vega-like stars. The ages of Vega-like stars derived from velocity dispersion is found to range from 10^8 yr to $2 - 3$ Gyr. However, in comparison with the normal field stars of similar spectral type, main sequence stars with dust disks are found to be younger, suggesting that the observable disks do not last for the entire lifetimes of the stars. We also find that the Vega-like stars of later spectral types are statistically older than stars of early type which implies longer debris disk lifetimes in low mass stars. Further, we find the fractional dust luminosity $f_d \equiv L_{dust}/L_*$ of main sequence stars with debris disks to fall steadily with increasing stellar age. We also find that the optical depth of the circumstellar disks around intermediate-mass stars systematically decreases with age from early pre-main sequence phase to late main sequence phase. Such an evolutionary trend is consistent with the pre-main sequence disks being the progenitors of main sequence debris disks.

Finally, in Chapter 6, we have studied the disk frequency and lifetimes in 12 nearby OB associations. The ages of these associations range from 5-50 Myr, which is poorly represented in the earlier studies of disk frequency in clusters and associations. We have identified stars with circumstellar disks in these OB associations based on their near-infrared excess emission and study the disk frequency with age. The fraction of stars with circumstellar disks in the OB associations studied is found to be very low at $< 5\%$. Most of the disks around young stars seem to be lost within 5 Myr or so, which is the age of the youngest association in our sample. This is consistent

with the disk evolution timescale being as short as < 5 Myr as found by Haisch et al. (2001) and Hillenbrand (2002). It is seen that though most of the inner disks are lost within a short timescale of < 5 Myr, a small fraction of stars retain disks longer (~ 10 Myr) than the average with relatively high accretion rates. However, by 10-15 Myr the near-infrared emitting inner disks are found to dissipate completely.

Thus it can be seen that the circumstellar environment around young stars show clear evolutionary trend as the stars age. The accretion rates steadily fall during the pre-main sequence evolution which is reflected in the weakening of emission line activity. The termination of accretion and dissipation of inner disks occur relatively rapidly in most young stars on a timescale that is as short as < 5 Myr. Also, the fractional dust luminosity of circumstellar disks, which is a measure of the optical thickness, is found to decline systematically with age from early pre-main sequence phase to late main sequence phase. The rapid decline of circumstellar activity in the pre-main sequence phase indicates a similarly short timescale ($\lesssim 5$ Myr) for the formation of planetesimals/planets in the circumstellar disks. The second generation debris disks produced by the breakup of the planetesimals and comets during the main sequence phase also continue to decline, but they can survive as long as $\sim 10^9$ yr.

Appendix A

OPTICAL SPECTRA OF HERBIG Ae/Be STARS

Table A.1: Log of spectroscopic observations

Object	Date of Observation	Resolution	Exposure time (sec)
BD+40 4124	19 May 2002	1300	600
HD 200775	22 October 2003	2190	30
HD 259431	24 October 2003	2190	150
HD 98922	09 April 2002	2600	600
Z CMa	27 January 2003	1300	420
BD+46 3471	22 October 2003	2190	210
HD 142527	9 April 2002	2600	900
HD 179218	24 October 2003	2190	300
HD 35929	22 October 2003	2190	210
51 Oph	19 May 2002	1300	180
BD+61 154	22 October 2003	2190	300
HD 37806	28 January 2003	1300	600
HD 85567	25 January 2003	1300	900

continued on next page

<i>continued from previous page</i>			
Object	Date of Observation	Resolution	Exposure time
UX Ori	14 March 2001	1300	900
HR 5999	19 May 2002	1300	600
VV Ser	30 May 2003	1300	1800
V1295 Aql	19 May 2002	1300	600
XY Per	27 January 2003	1300	600
HD 38120	22 October 2003	2190	390
AB Aur	24 October 2003	2190	30
NX Pup	20 January 2000	1300	900
HD 144432	2 June 2003	1300	1200
HD 31648	29 November 2002	1300	300
HD 150193	11 April 2002	2600	600
HD 36112	28 January 2003	1300	300
HD 163296	31 May 2003	1300	300
IP Per	22 October 2003	2190	300
HD 34282	20 November 2002	1300	900
HD 141569	19 May 2002	1300	300
KK Oph	30 May 2003	1300	1800
HD 100453	28 January 2003	1300	900
AK Sco	9 April 2002	2600	1800
HD 35187	14 January 2004	1800	600

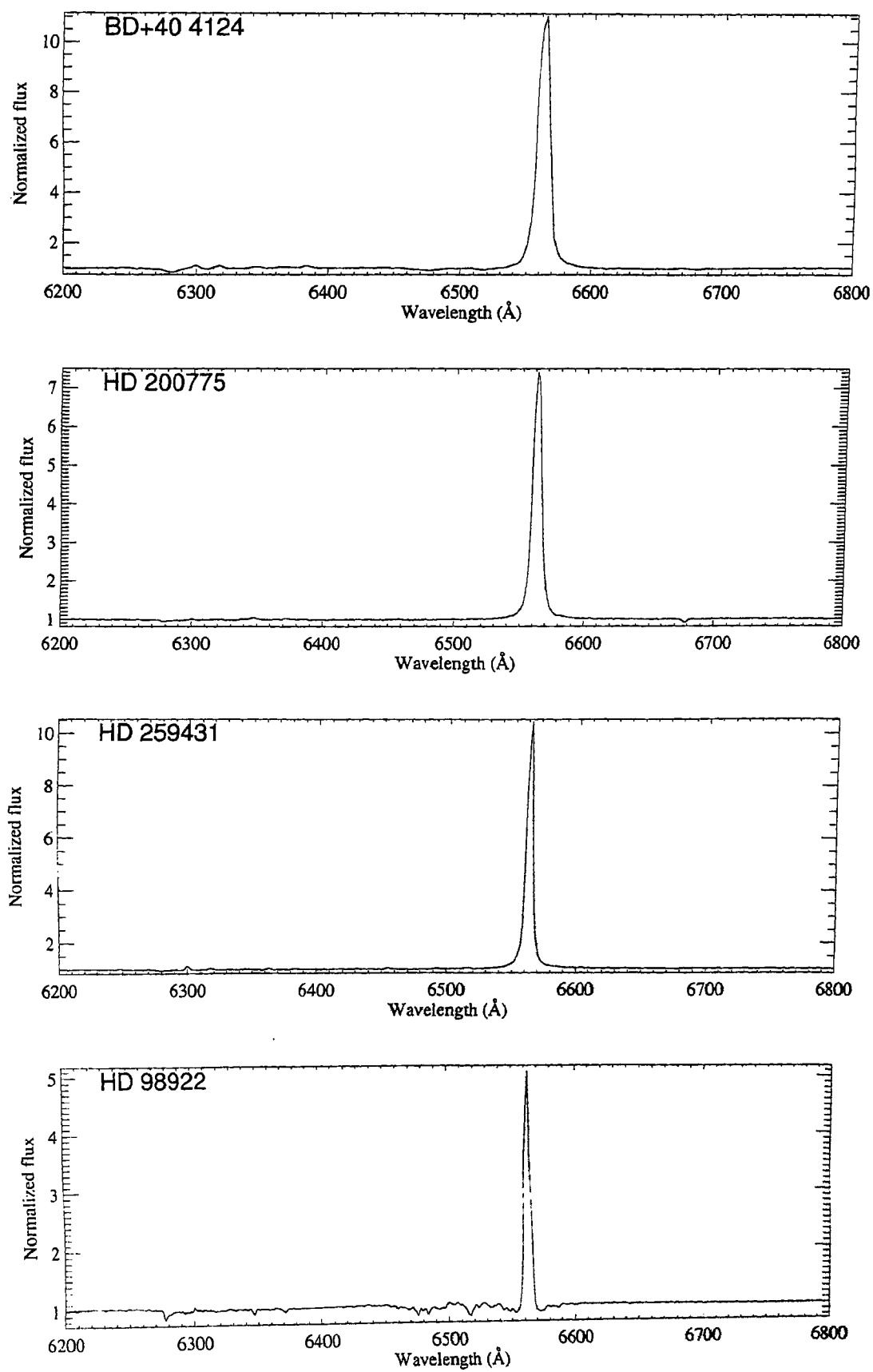


Figure A.1:

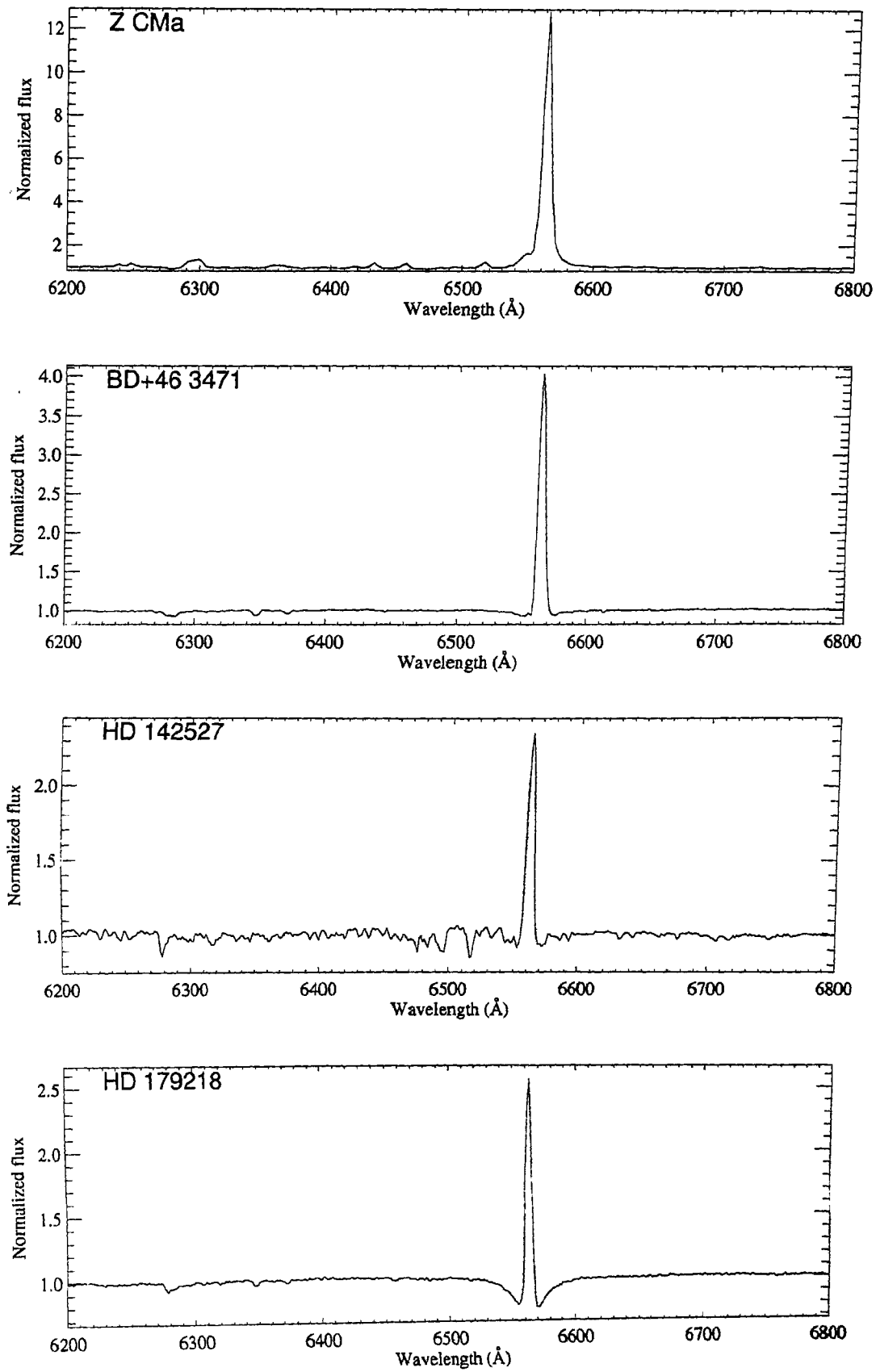


Figure A.1: conitnued

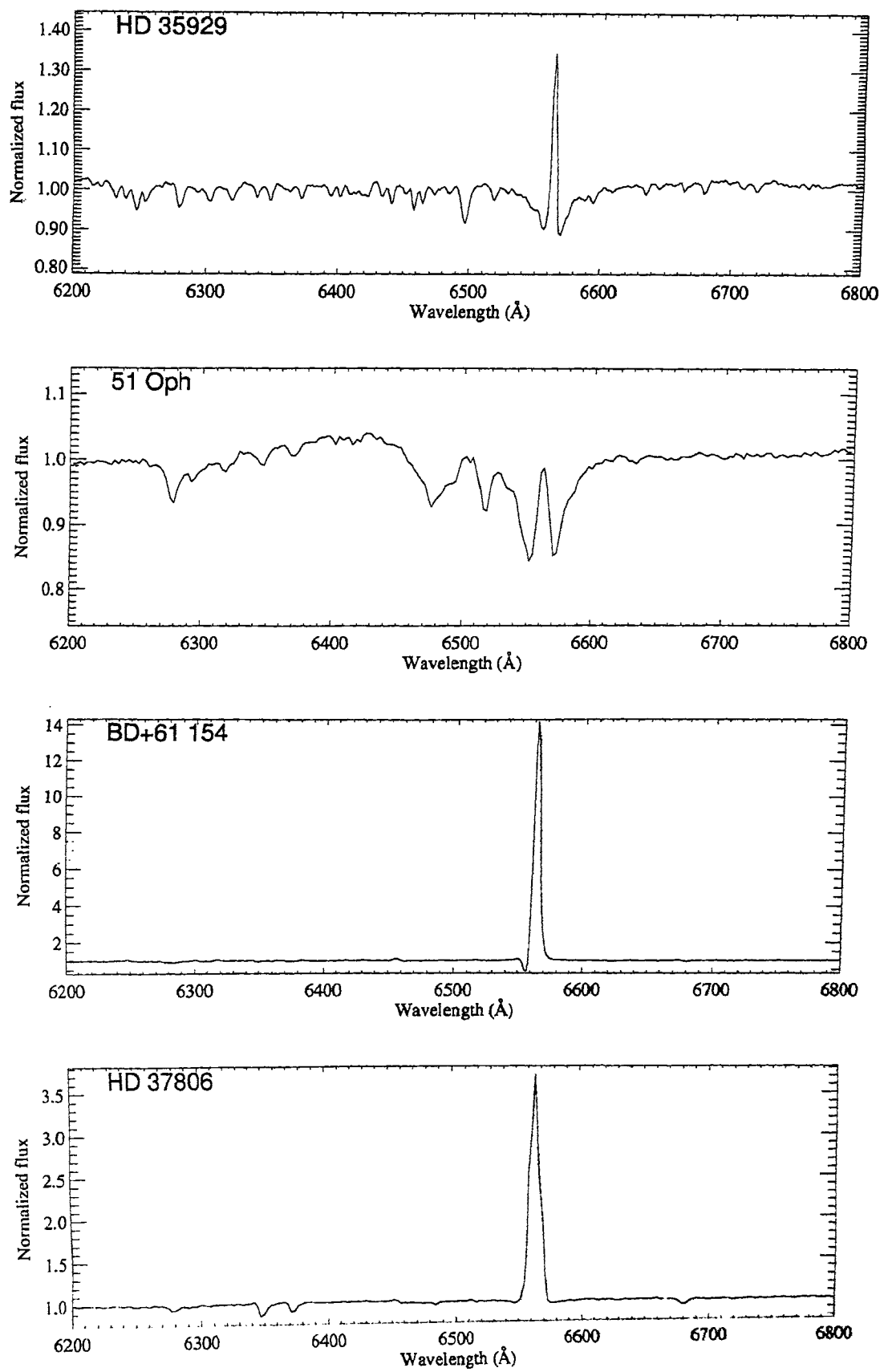


Figure A.1: continued

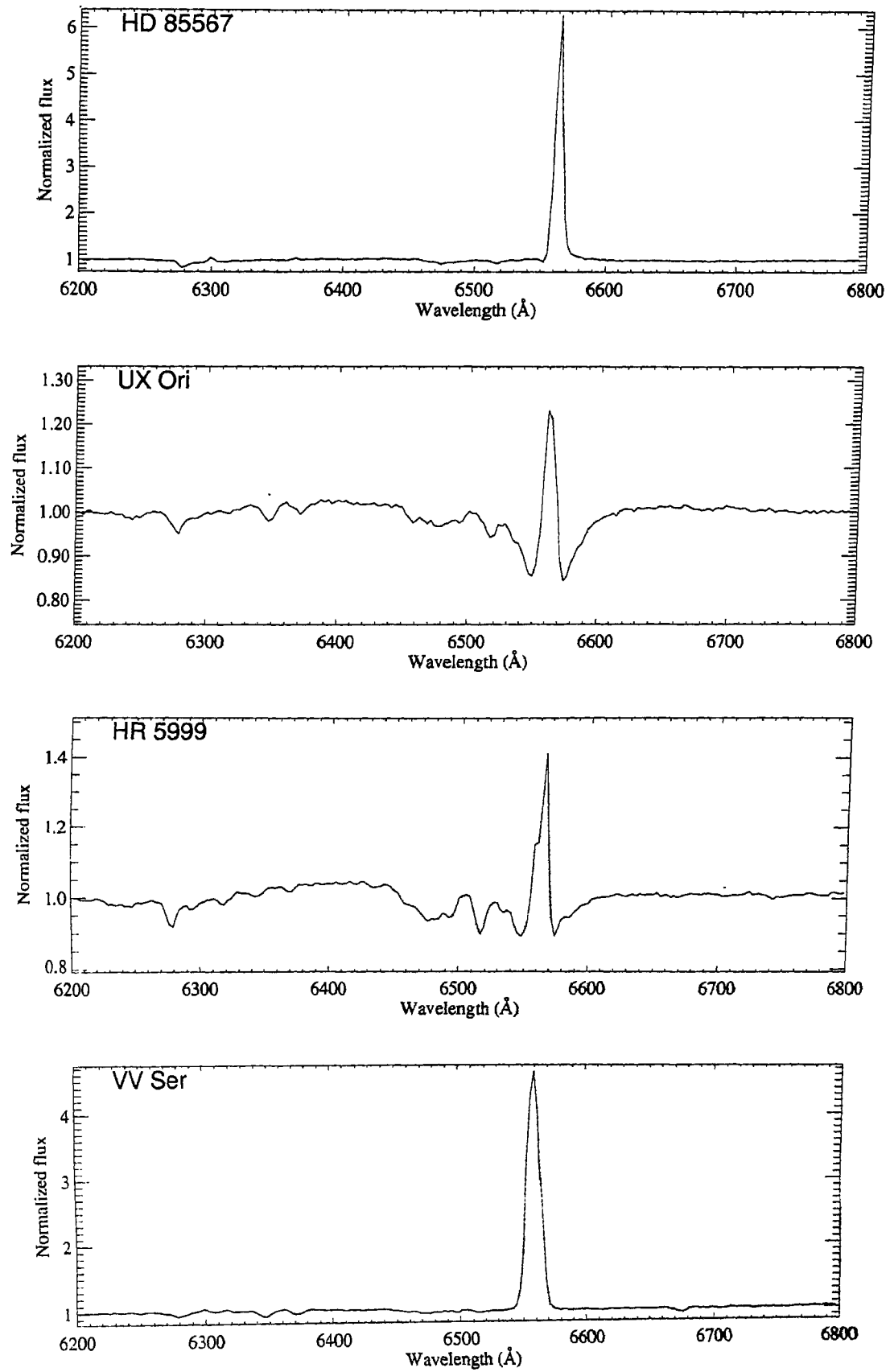


Figure A.1: continued

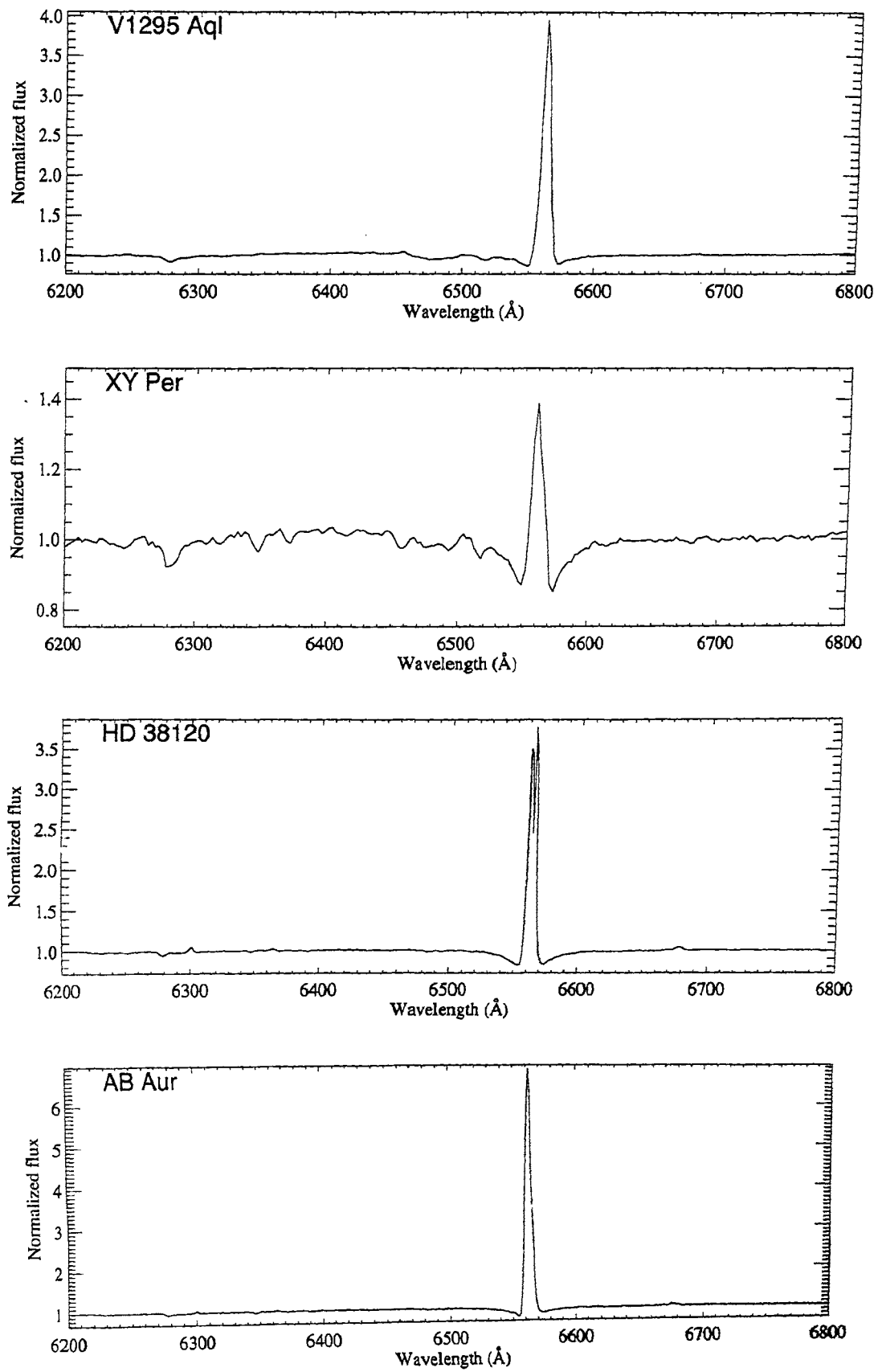


Figure A.1: continued

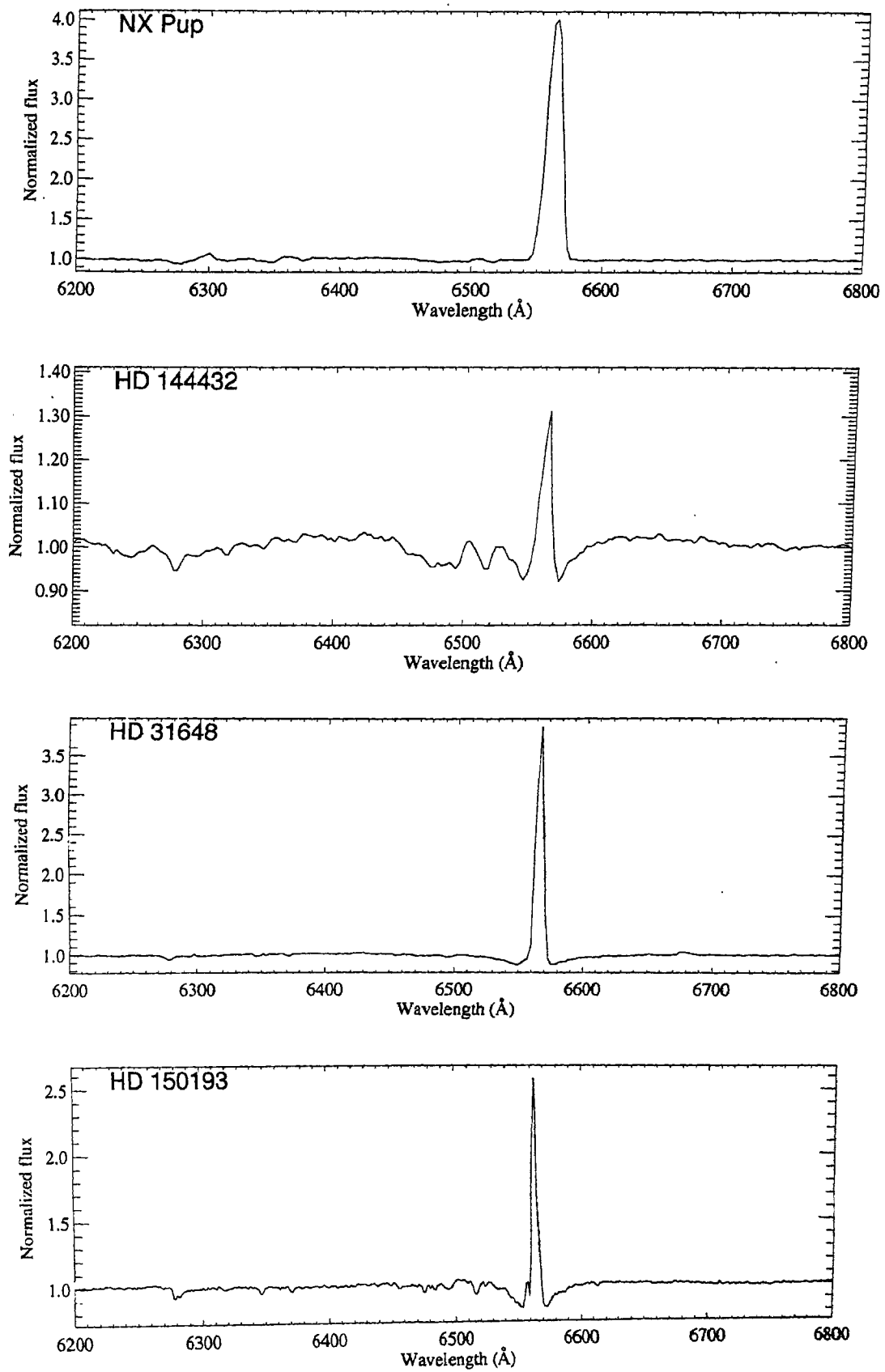


Figure A.1: continued

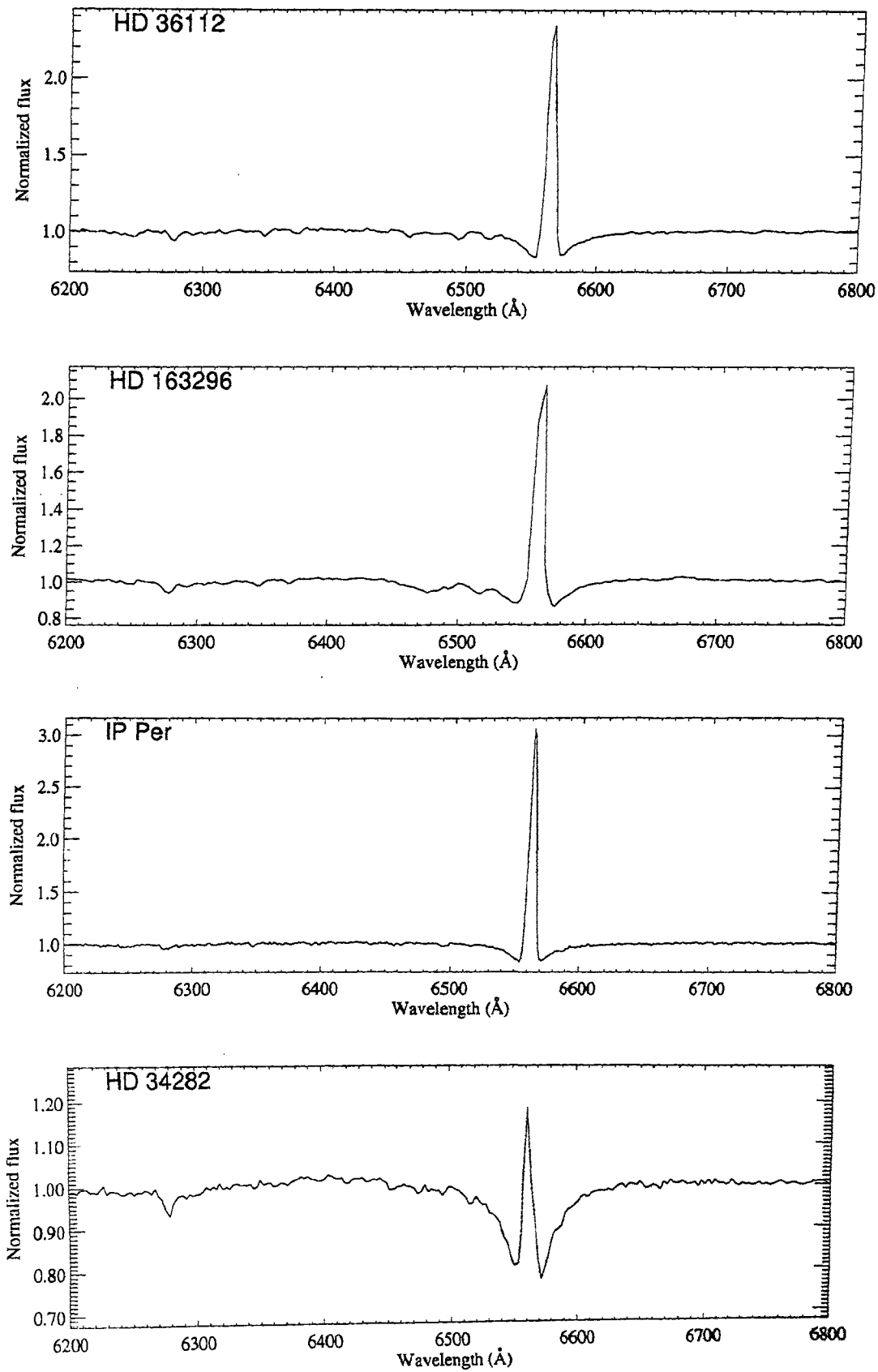


Figure A.1: continued

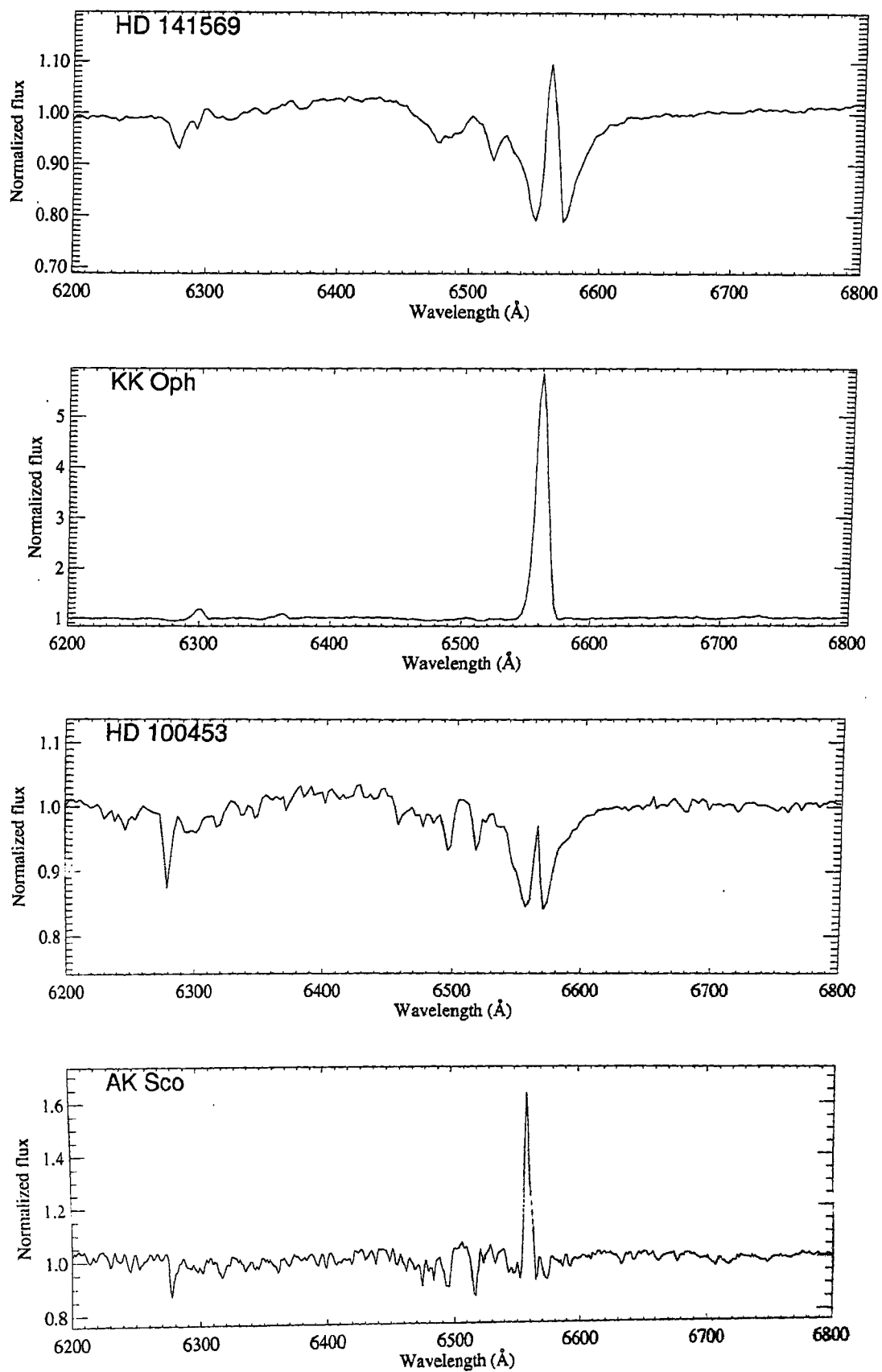


Figure A.1: continued

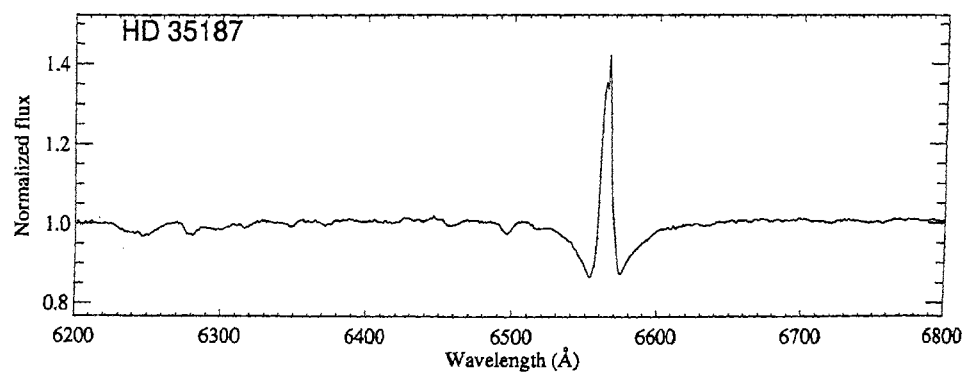


Figure A.1: continued

Bibliography

- Artymowicz, P. 1996, in *The Role of Dust in the Formation of Stars*, Proceedings of the ESO Workshop Held at Garching, Germany, 11 - 14 September 1995. Edited by Hans U. Käuffl and Ralf Siebenmorgen. Springer-Verlag Berlin Heidelberg New York. Also ESO Astrophysics Symposia (European Southern Observatory), 137
- Aumann, H. H., Beichman, C. A., Gillett, F. C., et al. 1984, *Astrophys. J. Lett.* , 278, L23
- Bachiller, R. & Tafalla, M. 1999, in NATO ASIC Proc. 540: *The Origin of Stars and Planetary Systems*, 227
- Backman, D. & Gillett, F. C. 1987, in LNP Vol. 291: *Cool Stars, Stellar Systems and the Sun*, 340
- Backman, D. E. & Paresce, F. 1993, in *Protostars and Planets III*, 1253–1304
- Barbanis, B. & Woltjer, L. 1967, *Astrophys. J.* , 150, 461
- Bastien, P. 1987, *Astrophys. J.* , 317, 231
- Bastien, P. 1988, in *Polarized Radiation of Circumstellar Origin*, 541–582
- Beckwith, S. V. W. 1999, in NATO ASIC Proc. 540: *The Origin of Stars and Planetary Systems*, 579
- Beckwith, S. V. W., Henning, T., & Nakagawa, Y. 2000, *Protostars and Planets IV* , 533
- Beckwith, S. V. W. & Sargent, A. I. 1996, *Nature* , 383, 139

- Berrilli, F., Corciulo, G., Ingresso, G., et al. 1992, *Astrophys. J.* , 398, 254
- Bertout, C., Basri, G., & Bouvier, J. 1988, *Astrophys. J.* , 330, 350
- Bhatt, H. C. 1996, *Astron. Astrophys. Suppl.* , 120, 451
- Bibo, E. A., The, P. S., & Dawanas, D. N. 1992, *Astron. Astrophys.* , 260, 293
- Binney, J., Dehnen, W., & Bertelli, G. 2000, *Mon. Not. R. astr. Soc.* , 318, 658
- Binney, J. & Merrifield, M. 1998, *Galactic astronomy* (Princeton, NJ, Princeton University Press, 1998)
- Binney, J. & Tremaine, S. 1987, *Galactic dynamics* (Princeton, NJ, Princeton University Press, 1987)
- Bohm, T. & Catala, C. 1993, *Astron. Astrophys. Suppl.* , 101, 629
- Böhm, T. & Catala, C. 1994, *Astron. Astrophys.* , 290, 167
- . 1995, *Astron. Astrophys.* , 301, 155
- Böhm, T. & Hirth, G. A. 1997, *Astron. Astrophys.* , 324, 177
- Bouret, J.-C. & Catala, C. 1998, *Astron. Astrophys.* , 340, 163
- Breger, M. 1974, *Astrophys. J.* , 188, 53
- Brown, A. G. A., Blaauw, A., Hoogerwerf, R., de Bruijne, J. H. J., & de Zeeuw, P. T. 1999, in *NATO ASIC Proc. 540: The Origin of Stars and Planetary Systems*, 411
- Cabrit, S., Edwards, S., Strom, S. E., & Strom, K. M. 1990, *Astrophys. J.* , 354, 687
- Calvet, N., D'Alessio, P., Hartmann, L., et al. 2002, *Astrophys. J.* , 568, 1008
- Carpenter, J. M. 2001, *Astron. J.* , 121, 2851
- Carpenter, J. M., Meyer, M. R., Dougados, C., Strom, S. E., & Hillenbrand, L. A. 1997, *Astron. J.* , 114, 198
- Catala, C. 1988, *Astron. Astrophys.* , 193, 222

- Catala, C. & Kunasz, P. B. 1987, *Astron. Astrophys.* , 174, 158
- Chiang, E. I. & Goldreich, P. 1997, *Astrophys. J.* , 490, 368
- Chiang, E. I., Joungh, M. K., Creech-Eakman, M. J., et al. 2001, *Astrophys. J.* , 547, 1077
- Cohen, M. & Kuhl, L. V. 1979, *Astrophys. J. Suppl.* , 41, 743
- Corcoran, M. & Ray, T. P. 1997, *Astron. Astrophys.* , 321, 189
- . 1998, *Astron. Astrophys.* , 331, 147
- Coulson, I. M., Walther, D. M., & Dent, W. R. F. 1997, in *Star Formation Near and Far*, 209
- Coulson, I. M., Walther, D. M., & Dent, W. R. F. 1998, *Mon. Not. R. astr. Soc.* , 296, 934
- de Bruijne, J. H. J. 1999, *Mon. Not. R. astr. Soc.* , 306, 381
- de Zeeuw, P. T., Hoogerwerf, R., de Bruijne, J. H. J., Brown, A. G. A., & Blaauw, A. 1999, *Astron. J.* , 117, 354
- Decin, G., Dominik, C., Waters, L. B. F. M., & Waelkens, C. 2003, *Astrophys. J.* , 598, 636
- Dehnen, W. & Binney, J. J. 1998, *Mon. Not. R. astr. Soc.* , 298, 387
- Dominik, C. & Decin, G. 2003, *Astrophys. J.* , 598, 626
- Dunkin, S. K. & Crawford, I. A. 1998, *Mon. Not. R. astr. Soc.* , 298, 275
- Eisner, J. A., Lane, B. F., Akeson, R. L., Hillenbrand, L. A., & Sargent, A. I. 2003, *Astrophys. J.* , 588, 360
- Emerson, J. P. 1988, in *NATO ASIC Proc. 241: Formation and Evolution of Low Mass Stars*, 193
- ESA. 1997, *The Hipparcos and Tycho Catalogues (ESA 1997)*, 1239

- Finkenzeller, U. & Mundt, R. 1984, *Astron. Astrophys. Suppl.* , 55, 109
- Fuente, A., Martín-Pintado, J., Bachiller, R., Rodríguez-Franco, A., & Palla, F. 2002, *Astron. Astrophys.* , 387, 977
- Garrison, L. M. & Anderson, C. M. 1978, *Astrophys. J.* , 221, 601
- Genzel, R., Reid, M. J., Moran, J. M., & Downes, D. 1981, *Astrophys. J.* , 244, 884
- Ghandour, L., Strom, S., Edwards, S., & Hillenbrand, L. 1994, in ASP Conf. Ser. 62: The Nature and Evolutionary Status of Herbig Ae/Be Stars, 223
- Gillett, F. C. 1986, in ASSL Vol. 124: Light on Dark Matter, 61–69
- Gledhill, T. M., Scarrott, S. M., & Wolstencroft, R. D. 1991, *Mon. Not. R. astr. Soc.* , 252, 50P
- Gorti, U. & Bhatt, H. C. 1993, *Astron. Astrophys.* , 270, 426
- Grady, C. A., Perez, M. R., & The, P. S. 1993, *Astron. Astrophys.* , 274, 847
- Grady, C. A., Polomski, E. F., Henning, T., et al. 2001, *Astron. J.* , 122, 3396
- Grinin, V. P. & Rostopchina, A. N. 1996, *Astronomy Reports*, 40, 171
- Gullbring, E., Hartmann, L., Briceno, C., & Calvet, N. 1998, *Astrophys. J.* , 492, 323
- Habing, H. J., Dominik, C., Jourdain de Muizon, M., et al. 1999, *Nature* , 401, 456
- Haisch, K. E., Lada, E. A., & Lada, C. J. 2001, *Astrophys. J. Lett.* , 553, L153
- Hamann, F. 1994, *Astrophys. J. Suppl.* , 93, 485
- Hamann, F. & Persson, S. E. 1992, *Astrophys. J. Suppl.* , 82, 285
- Hartmann, L. 1998. *Accretion processes in star formation* (Cambridge, UK : New York : Cambridge University Press, 1998. (Cambridge astrophysics series ; 32))
- Hartmann, L., Hewett, R., & Calvet, N. 1994, *Astrophys. J.* , 426, 669
- Hauck, B. & Jaschek, C. 2000, *Astron. Astrophys.* , 354, 157

- Heiles, C. 2000, *Astron. J.* , 119, 923
- Henning, T., Burkert, A., Launhardt, R., Leinert, C., & Stecklum, B. 1998, *Astron. Astrophys.* , 336, 565
- Herbig, G. H. 1960, *Astrophys. J. Suppl.* , 4, 337
- Herbig, G. H. 1994, in ASP Conf. Ser. 62: The Nature and Evolutionary Status of Herbig Ae/Be Stars, 3
- Herbig, G. H. & Bell, K. R. 1988, Catalog of emission line stars of the orion population : 3 : 1988 (Lick Observatory Bulletin, Santa Cruz: Lick Observatory, —c1988)
- Hillenbrand, L. A. 1997, *Astron. J.* , 113, 1733
- . 2002, astro-ph/0210520
- Hillenbrand, L. A., Strom, S. E., Calvet, N., et al. 1998, *Astron. J.* , 116, 1816
- Hillenbrand, L. A., Strom, S. E., Vrba, F. J., & Keene, J. 1992, *Astrophys. J.* , 397, 613
- Holland, W. S., Greaves, J. S., Zuckerman, B., et al. 1998, *Nature* , 392, 788
- Hoogerwerf, R. & Aguilar, L. A. 1999, *Mon. Not. R. astr. Soc.* , 306, 394
- Hsu, J.-C. & Breger, M. 1982, *Astrophys. J.* , 262, 732
- Jahreiß, H. & Wielen, R. 1983, in IAU Colloq. 76: Nearby Stars and the Stellar Luminosity Function, 277–287
- Jain, S. K. & Bhatt, H. C. 1995, *Astron. Astrophys. Suppl.* , 111, 399
- Jain, S. K., Bhatt, H. C., & Sagar, R. 1990, *Astron. Astrophys. Suppl.* , 83, 237
- Jain, S. K. & Srinivasulu, G. 1991, *Optical Engineering*, 30, 1415
- Jaschek, C. & Andrillat, Y. 1998, *Astron. Astrophys. Suppl.* , 130, 507
- Jaschek, C., Jaschek, M., Egret, D., & Andrillat, Y. 1991, *Astron. Astrophys.* , 252, 229

- Jaschek, M., Jaschek, C., & Andrillat, Y. 1988, *Astron. Astrophys. Suppl.* , 72, 505
- Jaschek, M., Jaschek, C., & Egret, D. 1986, *Astron. Astrophys.* , 158, 325
- Jayawardhana, R., Fisher, S., Hartmann, L., et al. 1998, *Astrophys. J. Lett.* , 503, L79
- Jayawardhana, R., Hartmann, L., Fazio, G., et al. 1999, *Astrophys. J. Lett.* , 520, L41
- Jura, M. 1999, *Astrophys. J.* , 515, 706
- Kalas, P. & Jewitt, D. 1997, *Nature* , 386, 52
- Kenyon, S. J. & Bromley, B. C. 2002, *Astrophys. J. Lett.* , 577, L35
- Kenyon, S. J. & Hartmann, L. 1987, *Astrophys. J.* , 323, 714
- . 1995, *Astrophys. J. Suppl.* , 101, 117
- Koenigl, A. 1991, *Astrophys. J. Lett.* , 370, L39
- Koerner, D. W., Jensen, E. L. N., Cruz, K. L., Guild, T. B., & Gultekin, K. 2000, *Astrophys. J. Lett.* , 533, L37
- Koerner, D. W., Ressler, M. E., Werner, M. W., & Backman, D. E. 1998, *Astrophys. J. Lett.* , 503, L83
- Koornneef, J. 1983, *Astron. Astrophys.* , 128, 84
- Lachaume, R., Dominik, C., Lanz, T., & Habing, H. J. 1999, *Astron. Astrophys.* 348, 897
- Lada, C. J. & Adams, F. C. 1992, *Astrophys. J.* , 393, 278
- Lada, C. J., Alves, J., & Lada, E. A. 1996, *Astron. J.* , 111, 1964
- Lada, C. J. & Lada, E. A. 2003, *Ann. Rev. Astron. Astrophys.* , 41, 57
- Lada, E. A. 1999, in NATO ASIC Proc. 540: The Origin of Stars and Planetary Systems, 441

- Lagrange, A.-M., Backman, D. E., & Artymowicz, P. 2000, *Protostars and Planets IV*, 639
- Lagrange-Henri, A.-M. 1995, *Astrophys. Space Sci.* , 223, 19
- Levato, H. & Abt, H. A. 1976, *Publ. Astr. Soc. Pacific.* , 88, 712
- Lissauer, J. J. 1993, *Ann. Rev. Astron. Astrophys.* , 31, 129
- . 2001, *Nature* , 409, 23
- Lisse, C., Schultz, A., Fernandez, Y., et al. 2002, *Astrophys. J.* , 570, 779
- Malfait, K., Bogaert, E., & Waelkens, C. 1998, *Astron. Astrophys.* , 331, 211
- Mamajek, E. E., Meyer, M. R., & Liebert, J. 2002, *Astron. J.* , 124, 1670
- Mannings, V. & Barlow, M. J. 1998, *Astrophys. J.* , 497, 330
- Mannings, V., Koerner, D. W., & Sargent, A. I. 1997, *Nature* , 388, 555
- Mannings, V. & Sargent, A. I. 1997, *Astrophys. J.* , 490, 792
- . 2000, *Astrophys. J.* , 529, 391
- Manoj, P., Maheswar, G., & Bhatt, H. C. 2002, *Mon. Not. R. astr. Soc.* , 334, 419
- Marcy, G. W. & Butler, R. P. 1999, in *NATO ASIC Proc. 540: The Origin of Stars and Planetary Systems*, 681
- Marcy, G. W., Cochran, W. D., & Mayor, M. 2000, *Protostars and Planets IV*, 1285
- Mayor, M. & Queloz, D. 1995, *Nature* , 378, 355
- McCaughrean, M. J. & O'dell, C. R. 1996, *Astron. J.* , 111, 1977
- McNamara, B. & Huels, S. 1983, *Astron. Astrophys. Suppl.* , 54, 221
- McNamara, B. J. 1976, *Astron. J.* , 81, 375
- Meeus, G., Waters, L. B. F. M., Bouwman, J., et al. 2001, *Astron. Astrophys.* , 365, 476

- Millan-Gabet, R., Schloerb, F. P., & Traub, W. A. 2001, *Astrophys. J.* , 546, 358
- Miroshnichenko, A., Ivezić, Z., & Elitzur, M. 1997, *Astrophys. J. Lett.* , 475, L41
- Mora, A., Merín, B., Solano, E., et al. 2001, *Astron. Astrophys.* , 378, 116
- Mundy, L. G., Looney, L. W., & Welch, W. J. 2000, Protostars and Planets IV, 355
- Muzerolle, J., Briceño, C., Calvet, N., et al. 2000, *Astrophys. J. Lett.* , 545, L141
- Muzerolle, J., Calvet, N., & Hartmann, L. 1998, *Astrophys. J.* , 492, 743
- . 2001, *Astrophys. J.* , 550, 944
- Natta, A. 2003, astro-ph/0304184
- Natta, A., Grinin, V., & Mannings, V. 2000, Protostars and Planets IV, 559
- Natta, A., Palla, F., Butner, H. M., Evans, N. J., & Harvey, P. M. 1993, *Astrophys. J.* , 406, 674
- Natta, A., Prusti, T., Neri, R., et al. 2001, *Astron. Astrophys.* , 371, 186
- Nisini, B., Milillo, A., Saraceno, P., & Vitali, F. 1995, *Astron. Astrophys.* , 302, 169
- Nordh, L., Olofsson, G., Abergel, A., et al. 1996, *Astron. Astrophys.* , 315, L185
- Oudmaijer, R. D., van der Veen, W. E. C. J., Waters, L. B. F. M., et al. 1992, *Astron. Astrophys. Suppl.* , 96, 625
- Palla, F. 1999, in NATO ASIC Proc. 540: The Origin of Stars and Planetary Systems, 375--+
- Palla, F. & Stahler, S. W. 1993, *Astrophys. J.* , 418, 414
- Pezzuto, S., Strafella, F., & Lorenzetti, D. 1997, *Astrophys. J.* , 485, 290
- Piétu, V., Dutrey, A., & Kahane, C. 2003, *Astron. Astrophys.* , 398, 565
- Plets, H., Waelkens, C., Oudmaijer, R. D., & Waters, L. B. F. M. 1997, *Astron. Astrophys.* , 323, 513

- Pollack, J. B., Hubickyj, O., Bodenheimer, P., et al. 1996, *Icarus*, 124, 62
- Prusti, T., Natta, A., & Palla, F. 1994, *Astron. Astrophys.* , 292, 593
- Ruden, S. P. 1999, in NATO ASIC Proc. 540: The Origin of Stars and Planetary Systems, 643
- Schmidt-Kaler, T. 1982, in Landolt-Bornstein: Numerical Data and Functional Relationships in Science and Technology, edited by K. Schaifers and H. H. Voigt (Springer-Verlag, Berlin), VI/2b
- Schneider, G., Smith, B. A., Becklin, E. E., et al. 1999, *Astrophys. J. Lett.* , 513, L127
- Serkowski, K. 1974, in IAU Colloq. 23: Planets, Stars, and Nebulae: Studied with Photopolarimetry, 135
- Shaw, S. J. 1975, *Astron. J.* , 80, 602
- Shu, F. H., Adams, F. C., & Lizano, S. 1987, *Ann. Rev. Astron. Astrophys.* , 25, 23
- Siebenmorgen, R., Prusti, T., Natta, A., & Müller, T. G. 2000, *Astron. Astrophys.* , 361, 258
- Silverstone, M. D. 2000, Ph.D. Thesis
- Skinner, C. J., Sylvester, R. J., Graham, J. R., et al. 1995, *Astrophys. J.* , 444, 861
- Skrutskie, M. F., Dutkevitch, D., Strom, S. E., et al. 1990, *Astron. J.* , 99, 1187
- Slettebak, A. 1982, *Astrophys. J. Suppl.* , 50, 55
- Smith, B. A. & Terrile, R. J. 1984, *Science*, 226, 1421
- Song, I. 2000, Ph.D. Thesis
- Song, I. 2001, in ASP Conf. Ser. 244: Young Stars Near Earth: Progress and Prospects, 221

- Spangler, C., Sargent, A. I., Silverstone, M. D., Becklin, E. E., & Zuckerman, B. 2001, *Astrophys. J.* , 555, 932
- Spitzer, L. J. & Schwarzschild, M. 1951, *Astrophys. J.* , 114, 385
- . 1953, *Astrophys. J.* , 118, 106
- Stahler, S. W. 1983, *Astrophys. J.* , 274, 822
- Strom, S. E., Edwards, S., & Skrutskie, M. F. 1993, in Protostars and Planets III, 837–866
- Strom, S. E., Strom, K. M., Yost, J., Carrasco, L., & Grasdalen, G. 1972, *Astrophys. J.* , 173, 353
- Sylvester, R. J. & Mannings, V. 2000, *Mon. Not. R. astr. Soc.* , 313, 73
- Testi, L., Palla, F., & Natta, A. 1998, *Astron. Astrophys. Suppl.* , 133, 81
- Thé, P. S. 1994, in ASP Conf. Ser. 62: The Nature and Evolutionary Status of Herbig Ae/Be Stars, 23
- Thé, P. S., de Winter, D., & Perez, M. R. 1994, *Astron. Astrophys. Suppl.* , 104, 315
- Tian, K. P., van Leeuwen, F., Zhao, J. L., & Su, C. G. 1996, *Astron. Astrophys. Suppl.* , 118, 503
- Uchida, Y. & Shibata, K. 1985, *Publ. Astr. Soc. Japan.* , 37, 515
- Valenti, J. A., Johns-Krull, C. M., & Linsky, J. L. 2000, *Astrophys. J. Suppl.* , 129, 399
- van Altena, W. F., Lee, J. T., Lee, J.-F., Lu, P. K., & Upgren, A. R. 1988, *Astron. J.* , 95, 1744
- van den Ancker, M. E., Bouwman, J., Wesselius, P. R., et al. 2000, *Astron. Astrophys.* , 357, 325
- van den Ancker, M. E., de Winter, D., & Tjin A Djie, H. R. E. 1998, *Astron. Astrophys.* , 330, 145

- van den Ancker, M. E., The, P. S., Tjin A Djie, H. R. E., et al. 1997, *Astron. Astrophys.* , 324, L33
- Vidal-Madjar, A. & Ferlet, R. 1994, in *Circumstellar Dust Disks and Planet Formation*, 7
- Vieira, S. L. A., Corradi, W. J. B., Alencar, S. H. P., et al. 2003, *Astron. J.* , 126, 2971
- Vrba, F. J., Schmidt, G. D., & Hintzen, P. M. 1979, *Astrophys. J.* , 227, 185
- Walker, M. F. 1969, *Astrophys. J.* , 155, 447
- Waters, L. B. F. M. & Waelkens, C. 1998, *Ann. Rev. Astron. Astrophys.* , 36, 233
- Weidenschilling, S. J. & Cuzzi, J. N. 1993, in *Protostars and Planets III*, 1031–1060
- Weinberger, A. J., Becklin, E. E., Schneider, G., et al. 2002, *Astrophys. J.* , 566, 409
- Wielen, R. 1977, *Astron. Astrophys.* , 60, 263
- Wilner, D. J. & Lay, O. P. 2000, *Protostars and Planets IV*, 509
- Wolk, S. J. & Walter, F. M. 1996, *Astron. J.* , 111, 2066
- Yudin, R. V. 2000, *Astron. Astrophys. Suppl.* , 144, 285
- Yudin, R. V. & Evans, A. 1998, *Astron. Astrophys. Suppl.* , 131, 401
- Zuckerman, B. 2001, *Ann. Rev. Astron. Astrophys.* , 39, 549
- Zuckerman, B. & Becklin, E. E. 1993, *Astrophys. J.* , 414, 793